Trinity College Dublin
Coláiste na Tríonóide, Baile Átha Cliath
The University of Dublin

The biology and ecology of regionally endothermic fishes in Irish waters

By

Haley Rose Dolton

BSc (double Hons.) Biology, Oxford Brookes University, 2011

MSc. (Distinction) Conservation and Biodiversity, University of Exeter, 2019

A thesis submitted in partial fulfilment of

the requirements for the degree of

DOCTOR OF PHILOSOPHY

2023

SCHOOL OF NATURAL SCIENCES

DISCIPLINE OF ZOOLOGY

TRINITY COLLEGE DUBLIN

IRISH RESEARCH COUNCIL
An Chomhairle um Thaighde in Éirinn

Declaration

I declare that this thesis has not been submitted as an exercise for a degree at this or any other university and it is entirely my own work. I agree to deposit this thesis in the University's open access institutional repository or allow the Library to do so on my behalf, subject to Irish Copyright Legislation and Trinity College Library conditions of use and acknowledgement. I consent to the examiner retaining a copy of the thesis beyond the examining period, should they so wish (EU GDPR May 2018).

Haley Rose Dolton

Summary

The waters surrounding Ireland are very productive due to cold water upwellings. This has led to Irish waters supporting many livelihoods such as those in tourism and fisheries, with some specialising in catching and observing regionally endothermic fishes. Endothermic fishes possess specialised anatomical structures such as centralised red muscle and *rete mirabile,* which generate and maintain body heat for long periods of time in certain tissues. These endothermic traits are thought to be advantageous for visual perception of prey, increased cruising speed and aiding in the recovery of metabolites after exercise. Most regionally endothermic fishes are rarely encountered due to their predominately pelagic lifestyle. However, anatomical and biologging studies are revealing more about the ecology and biology of these enigmatic species. In **chapter 2**, I investigated how a regionally endothermic fish, the Atlantic bluefin tuna (ABFT), behaves after a stressful catch-and-release (C&R) event. This highly tuned regional endotherm has the capacity to produce and retain body heat to such an extent that they are capable of overheating and dying during overexertion. Consequently, investigating how they behave after a stressful event is important to understand their behaviour and physiology, with the future aim of improving fishing practices of this ecologically and commercially important species. Catch and release fishing is thought to reduce mortality and stress of captured fish when compared to other fishery interactions. However, the fine-scale behavioural effects of C&R fishing of ABFT are unknown. To address this, I made use of an established C&R fishery and attached biologgers to assess how a regionally endothermic fish behaves after a C&R event. I found that ABFT make initial powered descents and have an elevated tailbeat frequency for approximately 5 to 10 hours post release potentially indicating recovery behaviour after an anaerobic event. I also found changes in the behaviour of fish that were handled differently during the capture event, with one fish suffering mortality. This could indicate that handling techniques of regionally endothermic fish can affect their chances of survival post-release and should be investigated further. Another historically important fish species in Irish waters, the basking shark *Cetorhinus maximus*, is currently found in large numbers off the west coastline of Ireland and although described as ectothermic in the literature (alongside 99.9% of all other fishes), it behaves in a similar way to regionally endothermic fish. For example, they have an elevated cruising speed and make fast oceanic migrations, indicating that basking sharks might not be full ectotherms. In addition to behaving like a regional endotherm, basking sharks are also found within the same order as regionally endothermic sharks, Lamniformes. In **Chapter 3** I investigate basking shark anatomy through dissections of stranded carcasses, and physiology through biologging to test the assumption the species is ectothermic. I found basking sharks have anatomical traits shared with regionally endothermic sharks such as red muscle found closer to the vertebrae at the trunk and a high percentage of compact tissue of the

heart (47%). Deploying internal temperature probes into shark species normally involves capture and restraining alongside a boat to insert a temperature logger. However, this is not possible for a planktivorous shark measuring up to 12 m in total length. Consequently, I co-designed and successfully implemented a new biologging technique of inserting and retrieving an internal temperature probe from a free-swimming basking shark. Data from these temperature loggers revealed that basking sharks are able to consistently elevate their body temperature by 1.0 to 1.5°C above ambient, and along with anatomical results from this chapter, demonstrates that basking sharks should now be classed as regionally endothermic. This finding was validated using estimations of heat transfer coefficients (HTC) and whole-body thermal conductance (or *k* coefficient) for a model ectothermic basking shark and similar-sized and fully ectothermic whale sharks *Rhincodon typus*. I showed modelled ectothermic shark body temperature quickly converged towards ambient, whereas body temperature data collected from basking sharks remained elevated above ambient. In **Chapter 4** I estimated the HTC of large regionally endothermic basking sharks and provided *k* estimates for the largest regionally endothermic fish species to date. I found basking sharks have a higher *k* value than predicted for their mass, with their *k* value increasing by approximately 100 times after a period of high mechanical effort (a triple breaching event). This is possibly explained by their filter-feeding life history increasing bulk flow rate of water over the gills, which in turn, may facilitate heat exchange at the gills. Despite a higher *k* value than predicted for their body mass, basking sharks are still able to maintain their body temperature above ambient and when increases in mechanical effort were recorded, white muscle temperature rapidly increased. Results from **Chapter 3 and 4** questioned when regional endothermy evolved within Lamniformes and which life histories it facilitated as it was a trait thought to be confined to apex predatory sharks. For example, the largest living shark species to have lived, the megatooth shark *Otodus megalodon*, is assumed to be regionally endothermic having reached that size partly due to its thermophysiology. In contrast, filter-feeding sharks were thought to have only reached their large size due to either their feeding ecology or thermoregulatory strategy. Regional endothermy and filter-feeding were never thought to have co-existed in the same Lamniformes species. However, finding the basking shark is a regional endotherm challenges our understanding of how many times this trait might have evolved in Lamniformes and when it may have evolved. In **chapter 5** I explored the presence of anatomical structures associated with regional endothermy in a more basal Lamniform, the smalltooth sand tiger shark *Odontaspis ferox*. I dissected carcasses, finding red muscle closer to the vertebrae and a high percentage of compact myocardium of the heart (48%). This suggests that perhaps this species is also regionally endothermic, supporting a one origin theory of regional endothermy in shark species and indicating further investigation into the anatomy and physiology of Lamniformes should be conducted to assess the prevalence of this trait within this largely assumed ectothermic order. In summary, I have addressed how hard-to-study

regionally endothermic fishes behave in their natural environment and challenged long-held assumptions regarding the anatomy and physiology of Lamniformes. These findings greatly enhance our understanding and knowledge of regional endothermy in fishes and also the evolutionary origin and purpose of this trait in shark species. Only by understanding more about a species are we able to effectively conserve them in an ever-changing environment.

Acknowledgements

This was hard and brutal at times of separation during a pandemic. But I've also had exhilarating, inspiring, surprising and the most breath-taking moments I've ever experienced during this PhD. I'm aware I'm an English voice speaking of research conducted in Irish waters, so first of all, thank you Ireland for having me and for those moments.

Thank you to my Supervisor, Dr Nicholas Payne for giving me this opportunity and for encouraging (even I know I've gone too far sometimes) my weird and wacky ideas! Your guidance, support, expertise and trust have gotten me here; a much better scientist. Thank you to my Co-Supervisors, Dr Andrew Jackson, and Dr Jonathan Houghton, I've learnt a lot from you both, if I've come away with a tiny bit of your knowledge and expertise, I'm doing well. Also, Jon, your constant support throughout my career has meant a lot to me, thank you. Thank you to my unofficial Co-supervisor Dr Edward Snelling – your knowledge, patience and guidance have been instrumental to my learning and PhD. To Dr Lucy Hawkes, Sue Sayer (MBE) and Dr Matthew Witt, thank you for your guidance and help when I couldn't see the wood for the trees, I wouldn't be here without you. Thank you to the Zoology Department for all your help throughout my PhD and the during times that were rapidly changing, you kept it all going. Thank you to the PhD, Post-doc and RA cohort I've been part of. The support in the department has been wonderful. I've worked with many wonderful Co-authors throughout this PhD – all experts, and luckily for me, all wonderful humans, thank you.

To my friends, Anna, Andrew, Harriet, Jax, Lorna, Lucie, Lucy B, Lucy R., Luz, Margaret, Michelle, Nina, Sarah, Tash, and the Tomlins. I'm so incredibly lucky to have you all. Your general disinterest in what I do, yet unwavering support whilst I've been away, have kept me on the straight and narrow and reminded me what's important in life. Thank you, I love you all very much. To my two PhD Lucy's, my chaos and my stay. The chaotic one, your support, kindness, and willingness to be silly with me saw me through some of the toughest POINTs of my life. Slimy buckles, I'm so lucky you were here. I simply could not have done this without you or with anyone else. You've been there through everything this PhD and beyond has thrown at me and I will never forget your kindness, strength and support, despite our cultural differences. Grace McNickles, your energy, and strength are admirable, a spark much needed in this world and I'm very glad you're in mine. Jessica Rudd, you have kept me going throughout so many bumps, your kindness, wisdom and support have been second to none. I'm your biggest clam-can fan!

To me family (Dad; Stephen, the Jameses and Bryans), thank you for always supporting me and my weird fascination with the sea and fish! It takes a village. Thank you to my Auntie Debbie for always encouraging my learning and being on hand for chemistry lessons! Everyone was with me during this, including the robins. My biggest thank you of all goes to my Ma (Joan) and Granny (Dot), you have always encouraged me to go after my dreams and live a life that makes me happy.

Your strength, sacrifices and unwavering support and love have gotten me where I am. A lived dream. Thank you, I stand on the shoulders of giants.

Thank you to all the fishers and members of the public I've worked with and met during my PhD. I've learnt loads and shared some awesome moments with you. Your passion for wildlife is infectious. Speaking of wildlife, I'm incredibly grateful and humbled to have contributed in any way to the knowledge base of these amazing animals in my PhD. I will forever be grateful to have worked with them.

Thank you to my main funders of this PhD, The Irish Research Council for their support, without which this PhD would not have been possible. Thank you to the other funders who have financially, or in-kind, supported my PhD: The Fisheries Society of the British Isles and SOFAR Oceans for Good.

This PhD *has* been hard. But a challenging privilege I'd choose again. Go raibh maith agat!

Table of Contents

Declaration ii

Summary iii

Acknowledgements vi

Table of Contents viii

List of Figures x

List of Tables xiv

Additional published work xv

1. Introduction 1

1.1. Thesis aims 4

2. Chapter 2 Short-term behavioural responses of Atlantic bluefin tuna to catch-and-release 5

2.1. Abstract 5

2.2. Introduction 5

2.3. Materials and Methods 7

2.3.1. Angling and tag attachment 7

2.3.2. Data analysis 8

2.4. Results 9

2.5. Discussion 13

3. Chapter 3 Regionally endothermic traits in planktivorous basking sharks *Cetorhinus maximus*. 16

3.1. Abstract 16

3.2. Introduction 16

3.3. Materials and Methods 18

3.3.1. Red muscle distribution and compact myocardium 18

3.3.2. Skeletal red muscle analysis 18

3.3.3. Body and ambient water temperature 19

3.3.4. Heat transfer coefficient model 19

3.4. Results 21

3.4.1. Red muscle distribution and compact myocardium 21

3.4.2. Body and ambient water temperature 23

3.4.3. Heat transfer coefficient model 23
3.5. Discussion 26
4. Chapter 4 Body temperature dynamics of regionally endothermic basking sharks 29
4.1. Abstract 29
4.2. Introduction 29
4.3. Materials & Methods 31
4.3.1. Biologging deployments 31
4.3.2. Data analysis 32
4.3.1. Heat Transfer Coefficient Modelling 33
4.4. Results 34
4.5. Discussion 40
5. Chapter 5 Centralised red muscle in the smalltooth sand tiger shark *Odontaspis ferox* and the prevalence of regional endothermy in sharks 43
5.1. Abstract 43
5.2. Introduction 43
5.3. Materials & Methods 45
5.4. Results and discussion 46
6. Discussion 49
6.1. Short-term behavioural responses of Atlantic bluefin tuna to catch-and-release fishing 49
6.2. Regionally endothermic traits in planktivorous basking sharks *Cetorhinus maximus* 50
6.3. Body temperature dynamics of regionally endothermic basking sharks 51
6.4. Prevalence and origin of regional endothermy in sharks 52
6.5. Regional endothermy in a changing environment 53
6.6. Implications and future research 53
7. Bibliography 55
Appendix A Supplementary information to Chapter 2: A.1
Appendix B Supplementary information to Chapter 3: B.5
Appendix C Supplementary information to Chapter 4: C.7
Appendix D Supplementary information to Chapter 5: D.10

List of Figures

Figure 2.1: Representative examples of tailbeat signal and depth for two ABFTs (tuna A and C) during initial minutes post-release (A, B). Vertical descent speed (m s^{-1}; yellow) and absolute depth (m; green) of tuna C during entire deployment (C). Vertical speed of ABFT during the initial minute post-release, represented by a GAM fitted to data (n = 9; D). Depth (m) of ABFT post-release (n = 9; E) and proportion of vertical space used by ABFT (%) during the first minute post-release (n = 9; F). ……..11

Figure 2.2: Examples of intermittent gliding behaviour shown in tailbeat acceleration (g) and depth (m) of tuna A and C immediately post-release (A, B, respectively) and some 5.5 hours post-release (C, D, respectively) ……12

Figure 2.3: Dominant tailbeat frequency (TBF) over the entire deployment period for nine individual tuna (A – I). To better visualise the data, dominant TBF was represented by a single data point every 12.5 minutes and smoothed using a generalised additive model. ……..13

Figure 3.1: Histological staining of red and white muscle in basking sharks. (A) Hematoxylin and eosin staining of white muscle and (B) red muscle, where the fibres are stained pink and nuclei are stained blue. (C – G) Nitro blue tetrazolium staining of red and white fibres from each transverse section collected from specimen B; location also show by the white curved horizontal lines on the dorsal profile of Figure 2A. Nitro blue tetrazolium stains for the mitochondrial enzyme, succinate dehydrogenase, which is abundant in oxidative fibres, and thus a dark blue stain is produced in red muscle fibres and a sparse speckled stain in white muscle fibres. (H) Control sample for nitro blue tetrazolium stain was also taken from Specimen B. ……..22

Figure 3.2: Anatomical measurements of red muscle distribution and compact myocardium in basking sharks. (A) Anterior to posterior red muscle distribution taken from transverse sections of Specimen A at positions indicated by the white curved vertical lines on the shark. Photographs of transverse sections are incomplete half sections that have been mirrored to aid visual representation (we have not extrapolated distribution anteriorly or posteriorly beyond the extents of our cross-section samples). (B) Ventricular cross-section showing the outer compact separated by inner spongy myocardium, taken from the atrioventricular junction of Specimen C. ……..23

Figure 3.3: Biologging tag package and subcutaneous body temperature in free-swimming basking sharks. (A) Titanium anchor deployed into white muscle (between 5 to 7 cm under the subcutaneous layer) below the dorsal fin with a biologging device recording temperature (LAT1810S), and a towed float recovery package (shown in red behind the shark's dorsal fin) consisting of a VHF transmitter (model MM120, Advanced Telemetry Systems) and a satellite position only tag (model 258, Wildlife Computers). (B) Subcutaneous white muscle temperature

(red lines) compared with ambient water temperature (blue lines) in four free-swimming basking sharks across entire deployment periods. ……..25
Figure 3.4: Measured basking shark subcutaneous white muscle temperature and modelled hypothetical ectothermic sharks of a similar body size. Red and blue lines represent measured subcutaneous white muscle temperature and ambient temperatures collected by 'basking shark 1', respectively. The black line, dashed light green line and dotted dark green line represent a modelled hypothetical fully ectothermic basking shark as well as two whale sharks (7.0, 7.0 and 7.2 m total length), respectively. ……26
Figure 4.1: Temperature, depth and acceleration data from sharks 6 (A and B) and 7 (C and D). (A and C) Subcutaneous white muscle temperature (°C; gold line) and ambient water temperature (°C; steel blue line), respectively during the entire deployment period. (B and D) tailbeat acceleration (g; blue dots), pitch (°; teal line), roll (°; yellow line) and depth (m; shaded grey). ……36
Figure 4.2: Entire time-series of water temperature, subcutaneous white muscle temperature and heat transfer coefficient estimates of four basking sharks. (A, B, C and D) subcutaneous white muscle temperature (gold lines) compared with fixed heat transfer coefficient model $\widehat{T_m}$ (orange dashed lines) and ambient water temperature (steel blue lines) in four free-swimming basking sharks (panels A, B, C and D are sharks 1, 3, 4 and 7, respectively). ……37
Figure 4.3: Relationship between body mass and heat transfer coefficient at cooling. Reproduced from Nakamura et al., 2020. Modified plot from Nakamura et al., 2020 of the relationship between body mass (kg) and heat transfer coefficients (°C min^{-1} $°C^{-1}$) at cooling from ectothermic fish (blue triangles), regionally endothermic fish (red diamonds). Fixed *k* estimates of regionally endothermic basking sharks are shown as red squares and a fixed *k* estimate after breaching is indicated by a red circle. The line through the data points was reproduced using the log intercept and slope given in Nakamura et al., 2020. ……..38
Figure 4.4: Time-series examples of increases in mechanical effort and associated subcutaneous musculature temperature increase from shark 7. (A and C) Subcutaneous white muscle temperature (°C; gold line) and ambient water temperature (°C; steel blue line). (B and D) Tailbeat acceleration (g; blue dots), pitch (°; teal line), roll (°; yellow line) and depth (m; shaded grey). ……39
Figure 4.5: Subcutaneous white muscle temperature and heat transfer coefficient modelling of a cool down period after a triple breach event of shark 7. (A) Subcutaneous white muscle temperature (°C; gold line), ambient water temperature (°C; steel blue line) and fixed heat transfer coefficient model $\widehat{T_m}$ (orange dashed line). (B) Tailbeat acceleration (g; blue dots), pitch (°; yellow line), roll (°; teal line) and depth (m; shaded grey). ……..40
Figure 5.1: Red muscle distribution and prevalence of regional endothermy in Lamniformes. (A) Diagram of the smalltooth sand tiger shark showing location of transverse section indicated by black dashed line taken from specimen 1. (B). Posterior facing transverse section showing centralised

(medial to lateral band) red muscle (red highlighted area) typical of regionally endothermic sharks. (C) Phylogram of Lamniformes adapted from Compagno 1990 and Piemento et al. 2019. Only extant species whose red muscle have been investigated are depicted by red lines on shark silhouettes on the reconstructed phylogram (Table D.1), and megatooth shark is also shown for context. Confirmed regional endothermy and centralised red muscle along the trunk (pink shark silhouette), confirmed laterally placed red muscle and probable ectothermy (light blue shark silhouette) and unconfirmed thermoregulatory strategy (grey silhouettes) with extinct species having a cross. Proposed single origin of regional endothermy indicated by red rectangle. Species depicted are numbered as followed: (1.) *Mitsukurina owstoni* (2.) *Carcharias taurus* (3.) **Odontaspis ferox* (4.) *Odontaspis noronhai* (5.) *Pseudocarcharias kamoharai* (6.) *Megachasma pelagios* (7.) *Alopias superciliosus* (8.) *Alopias pelagicus* (9.) *Alopias vulpinus* (10.) *Cetorhinus maximus* (11.) *Lamna ditropis* (12.) *Lamna nasus* (13.) *Carcharodon carcharias* (14.) *Isurus oxyrinchus* (15.) *Isurus paucus* (16.) *†Otodus megalodon*. ……47

Figure A.1: Biologging package and clamp attachment. Biologging package containing a multi-channel data logger (recording tri-axial acceleration), a very high frequency transmitter and Satellite Position Only Tag. A clamp is held open with a block of wood in preparation for deployment. Recovery telephone number has been obscured on red float material. ……A.1

Figure A.2: Deployment locations (circle shapes) of Atlantic bluefin tuna (tuna ID indicated on the map) tagged off the coast of Donegal, Ireland. Black dashed line indicates a connecting line between deployment location and pop-off location (star shape) of the biologging package. It does not represent actual movement of Atlantic bluefin tuna. The biologging package came off of Tuna C within 1.0 km of the deployment location. Consequently, there is no connecting black dashed line. Tuna X is not shown due to a suspected mortality event within minutes of release. ……A.2

Figure A.3: Vertical speed and depth use of Atlantic bluefin tuna during the respective whole deployment. Vertical speed (m s^{-1}) (yellow) and depth (m) (green) use of Atlantic bluefin tuna tagged in this study. Atlantic bluefin tuna identification shown in plots. ……A.3

Figure A.4: Suspected mortality event of tuna X. Release event of tuna X showing unfiltered acceleration (teal line (g)) and smoothed depth data (blue line (m)). ……A.4

Figure A.5: Classic intermittent locomotion of Atlantic bluefin tuna. (A) Examples of classic intermittent locomotion of tuna A 6 hours post-release and (B) tuna C 16 hours post-release. Increased tailbeat activity (teal line (g)) is seen on ascents and gliding on descents (depth shown with a blue line (m)). ……A.4

Figure B.1: Lateral subcutaneous vessels of basking sharks. Within the connective tissue there appears a small lateral subcutaneous artery and large lateral subcutaneous vein located near the lateral extents of the red muscle. Image taken from specimen A from near the pectoral fin region. ……B.6

Figure C.1: Biologging configurations. Tag deployment set up (solid black line represent monofilament line and dashed black lines represent cable ties). (A) Titanium anchor deployed into white muscle using a modified tagging spear as described in Dolton et al 2023. (B) Two titanium anchors used to hold internal temperature in the musculature. Steel H frame used to transmit force down the extension pole to steel baseplate and steel applicators. Biologging devices (Lotek LAT100ST, Technosmart 720hp video camera, and PD3GT Little Leonardo accelerometer) secured onto baseplate. Steel frame and extension pole removed from shark upon deployment. (C) Fishing dart used to deploy internal temperature probe (Lotek LAT100ST) into the musculature. Steel A frame used to transmit force down the extension pole to steel baseplate (held in place with hard foam) and fishing dart. Biologging devices (Lotek LAT100ST and PD3GT Little Leonardo accelerometer) secured onto baseplate, with Technosmart 720hp video camera secured to the anchor line. Steel frame, hard foam and extension pole removed from shark upon deployment. ……C.7

Figure C.2: Entire time-series of water temperature, subcutaneous white muscle temperature and heat transfer coefficient estimates of three basking sharks. (A, B, and C) subcutaneous white muscle temperature (gold lines) compared with fixed heat transfer coefficient model $\widehat{T_m}$ (orange dashed lines) and ambient water temperature (steel blue lines) in three free-swimming basking sharks (panels A, B and C are sharks 2, 6, and 5, respectively). ……C.9

Figure C.3: Time-series examples of rolling events from shark 6 and 7. (A and C) Subcutaneous white muscle temperature (°C; gold line) and ambient water temperature (°C; steel blue line) of two separate rolling events. (B and D) Tailbeat acceleration (g; blue dots), pitch (°; teal line), roll (°; yellow line) and depth (m; shaded grey) of rolling events of shark 6 and 7, respectively. ……C.10

Figure D.1: Red muscle distribution of the smalltooth sand tiger shark *Odontaspis ferox*. (A) Diagram of the smalltooth sand tiger shark showing location of transverse sections. (B) Transverse cross sections of specimen 1 taken from locations indicted on panel A as black dashed lines. (C) Transverse cross sections of specimen 2 taken from locations indicted on panel A as white and black dashed lines. The first dashed line on the left matching first transverse cross section on the left in panels B and C. ……D.11

List of Tables

Table 2. 1: Tag attachment metadata for ten Atlantic bluefin tuna *Thunnus thunnus*. Deployment duration rounded to nearest hour. 10

Table 4. 1: Metadata and estimated temperature parameters from heat transfer coefficient (HTC) modelling. *Potential shallow internal temperature sensor placement. ……..……..3535

Table A.1: Metrics (measured in cm) and weight (g) of biologging package contents used during this study. Length, width, and height measurements were made at the maximum point of the main body of devices or clamp package. ……A.1

Table C.1: basking shark identification from Chapters 3 and 4 including deployment latitude, longitude and total length of each relevant shark……C.8

Table D.1: Species in the order Lamniformes that have regionally endothermic anatomical traits (yes; Y, no; N or Unknown) and thermoregulatory life history investigated (Regional endotherm, Ectotherm or Unknown). ……D.12

Additional published work

1. Rudd JL, Bartolomeu T, **Dolton HR**, Exeter OM, Kerry C, Hawkes, LA, Henderson SM, Shirley M, Witt MJ (2020). Basking shark sub-surface behaviour revealed by animal-towed cameras. *PLOS ONE*, 16(7), e0253388. https://doi.org/10.1371/journal.pone.0253388.

   Contribution – I co-analysed data and edited manuscript drafts.

2. Harding L, Gallagher A, Jackson AL, Bortoluzzi J, **Dolton HR**, Shea B, Harman L, Edwards D, Payne NL (2022). Capture heats up sharks. Conservation Physiology, 10(1), coac065. doi: https://doi.org/10.1093/conphys/coac065

   Contribution – I collected data and edited manuscript drafts.

3. Curnick DJ, Deaville R, Bortoluzzi J, Cameron L, Carlsson J, Carlsson J, **Dolton HR**, Gordon CA, Hosegood P, Nilsson A, Perkins MW, Purves KJ, Spiro S, Vecchiato M, Williams R, Payne NL (2023). Northerly range expansion and first confirmed records of the smalltooth sand tiger shark, Odontaspis ferox, in the United Kingdom and Ireland. *Journal of Fish Biology*. Accepted Author Manuscript.

   Contribution – I collected data and edited manuscript drafts.

1. Introduction

Ireland's territorial waters are ten times the size of Ireland's land mass with many sectors relying on the sea for financial support in the past and present. For example, a large basking shark *Cetorhinus maximus* fishery was based off Achill Island, Co. Mayo, between 1946 to 1976, catching thousands of basking sharks for harvest before ultimately collapsing due to overexploitation (McNally 1976). Similarly, Atlantic bluefin tuna *Thunnus thynnus* (ABFT) have historically suffered overexploitation in Irish waters and as such, a catch-and-release (C&R) programme currently exists in Irish waters as part of stock management (Horton et al. 2020). If well managed, C&R programmes can support local economies whilst reducing capture-related injuries and mortalities of ecologically important predatory species such as ABFT (Policansky 2002, Cooke & Schramm 2007, Cosgrove et al. 2008). Atlantic bluefin tuna have specialised anatomy and physiology facilitating their predatory life history associated with regional endothermy, or the ability to generate and retain metabolic heat (Bernal et al. 2001a). This is in contrast to 99.9% of all other fishes that are ectothermic where body temperature closely matches ambient temperature (Wegner et al. 2015). Several species within billfish, tuna and shark taxa have convergently evolved the rare trait of regional endothermy, meaning these fishes can internally generate and maintain elevated temperatures within certain body tissues such as the red muscle, viscera, eyes and brain, which is thought to facilitate an apex predatory lifestyle (Carey & Teal 1969, Carey & Lawson 1973, Graham 1975, Graham et al. 1983, Bernal et al. 2001b, 2003a). It has been proposed that regionally endothermic fishes might be more resistant to environmental stressors such as climate change and fisheries pressures, but perhaps more vulnerable to short term stressors such as C&R if increased metabolic costs cannot be repaid rapidly through behaviours such as feeding (Carey & Lawson 1973, Block 1991, Dickson & Graham 2004, Horodysky et al. 2016). There remain large assumptions as to the function of regional endothermy and which species possess it, particularly within sharks (Bernal et al. 2001a, Sternes et al. 2023). For example, all currently described regionally endothermic sharks belong to the order Lamniformes and are apex predatory sharks (family; Lamnidae and Alopiidae). However, perhaps due to their differing life histories, the remaining members of this order were assumed to be ectothermic with regional endothermy thought to have convergently evolved several times within the order (Bernal et al. 2001a, Bernal & Sepulveda 2005). Other members of this order, such as the basking shark, display similar behaviours to regionally endothermic fishes, such as making vast oceanic migrations over short periods of time (approximately 95000 km in 82 days) and they are also closely related to regionally endothermic sharks (Compagno 1990, Sims 2000, Bernal et al. 2001a, Gore et al. 2008). This thesis aims to assess how an ecologically and commercially important species like the regionally endothermic ABFT behaves after a physiologically demanding event and

to reassess the anatomy and physiology of Lamniformes. In doing so, it will provide accurate physiological and behavioural information about difficult to study fishes, which can be used in future comparative analysis and population and distribution forecasting used to inform management decisions (Kearney & Porter 2009).

Large regionally endothermic fish are challenging to study due to their rarity and pelagic life history (Bernal et al. 2001b). Nonetheless, in part due to their commercial importance, the extreme endpoint of C&R (i.e., mortality) has been studied in ABFT by using pop-up satellite archival tags with 3.4% mortality rate considered a 'best case scenario' (Stokesbury et al. 2011). However, the sublethal physiological or behavioural effects of this fishery are largely unknown for ABFT (Stokesbury et al. 2011, Marcek & Graves 2014). Biologging devices such as accelerometers, which record tri-axial body movement, have been used to study the fine-scale behavioural effects of C&R for a variety of popular sports fish such as sharks and freshwater fishes (Brownscombe et al. 2014, 2017, Whitney et al. 2017, Hounslow et al. 2019, Holder et al. 2020). With C&R programmes extending to other countries such as the United Kingdom, it is of high importance that the fine-scale response of this large regional endotherm to exhaustive exercise associated with C&R is assessed and integrated into stock management considerations. I aim to address this knowledge gap in **Chapter 2** by recording the fine-scale behavioural response of ABFT in the hours immediately post-release of a C&R event.

A regionally endothermic life history of fishes is metabolically costly, especially following anaerobic events such as those described in **Chapter 2** (Bennett & Ruben 1979, Brill & Bushnell 1991, Harding et al. 2022). Most heat generation in shark species is thought to occur within centralised red muscle and along with other anatomical structures such as a high percentage of compact myocardium of the heart (typically associated with elevated blood pressure), is thought to facilitate a regionally endothermic apex predatory life history (Braekken 1959, Brill & Bushnell 1991, Bernal et al. 2001a, 2003a, Bernal & Sepulveda 2005). The basking shark (family; Cetorhinidae) is sister to Lamnidae, and shares behaviours typically associated with regionally endothermic fishes such as a fast-cruising speed when compared to ectothermic fishes and migrating over large distances in short time periods of time (Compagno 1990, Bernal et al. 2001a, Gore et al. 2008). However, basking sharks have always been assumed to be ectothermic in the literature with associated ectothermic anatomical features such as lateral red muscle distribution (e.g., Bernal et al. 2001a). Due to the size and planktivorous feeding ecology of basking sharks it remains challenging to study the anatomy and physiology of the species. However, stranding events of fresh carcasses provide opportunities to investigate the anatomy of basking sharks, such as red muscle distribution and percentage of compact myocardium of the heart. When anatomical analysis is combined with physiological study, such as deploying internal temperature probes, it

becomes possible to assess whether basking sharks are fully ectothermic as suggested by the literature. I aim to formally test this assumption in **Chapter 3**.

Body temperature data collected via biologging can be used to estimate the rate of heat exchange between fishes and the surrounding water through calculating a heat transfer coefficient (HTC) and to determine whether a fish is ectothermic or regionally endothermic (Nakamura et al. 2020, Watanabe et al. 2021). The HTC of a species includes thermal conductance of body mass and shape, which is termed a *k* coefficient. Typically, smaller fish exchange heat with the environment faster than larger fish following Newton's law of cooling (with increasing body mass associated with decreasing *k* coefficient (Nakamura et al. 2020)). The HTC can vary among species, individuals and throughout time. For example, the largest extant fish is the ectothermic whale shark *Rhincodon typus,* and HTC estimation revealed this species cools down at a slower rate than it heats up (i.e., $k_{cooling} < k_{heating}$) when experiencing changing ambient temperature, and that internal heat production does not notably change muscle temperature, confirming an ectothermic life history (Nakamura et al. 2020). This suggests whale sharks might be able to make forays to colder, deeper waters without the metabolic cost of regional endothermy. The basking shark is the closest in size to the whale shark (12 and 18 m total length, respectively (Sims 2008, Dove & Pierce 2021)) but it is unknown how the large size of basking sharks may affect thermoregulatory ability or whether they follow established HTC relationships regarding the rate of heat exchange in relation to body mass. In addition to this, it unknown whether acute increases in mechanical effort might affect body temperatures of basking sharks. **Chapter 4** aims to estimate the HTC of a large, ram ventilating, filter-feeding shark for the first time to increase the knowledge of the physiology and life history of basking sharks.

Heat transfer coefficient estimations of sharks have been used to confirm thermophysiological strategies of shark species in the past (Carey et al. 1982, Bernal et al. 2001b, Nakamura et al. 2020). However, thorough investigations of the thermophysiology of the entire Lamniformes order has not been conducted. Within Lamniformes, only two species have been confirmed to be ectothermic through dissections and measurement of muscle temperature (the pelagic *Alopias pelagicus* and big eye thresher shark *Alopias superciliosus* (Bernal et al. 2003a, Pimiento et al. 2017)), five species are regionally endothermic (Bernal et al. 2003a for a review, Bernal & Sepulveda 2005), and eight species within this order are assumed ectotherms (Bernal et al. 2003a, Pimiento et al. 2017, Sternes et al. 2023). By dissecting stranded carcasses of more basal Lamniformes species, **Chapter 5** aims to address the prevalence of regionally endothermic traits within the order. In doing so, results from these anatomical dissections may provide additional evidence as to the evolutionary appearance and importance of regional endothermy in shark species.

Studying the ecology and physiology of regionally endothermic fish in Irish waters is of great interest to me as Irish waters are incredibly diverse and productive, which provides a unique opportunity to study species which are often difficult to see anywhere else in the world. Both ABFT and basking sharks are of ecological and conservation interest, with AFBT being commercially valuable and basking sharks being classified as globally 'Endangered' (Rigby et al. 2021). Additionally, both species are large and relatively predictable in terms of seasonality in Irish waters, providing an opportunity to deploy new technology such as those used in biologging to learn more about how large regional endotherms might respond in, and to, their environment. In addition to the use of state-of-the-art technology such as biologging, strandings provide a unique opportunity to learn more about species which are typically difficult to examine up close. Anatomical and histological analysis were the foundation of pioneering fish physiological studies in the past and when combined with modern technology today have the potential to inform where new technology should be placed on the body of a fish, which may reduce tagging related impacts on the wild animals studied. Furthermore, understanding the physiology and behaviour of regionally endothermic fish is becoming increasingly important when taken in the frame of our changing global environment.

The results of this thesis will likely be of use to a variety of stakeholders, including but not limited to, fisheries managers who can incorporate results from **Chapter 2** into species-specific C&R guidelines and future studies of ABFT, and conservation planners whose future predictions of population trends or distribution shifts may alter with new anatomical and physiological evidence for Lamniformes species (**Chapters 3, 4 and 5**). In terms of scholarly understanding this thesis aims to update and evaluate existing literature, such as challenging assumptions relating to shark species anatomy and physiology. If my findings contradict the current literature on regional endothermy in sharks it will greatly enhance and revise our knowledge of regional endothermy in fishes, especially within shark research. Additionally, new avenues of investigation could be opened up including reassessing assumed thermophysiology of shark species and the estimation of metabolic rates of large free-swimming fish species.

1.1. Thesis aims

1. To understand the behavioural effects of a C&R event on a regionally endothermic fish (**Chapter 2**).
2. To test the assumption that basking sharks have an ectothermic anatomy and physiology (**Chapter 3**).
3. To determine heat transfer coefficients of basking sharks and assess whether this species follows established cooling rates of fishes (**Chapter 4**).
4. To assess the prevalence of regionally endothermic traits within the order Lamniformes (**Chapter 5**).

2. Chapter 2 Short-term behavioural responses of Atlantic bluefin tuna to catch-and-release

Authors: Haley R. Dolton, Andrew L. Jackson, Alan Drumm, Lucy Harding, Niall Ó Maoiléidigh, Hugo Maxwell, Ross O'Neill, Jonathan D. R. Houghton, Nicholas L. Payne.

Author contribution: Overall conception by NLP, NOM, AD and HRD Fieldwork undertaken by HRD, NLP, AD, RON, LH, JDRH and HM. Data analysis undertaken by HRD and NLP Writing led by HRD and NLP with contribution from all authors. All authors read, edited and discussed the manuscript.

Status: This manuscript was published in *Conservation Physiology* in September 2022.

2.1. Abstract

Catch-and-release (C&R) angling is often touted as a sustainable form of ecotourism, yet the fine-scale behaviour and physiological responses of released fish is often unknown, especially for hard-to-study large pelagic species like Atlantic bluefin tuna (ABFT; *Thunnus thunnus*). Multi-channel sensors were deployed and recovered from 10 ABFTs in a simulated recreational C&R event off the west coast of Ireland. Data were recorded from 6 to 25 hours, with one ABFT (tuna X) potentially suffering mortality minutes after release. Almost all ABFTs ($n = 9$, including tuna X) immediately and rapidly (vertical speeds of approximately 2.0 m s^{-1}) made powered descents and used 50 to 60% of the available water column within 20 seconds, before commencing near-horizontal swimming approximately 60 seconds post-release. Dominant tailbeat frequency was approximately 50% higher in the initial hours post-release and appeared to stabilize at 0.8 to 1.0 Hz some 5 to 10 hours post-release. Results also suggest different short-term behavioural responses to noteworthy variations in capture and handling procedures (injury and reduced air exposure events). Our results highlight both the immediate and longer-term effects of C&R on ABFTs and that small variations in C&R protocols can influence physiological and behavioural responses of species like the commercially valuable and historically over-exploited ABFT.

2.2. Introduction

Catch-and-release (C&R) fishing is an increasingly popular practice, providing important social and economic benefits to communities while also being presented as sustainable (Policansky 2002). Atlantic bluefin tunas (ABFTs) *Thunnus thunnus* are active, predatory fish historically over-exploited in commercial fishing and are a popular sport fish in C&R fisheries (Taylor et al. 2011) due to their size and power. The International Commission for the Conservation of Atlantic Tunas (ICCAT) manage ABFTs as two stocks (although there may be more genetically distinct spawning

stocks in the NE Atlantic (Rooker et al. 2008, 2014, Rodríguez-Ezpeleta et al. 2019)): as an 'eastern stock' and 'western stock', which is separated along the 45°W meridian (ICCAT 2002, Block et al. 2005). The eastern stock is estimated to have declined to 33% of the historical levels in the early 2000s due to overfishing (Taylor et al. 2011) and in 2007 ICCAT began a stock rebuilding program, with the most recent assessment suggesting the eastern stock biomass is no longer decreasing (ICCAT 2020). Despite the scientific assessment carried out by ICCAT, there remains a question surrounding the actual biomass of the 'western' or 'eastern' stock of ABFTs due to uncertainties surrounding the size of sexually mature individuals from each stock (Corriero et al. 2020, Medina 2020) and the reconciliation between the use of 'eastern' or 'western' areas by each stock for important life history events, with mixing between the stocks now widely accepted to occur (Block et al. 2005, Stokesbury et al. 2007, Rooker et al. 2014, Hanke et al. 2018, Horton et al. 2020).

Recreational C&R assumes released individuals recover from the interaction and contribute to future reproductive potential of the population (Cooke & Schramm 2007, Donaldson et al. 2008). If managed well, this approach can allow communities to benefit substantially, while helping to safeguard stocks (Cosgrove et al. 2008). However, the sustainability of a C&R fishery for a particular species is underpinned ultimately by survivorship rates post-release including, but not limited to, suitability of fishing equipment, angler experience, species physiology and ecology and environmental conditions (Arlinghaus et al. 2007, Cooke & Schramm 2007, Davis 2007, Brownscombe et al. 2017). Consequently, methods to mitigate mortality during C&R events have been investigated in many teleost species (see Muoneke et al. 2008, Brownscombe et al. 2017 for a review). However, due to the difficulty of studying large, marine species in situ, there remains significant uncertainties surrounding best C&R practices and mortality rates due to species-specific responses to capture (Bartholomew & Bohnsack 2005, Muoneke et al. 2008, Gallagher et al. 2014). For example, survival rates of large sport fish appear highly variable, with reported survivorship rates varying from 22% to 100% for common thresher sharks *Alopias vulpinus* (Sepulveda et al. 2015), 90% for shortfin mako sharks *Isurus oxyrinchus* (French et al. 2015), 100% for yellowfin tunas *Thunnus albacares* and bigeye tunas *Thunnus obesus* (Holland et al. 1990) and 94 to 100% for ABFTs (Stokesbury et al. 2011, Marcek & Graves 2014). Such variation indicates areas for improvement and refinement regarding C&R practices with species-specific guidelines suggested to reduce mortality and sub-lethal effects (Cooke & Suski 2005).

Survivorship rates represent the extreme endpoint metric of a C&R interaction. However, a range of sub-lethal impacts can have substantial consequences on the post-release fitness of individual fish and may have negative effects at the population level. These include physical injuries such as puncture wounds to the skin and sensitive tissues like the gills and eyes (reviewed in Brownscombe et al. 2017) and possible impacts on suggested fitness measures such as elevated

energy expenditure, increased predation risk and potential interruption of important activities such as feeding, growth and reproduction (Cooke et al. 2002, Cooke & Suski 2005, Raby et al. 2013, Brownscombe et al. 2014, 2017). Sub-lethal behavioural studies typically measure and describe stress proxies such as reflex impairment prior to fish release (Brownscombe et al. 2013, 2017, McArley & Herbert 2014), with the realised short-term physiological or behavioural fate of the animal post-release largely unknown. Recently, biologging devices have emerged as useful tools for measuring fine-scale behavioural, ecological and physiological parameters to assess biological function in fish (Cooke et al. 2004, Watanabe et al. 2008, Watanabe & Sato 2008, Payne et al. 2014) and to measure the post-release response in popular species targeted in C&R fisheries such as sharks (Whitney et al. 2016, 2017, Brewster et al. 2018, Hounslow et al. 2019). Accelerometers, which can record high-resolution tri-axial acceleration, have been used to record body movements of bony fish after C&R to assess short-term impacts on behaviours such as swimming and predator avoidance (Brownscombe et al. 2014, 2017, Holder et al. 2020, LaRochelle et al. 2021). Short-term effects on behaviour have been shown to indicate the long-term fate of fish, including survivability (Beitinger 1990, Brownscombe et al. 2014, Lennox et al. 2018). However, despite their popularity as a sport fish, little is known about the short-term physiological and behavioural impact that C&R has on ABFTs beyond what can be inferred from lower resolution methods such as pop-off satellite archival tags (Stokesbury et al. 2011, Marcek & Graves 2014). We deployed accelerometers on 10 ABFTs captured during a simulated C&R event off the Northwest coast of Ireland. Our aim was to document the impact of C&R on the fine-scale behaviour of ABFTs immediately post-release and several hours thereafter.

2.3. Materials and Methods

2.3.1. Angling and tag attachment

Ten ABFTs were tagged under license from Health Products Regulatory Authority of Ireland between 2017 and 2020 (2017, *n* = 3; 2018, *n* = 4; 2019, *n* = 2 and 2020, *n* = 1) as part of a simulated recreational C&R event. As recreational fishing of ABFT is not permitted in Irish waters, a simulated C&R event was created whereby ABFTs were caught by anglers and brought to the boat for the purpose of a scientific procedure, as authorized within the Tuna Catch-and-Release Tagging (CHART) programme. A 120 to 200 lb line with 400 lb leader was used on a Class Rod (80 to 130 lb strength) to troll with squid lures on a spreader bar. Hooks (IO/O Mustad J hooks) were removed from fish immediately when brought on deck. All ABFTs were captured using this method within 20 km of the Donegal coastline, Ireland. Once close to the boat a lip hook was inserted into the mouth and out under the jaw to either secure the ABFT alongside the boat (*n* = 1) or to bring the ABFT on deck (*n* = 9). The use of lip hooks forms an important aspect of our simulated C&R study as they are

used under the Irish CHART programme. Once on board ABFTs were placed on a padded mat with a deck hose inserted immediately in the mouth to ventilate the gills, a damp cloth placed over the eyes to reduce stress (following Block et al., 2005) and the lip hook removed (lip hooking lasted approximately 10 seconds in duration). One fish was towed alongside the boat using a lip hook at one to two knots to ventilate the gills and was tagged while remaining partially submerged. Fork length (cm), half girth (cm), fish landing time, release condition, release time and position of capture were recorded. A floy tag was inserted near the second dorsal fin, and a tissue biopsy was taken from each fish as part of a wider study of ABFTs. A sterile fin clamp package containing a multi-channel data logger recording tri-axial acceleration at 20 Hz (resolution: 0.01 g) and 25 Hz (resolution: 0.01 g; Little Leonardo Corp. ORI1300 3MPD3GT, *n* = 7; and TechnoSmart AGM-1, *n* = 3, respectively) and depth at 1 Hz (resolution: 0.4 m and 0.1 m, respectively) was deployed on the second dorsal fin (Huveneers et al. 2018). Tri-axial acceleration was recorded at different frequencies due to logistical constraints. The package also contained a radio tag very high frequency transmitter (Advanced Telemetry Systems MM170B) and Satellite Position Only Tag (Wildlife Computers Model 258) to aid in recovery of the package (Figure A.1; for package metrics, see Table A.1). As ABFTs are highly migratory, a galvanic timed release (rated for one or two days) was manually corroded down in a bucket containing seawater to 12 to 15 hours and used to hold the biologging package to the fin clamp. Manual corrosion of galvanic timed releases allowed the package to detach from the fin 6 to 25 hours later following submergence in seawater and to be successfully recovered. A second corrodible link in the fin clamp itself dissolved some 3 to 5 days later allowing all equipment to completely detach from the fish.

2.3.2. Data analysis

Multi-channel data were initially analysed in Igor Pro 6.3 (WaveMetrics Inc., Portland, OR, USA) with the Ethographer package (Sakamoto et al., 2009). A low-pass filter was used to remove static (gravitational) from dynamic (body movement) components of the accelerometer data (following Watanabe & Takahashi 2013). The clearest tailbeat signal on a dynamic wave was used in R Studio (R Development Core Team 2020) to determine the dominant tailbeat frequency (TBF) for each individual (*n* = 9; one ABFT possibly suffered mortality and was excluded from this analysis). A loop function was created to run over every 12.5 minutes of data using an autoregression model to compute spectral density using the 'stats' package in base R. Trends in dominant TBF through time (as identified by the spectral density function) was visualized using the 'stat_smooth' function in R to produce a generalized additive model (GAM) using the formula y ~ s(x) (family = loess).

Deployment locations were matched to 10 m resolution bathymetry data obtained from the Integrated Mapping for the Sustainable Development of Ireland's Marine Resource in QGIS software (QGIS Development Team 2018) to find release site depth. Tuna G was excluded from

depth data analysis as the multi-channel data logger failed to record pressure. Depth data were analysed with a GAM using the formula y ~ s(x) (family = loess) to plot vertical speed data using ggplot in R. Depth data were also smoothed (*n* = 9) in Igor Pro 6.3 (WaveMetrics Inc., Portland, OR, USA) using an 8-point moving average smoother and the difference between two subsequent smoothed depth recordings were calculated producing vertical speeds whereby positive and negative values represent descents and ascents, respectively. Smoothed depth data from the initial 60 seconds post-release were plotted in R using ggplot as absolute terms and also as a proportion of the release site depth (%).

2.4. Results

Between 2017 and 2020, large ABFTs ranging from 200 to 235 cm in length were tagged with multi-channel data loggers (*n* = 10) (Table 2.1) off the northwest coast of Ireland. Biologging packages stayed on the fin for 6 to 25 hours (Table 2.1; Figure A.1), with packages detaching from the ABFT within 55 km (minimum straight-line distance) of the tagging site (Figure A.2); fight time ranged from 13 to 24 minutes, and handling time (the duration from when ABFT were brought onto deck or secured alongside the boat to release) ranged from 2 to 9 minutes (Table 2.1). Initial tailbeat acceleration and depth data post-release revealed that the ABFTs undertook initial powered (associated with clear tailbeats) descents for several seconds, followed by a period of gliding that culminated with a tailbeat signal (displaying little variance between beats) within one-minute post-release and horizontal swimming (Figure 2.1A; B). The vertical speed of initial descent immediately post-release was noticeably higher (1.5 to 2.5 m s^{-1}; Figure 2.1C; D) than vertical descent speeds over the remaining time series, which were typically <0.5 m s^{-1} (Figure A.3). Following the initial rapid descent, the ABFTs began to reduce their vertical speed and approach near horizontal swimming (i.e., stop their descent) some 60 seconds post-release (Figure 2.1D) at a depth of 45 to 80 m (Figure 2.1E) using 66 to 98% of the proportional water column (Figure 2.1F). Tuna C, which remained partially submerged during the handling and tagging process, displayed a slightly slower return to near horizontal swimming during this time than the other ABFTs. Tuna D, which received a hooking injury to the eye, exhibited a noticeably different initial depth pattern to all other ABFTs, initially descending slowly and staying within 10 m of the surface and reaching its maximum vertical descent speed approximately 40 seconds after release (whereas others reached peak descent speeds <20 seconds after release; Figure 2.1D).

Table 2.1: Tag attachment metadata for ten Atlantic bluefin tuna *Thunnus thunnus*. Deployment duration rounded to nearest hour.

Tuna ID	Date	Deployment latitude (°N)	Deployment longitude (°W)	Fork length (cm)	Fight time (minutes)	Handling time (minutes)	Deployment duration (hours)
A	18/10/2017	54.773	8.715	200	N/A	5	10
B	29/10/2017	54.901	8.693	235	N/A	4	7
C*	04/10/2018	54.544	8.850	205	20	9	25
D	04/10/2018	54.542	8.855	220	14	3	8
E	14/10/2018	54.513	8.855	220	17	2	16
F	31/10/2018	54.569	8.774	211	13	3	7
G	31/10/2019	54.490	8.719	222	19	4	11
H	31/10/2019	54.499	8.734	215	24	6	6
I	15/09/2020	54.576	8.828	207	19	5	16
X†	02/11/2017	54.892	8.649	200	N/A	7	N/A

*not brought on deck, tagged in water

† possibly suffered mortality immediately after release

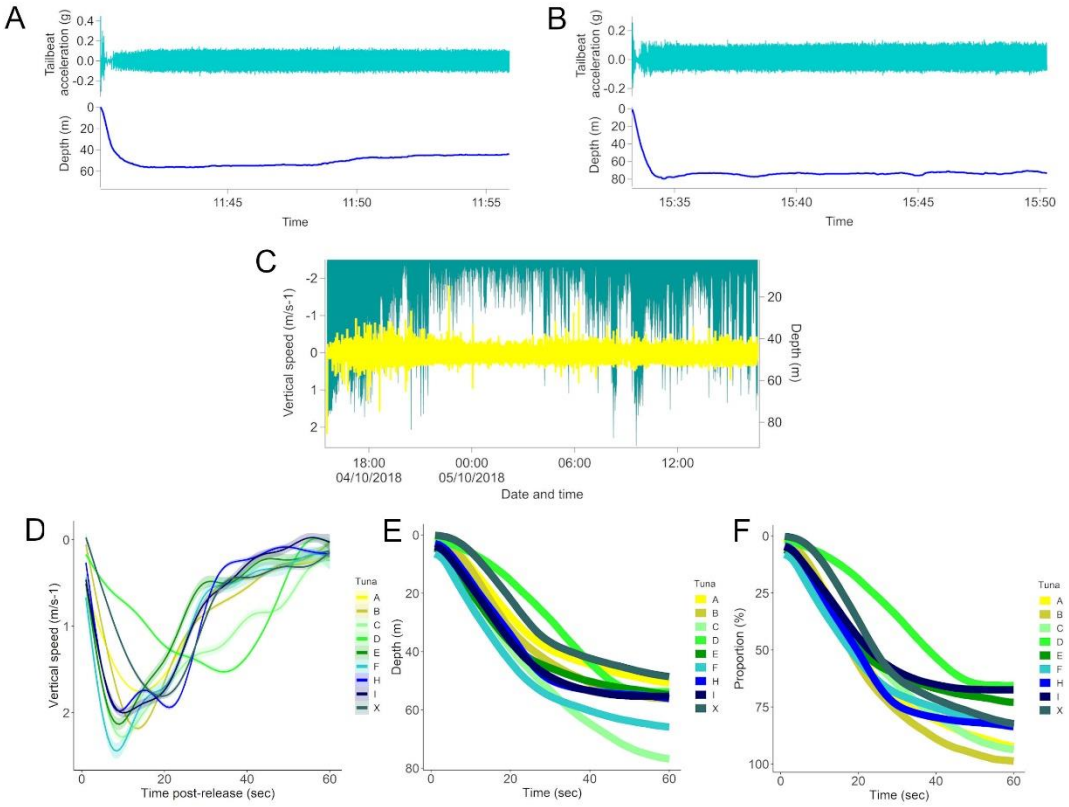

Figure 2.1: Representative examples of tailbeat signal and depth for two ABFTs (tuna A and C) during initial minutes post-release (A, B). Vertical descent speed (m s−1; yellow) and absolute depth (m; green) of tuna C during entire deployment (C). Vertical speed of ABFT during the initial minute post-release, represented by a GAM fitted to data (n = 9; D). Depth (m) of ABFT post-release (n = 9; E) and proportion of vertical space used by ABFT (%) during the first minute post-release (n = 9; F).

Tuna X, which may have suffered mortality upon release (Figure A.4), had the longest time on deck (seven minutes; although was not a major outlier) and appeared to follow a similar pattern of descent as the other individuals, which lasted approximately 30 seconds, with a weak possible tailbeat signal lasting approximately 60 seconds. After this latter period, larger peaks in tailbeat amplitude were seen regularly through the time series for approximately three minutes with unusual accelerations, remaining relatively still on the seabed at a final depth of 65 m (Figure A.4). It is possible that the clamp had detached from the animal; however, the variable rate of descent was not consistent with such an event.

The percentage of proportional vertical space used within the water column by the ABFTs tagged on deck varied between 50 to 60% within approximately the first 20 seconds and 66 to 98% during the remaining 60 seconds post-release (Figure 2.1F). Tuna D displayed a different descent response in relation to proportional vertical space use, using approximately 12.5% of the water

column within the first 20 seconds (Figure 2.1E; F). During the initial descent period, the ABFTs used intermittent tailbeat and gliding, a pattern also seen hours after release (Figure 2.2; Figure A.5).

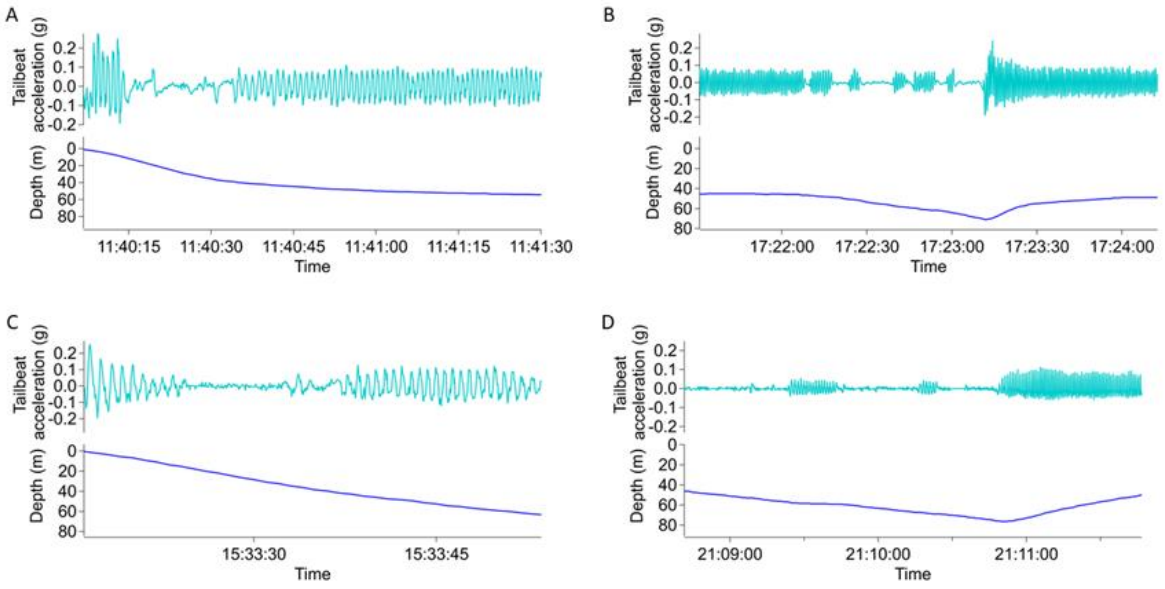

Figure 2.2: Examples of intermittent gliding behaviour shown in tailbeat acceleration (g) and depth (m) of tuna A and C immediately post-release (A, B, respectively) and some 5.5 hours post-release (C, D, respectively).

Spectral analysis over the entire deployment period of each ABFT revealed that dominant TBF was approximately 50% higher within the first few hours post-release (Figure 2.3), and subsequently appeared to stabilize at 0.8 to 1.0 Hz some 5 to 10 hours post-release. However, several traces (e.g., tunas A, F and H) continued to decrease for some of the shorter deployments (≤10 hours), suggesting dominant TBF had not stabilized at this time.

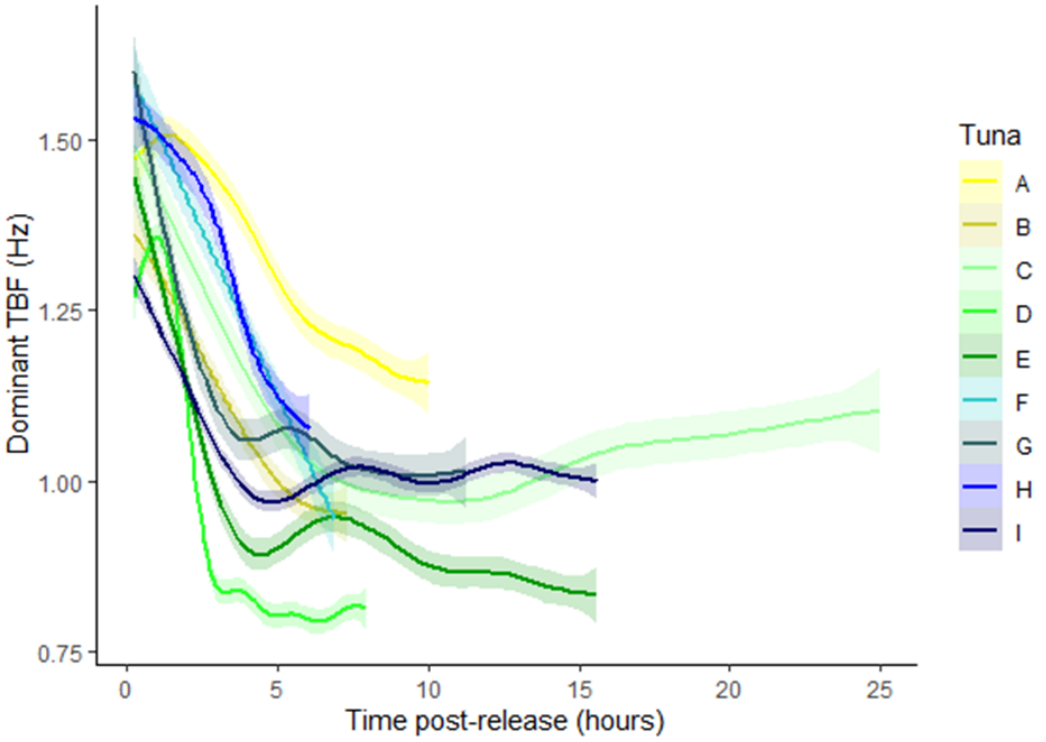

Figure 2.3: Dominant tailbeat frequency (TBF) over the entire deployment period for nine individual tuna (A – I). To better visualise the data, dominant TBF was represented by a single data point every 12.5 minutes and smoothed using a generalised additive model.

2.5. Discussion

We used high-resolution accelerometery and depth data to demonstrate the behavioural responses of ABFTs to C&R angling. Individuals tagged on deck descended rapidly (i.e., four-fold faster than subsequent descents) in the 20 seconds immediately after release, using 50 to 60% of the available water column, before gradually arresting their descent speeds and resuming horizontal swimming approximately 60 seconds post-release at a depth of 50 to 80 m. Thereafter, the ABFTs swam with an elevated TBF for 3 to 7 hours before activity levels stabilized. These patterns were relatively consistent between individuals but punctuated by some notable exceptions. For example, one individual obtained an eye injury, and another remained partially submerged during the handling process, with both exhibiting slightly different depth patterns than other ABFTs. Additionally, the individual with the longest time on deck may have suffered mortality.

The initial seconds post-release provided the first opportunity for the ABFTs to ventilate their gills after an anaerobic event and to metabolize waste products such as lactate, which may have accumulated during the fight time and on deck or aside vessel (Arends et al. 1999, Cooke & Suski 2005, French et al. 2015). The rate of vertical ascent should be a strong determinant of total gas and heat exchange, given ABFTs are obligate ram ventilators, and so could be an important initial period of reoxygenation and heat exchange. Gleiss et al. (2019) found ABFTs use gliding

descents upon release thought to agree with Weihs' two-stage locomotion model allowing conservation of energy on descents during gravity-assisted locomotion (Weihs 1973). However, during the first 60 seconds post-release the ABFTs used between 66% and 98% of the available water column, and while ABFTs are negatively buoyant, the descent was powered by intermittent locomotion despite a marked increased locomotor effort thought to not be needed to overcome the hydrostatic force of a gas bladder during depth changes of ABFTs (Gleiss et al. 2019). The extent to which this initial powered descent represents an 'escape' or 'stress' response (e.g., triggered by adrenaline production) versus a recovery from anaerobic exercise could be an important question for future work and to identify lower limits of water depth over which ABFTs can be safely released.

As with the relatively similar responses of ABFTs in the first minute after release, there was a strikingly consistent pattern of TBF being approximately 50% higher post-release than TBFs reached 5 to 10 hours later. While TBF for some of the shorter deployment durations seemed to still be declining when the biologging tags detached from the animal, the first 5 to 10 hours post-release is characterized by higher activity levels and increased mechanical output, with potential baseline activity levels reached thereafter. While we do not have data extending beyond 25 hours, a previous study from the east Atlantic (Gleiss et al. 2019) showed similar trends of TBF to our study with tailbeat frequencies remaining elevated for several hours post-release (approximately ≥1.5 Hz) and gradually declining to <1 Hz some six hours post-release establishing a potential TBF baseline that was similar several days later. The physiological driver of this extended period of elevated activity is unknown, but has also been reported in sharks following a C&R event (Whitney et al. 2016), and will represent a large increase in energy expenditure of animals subjected to C&R compared with those that do not (since metabolic rate scales exponentially with swimming speed (Weihs 1973, Jacoby et al. 2015, Ryan et al. 2015).

A variety of C&R factors are known to influence fish fitness and mortality post-release (see Brownscombe et al. 2017, for a review). For example, common thresher sharks caught in recreational fisheries display significantly elevated lactate levels with increased fight time (Sepulveda et al. 2015), with air exposure also known to increase lactate and mortality levels (Lennox et al. 2015, Brownscombe et al. 2017, Mohan et al. 2020). Our study represented a simulated C&R event with experienced anglers that bring ABFTs to the boat quickly and efficiently. However, most ABFTs were assisted onto deck by using lip hooks, a practice that is often advised against for C&R fisheries, and briefly exposed to air during the tagging process prior to the hose being introduced to the mouth for irrigation (Danylchuk et al. 2008, Brownscombe et al. 2017). The one ABFT that was tagged in the water exhibited a slightly different depth response to other ABFTs, so it could be instructive to further explore the extent to which bringing ABFTs on deck influences subsequent behaviour and physiology. Further refinements in biologging techniques and addition

of sensors such as video cameras could also enhance detection of important post-release behaviours such as active resumption of feeding, which is indicative of good physiological status (Del Caño et al. 2021) after capture.

Developing species-specific guidelines can aid in the development of a sustainable C&R fishery for a species that is vulnerable to overexploitation. Our study demonstrated a notable similarity in initial depth use in the first minute post-release and a decline in dominant TBF several hours later. However, an individual hooked in the eye and an individual who remained partially submerged during tagging displayed different responses to other ABFTs in this study. These two exceptions could serve to motivate further exploration of how variations in C&R procedures influence subsequent welfare outcomes for ABFTs. With the number of C&R programmes of ABFTs in the north-east Atlantic likely to increase, careful monitoring of fishing techniques and the species-specific behavioural responses to C&R will help safeguard sustainable fishing of the commercially vulnerable and valuable ABFT.

3. Chapter 3 Regionally endothermic traits in planktivorous basking sharks *Cetorhinus maximus*.

Authors: Haley R. Dolton, Andrew L. Jackson, Robert Deaville, Jackie Hall, Graham Hall, Gavin McManus, Matthew W. Perkins, Rebecca A. Rolfe, Edward P. Snelling, Jonathan D. R. Houghton, David W. Sims, Nicholas L. Payne.

Author contribution: Overall conception by HRD, ALJ, EPS, JDRH and NLP. Fieldwork undertaken by HRD, NLP, RD and MWP. Histology analysis undertaken by HRD, NLP, GM and RAR. Data analysis undertaken by HRD, NLP and ALJ. Writing led by HRD, EPS and NLP with contribution from all authors. All authors read, edited and discussed the manuscript.

Status: This manuscript was published in July 2023 in *Endangered Species Research*. For inclusion in my thesis supplementary information in the published manuscript regarding musculature analysis and heat transfer coefficient modelling has been moved into the main text of Chapter 3.

3.1. Abstract

Few fast-swimming apex fishes are classified as 'regional endotherms', having evolved a relatively uncommon suite of traits (e.g., elevated body temperatures, centralised red muscle, and thick-walled hearts) thought to facilitate a fast, predatory lifestyle. Unlike those apex predators, endangered basking sharks *Cetorhinus maximus* are massive filter-feeding planktivores assumed to have the anatomy and physiology typical of fully ectothermic fishes. We combined dissections of stranded specimens with biologging of free-swimming individuals and found basking sharks have red muscle found medially at the trunk, almost 50% compact myocardium of the ventricle, and subcutaneous white muscle temperatures consistently 1.0 to 1.5°C above ambient. Collectively, our findings suggest basking sharks are not full ectotherms, instead sharing several traits used to define a regional endotherm, thus deviating from our current understanding of the species and questioning the link between physiology and ecology of regionally endothermic shark species. With successful forecasting of population dynamics and distribution shifts often improved by accurate physiological data, our results may help explain movement patterns of the species which could ultimately facilitate conservation efforts.

3.2. Introduction

Fast swimming is thought to be greatly facilitated in some groups of fish by anatomical and physiological traits that purportedly enhance sustained metabolic and mechanical power (Bernal et

al. 2003a). Several lineages of active predatory fishes (e.g., sharks and tunas), have evolved centralisation of the skeletal red muscle at the trunk, and other anatomical structures such as the *rete mirabile* heat exchanger, which limit conductive and convective heat loss (Carey et al. 1982). Consequently, these species tend to maintain their red muscle at temperatures above ambient and so are often referred to as 'regional endotherms' (Watanabe et al. 2015). Regional endotherms swim faster than similar-sized ectothermic fishes (Harding et al. 2021) and generally have elevated metabolic rates (relative to body mass (Payne et al. 2015)), with specialisations such as comparatively large gill surface areas and, often, thick-walled hearts that have a high proportion of compact myocardium (although some exceptions exist (Brill & Bushnell 1991)).

Several hypotheses attempt to explain the key ecological advantages of regional endothermy, including expansion of spatial and temporal thermal niches (Weng et al. 2005), faster cruising speeds (Watanabe et al. 2015, Harding et al. 2021), and enhanced environmental perception (Block & Carey 1985). The order Lamniformes contain the only regionally endothermic sharks described in the literature (Lamnidae and Alopiidae (Carey & Teal 1969, Bernal et al. 2001a, 2003a)). All are fast, high-performance, apex predators, so an intuitive link can be drawn between their shared anatomy, physiology, and ecology. The basking shark *Cetorhinus maximus* is a sister taxon to the predatory Lamnidae (Bernal et al. 2001a), is explicitly considered an ectothermic species (Bernal et al. 2001a, Watanabe et al. 2015, Ciezarek et al. 2016) and is a low trophic-level filter-feeder that specialises on zooplankton (Sims 1999, 2000). Nevertheless, their cruising swim speed (approximately 1.1 m s^{-1} (Sims 1999, 2000)) and migration speed (e.g., 9589 km in 82 days (Gore et al. 2008)), is more similar to that of regionally endothermic sharks than similarly sized ectothermic fish (Watanabe et al. 2015, Harding et al. 2021). Accordingly, there are both phylogenetic and behavioural reasons to suspect that basking sharks may exhibit anatomical and physiological traits more typical of 'regional endotherms' than full ectotherms.

Basking sharks are globally 'Endangered' (Rigby et al. 2021) and their anatomy and physiology is difficult to study because of the paucity of freshly dead specimens from strandings or accidental capture. Studying the physiology of very large free-swimming sharks is challenging with no direct internal temperature measurements ever made, to our knowledge, for free-swimming basking sharks. Accurate physiological data can inform robust predictions of population shifts and changes in distribution patterns under climate change (Kearney & Porter 2009), which may help refine future spatial conservation efforts. In this study, we combined opportunistic beach dissections with subcutaneous white muscle temperatures recorded from biologging tags to determine whether red muscle distribution, proportion of compact myocardium and body temperatures were more similar to regionally endothermic shark species or to their fully ectothermic counterparts.

3.3. Materials and Methods

3.3.1. Red muscle distribution and compact myocardium

In 2020, beach dissections were conducted in England on carcasses of two stranded male basking sharks measuring 3.8 m total length (TL) and 4.5 m TL (Specimens A and B, respectively). Logistical constraints and local government environmental health regulations prevented us from taking full transverse sections through the body of the sharks. Instead, 13 approximate half cross-sections were made on Specimen A and five from Specimen B. Images were taken of either the anterior or posterior side of the cross-sections. A three-dimensional reconstruction of skeletal red muscle distribution was created in Computer Aided Design software (Autodesk 3ds Max 2021, Autodesk Media and Entertainment) using images of whole animals, with red muscle position estimated throughout using images of cross-sections from Specimens A and B.

In 2021, hearts were collected from carcasses of a further two basking sharks stranded on the west coast of Ireland, comprising a 6.9 m TL female and a 4.8 m TL male (Specimens C and D, respectively). Hearts were extracted and kept on ice for <24 h before removal of chamber blood, and dissection and weighing of the ventricle's compact and spongy components. Because the ventricle's compact and spongy components were distinguishable by eye, the two tissues were dissected and individually weighed by digital scale.

3.3.2. Skeletal red muscle analysis

To confirm putative red muscle, ca. 5 × 5 × 10 cm muscle samples were taken from Specimen B at each half-transverse cross-section to allow for staining of succinate dehydrogenase (SDH), a mitochondrial-bound enzyme found in high abundance in oxidative muscle fibres, and hematoxylin and eosin (H&E) staining (Nachlas et al. 1957, Kielhorn et al. 2013). All muscle samples were initially frozen at -80°C prior to processing. A day later, sub-samples from each of these (measuring ca. 2 × 5 × 10 cm) were placed into 10% neutral buffered formalin and kept at 4°C until H&E staining. Remaining portions of samples were retained at -80°C until analysis.

Within 3 months of the stranding, samples measuring ca. 2 × 2 × 3 cm were taken from deep within the frozen muscle stored at –80°C of each transverse section. SDH staining is routinely conducted on freshly frozen tissue. Consequently, a protocol from Nachlas et al. 1957 was adapted to suit lower tissue quality. Samples of frozen tissue were defrosted allowing for tissue samples measuring ca. 0.5 × 0.5 × 0.5 cm to be cut with a scalpel rather than a cryotome. Sections were incubated in 0.2 mol L^{-1} phosphate buffer with nitro blue tetrazolium (NBT), menadione solution and 0.2 mol L^{-1} sodium succinate for 15 minutes at room temperature and 30 minutes at 37°C. After sufficient staining was observed, sections were gently rinsed in saline for three minutes, fixed in

10% formalin solution for 10 minutes and dehydrated in 15% ethanol for five minutes (Nachlas et al. 1957, Kroeger et al. 2020). A control sample was also placed in an NBT solution without the substrate and subjected to the same conditions and fixing protocol. Samples were placed on slides and imaged on an Olympus BX51 light microscope coupled to an Olympus DD73 camera.

Samples of white and putative red muscle measuring ca. 1.0 × 0.5 × 0.5 cm were taken for standard H&E staining (Humason 1979). Samples were dehydrated in a graded ethanol series, cleared in xylene, and then embedded in paraffin wax allowing 5 µm sections to be cut on a Leica RM2235 microtome. Sections were mounted on glass slides (SuperFrost®Plus, Menzel-Glaser, Germany) using glycerine mounting jelly. Sections were imaged once again on the Olympus BX51 with the DD73 camera. SDH and H&E staining confirmed red muscle fibre type due to the uptake of NBT stain and small size of fibres.

3.3.3. Body and ambient water temperature

A new electronic biologging tag package was deployed for body temperature measurements without the need for capture or handling for sensor attachment, reducing potential stress to the animal. Subcutaneous white muscle and ambient water temperature sensors (LAT1810S, accuracy of 0.02°C, Lotek Wireless Inc., Newmarket, ON, Canada) were engineered into the package under license from the Health Products Regulatory Authority of Ireland (#AE19136/P127), on four free-swimming basking sharks off the coast of Ireland in 2021. Tagged basking sharks measured between 5 and 8 m TL. The internal temperature sensor (200 mm flexible stalk with 70 mm bend relief) was deployed on free-swimming sharks using a custom-designed pole spear to insert the sensor with a titanium M-style dart (Wildlife Computers) no more than 10 cm into the white muscle, with sensor depths estimated between 5 and 7 cm below the subcutaneous layer. A galvanic timed-release link detached from the anchor line approximately 12 hours after deployment. Buoyancy and drag of the syntactic foam flotation (surrounding transmitters used to locate the tag post release; VHF transmitter model MM120, Advanced Telemetry Systems and Satellite Position Only Tag model 258, Wildlife Computers) forced the internal temperature sensor from the body upon release. Apart from the titanium dart that pierced the white muscle, sharks were not handled in any other way, and all four were seen feeding at the surface within minutes of tag deployment. Calibrated external ambient water temperature and subcutaneous white muscle temperature data were collected at 0.1 Hz and plotted against time in R Studio (R Development Core Team 2020).

3.3.4. Heat transfer coefficient model

To check for the contribution of thermal inertia to basking shark body temperature, we adopted an allometric relationship between body mass and heat-transfer coefficients to simulate how body temperature of large basking sharks should vary if they were a full ectotherm. We then compared those models to our measured basking shark data to help understand respective roles of body mass versus other potential mechanisms in determining body temperature of basking sharks relative to water temperature.

We adopted differential equations as described in Malte et al. 2007, Nakamura et al. 2020 and Watanabe et al. 2021:

$$\frac{dT_m(t)}{dt} = k\left(T_a(t) - T_m(t)\right) + \dot{T}0$$

where *k* is the whole-body heat transfer (°C sec^{-1} °C^{-1}), T_a is the ambient water temperature (°C) at time (t), T_m is the subcutaneous white muscle temperature (°C) at time (t) and $\dot{T}0$ is a temperature elevation term arising from heat production and retention (°C sec^{-1}).

Body weight (kg) of a 7.0 m TL basking shark was calculated as a length-weight relationship; W = aLb where W is weight (kg), a and b are species specific coefficients and L is total body length. The equation above was applied to a hypothetical ectothermic basking shark based on temperature data collected by 'basking shark 1', which measured approximately 7.0 m TL, as well as two ectothermic whale sharks *Rhincodon typus* of similar body size (approximately 7.0 m TL). Whale shark constant *k* estimates were taken from Nakamura et al. 2020, while basking shark fixed *k* estimates were assumed from an allometric plot of body mass and calculated *k* values from ectothermic and regionally endothermic fish species after we corrected for the scale bar errors present in the original Nakamura et al. 2020 publication. The term $\dot{T}0$ was assumed to be 0.0°C due to ectothermic sharks lacking the anatomical and physiological traits to retain body heat and because heat transfer models provide a better fit for ectothermic sharks without the term included (Nakamura et al. 2020). Model sharks were assumed to have the same starting muscle temperature as 'basking shark 1'. An ODE solver model ['deSolve' (Soetaert et al. 2010) and 'tidyverse' (Wickham et al. 2019) packages in R Studio (R Development Core Team 2019)] that minimized the fit of *k* and $\dot{T}0$ by using Nelder-Mead optimisation to minimize the fit of the squared residuals over time to produce hypothetical ectothermic subcutaneous white muscle temperatures.

3.4. Results

3.4.1. Red muscle distribution and compact myocardium

Beach dissections of Specimens A and B confirmed musculature type (Figure 3.1) and revealed basking shark red muscle was not distributed laterally along the trunk, but rather extended from the vertebrae to the edge of a subcutaneous layer of connective tissue (Figure 3.2A). Within this connective tissue, and near the lateral extents of red muscle, there appears a paired small artery and large vein (Figure B.1). The red muscle then becomes increasingly lateral towards the caudal fin (Figure 3.2A).

Ventricles from Specimens C and D were thick-walled, both having 47% compact myocardium (Figure 3.2B).

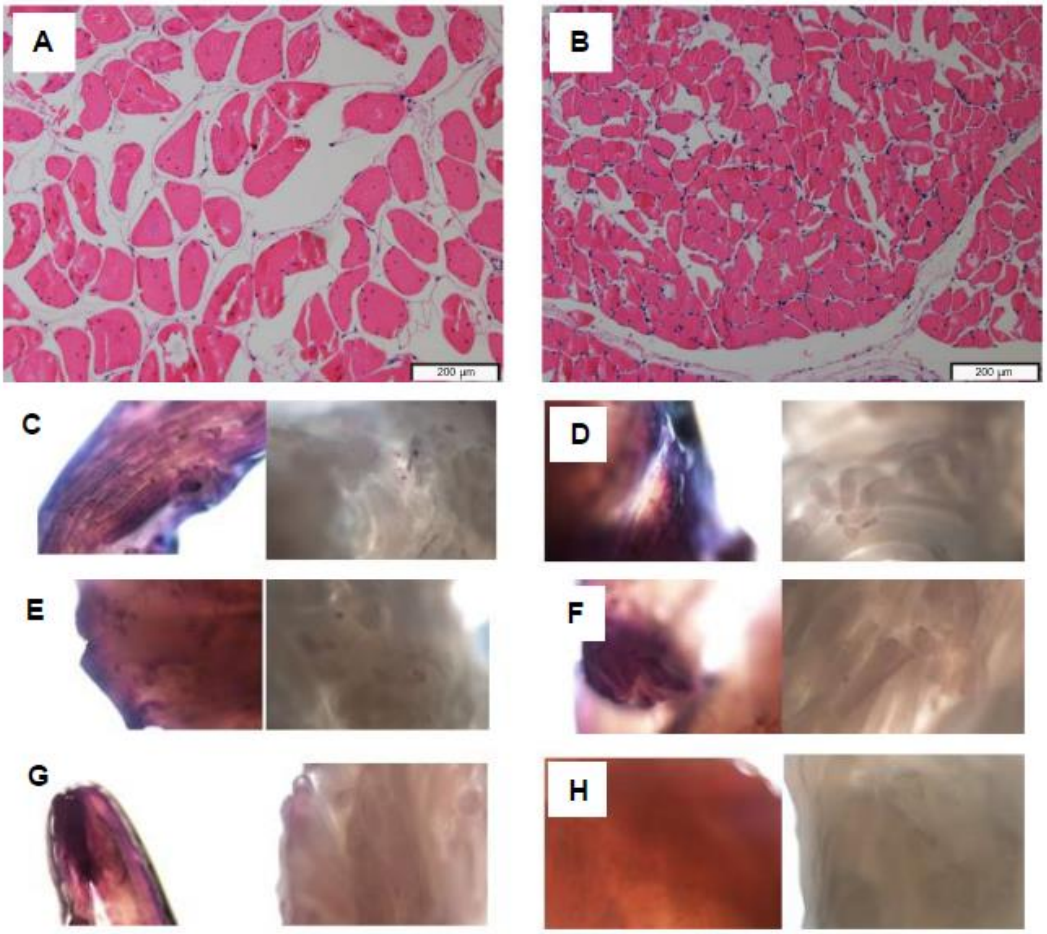

Figure 3.1: Histological staining of red and white muscle in basking sharks. (A) Hematoxylin and eosin staining of white muscle and (B) red muscle, where the fibres are stained pink and nuclei are stained blue. (C – G) Nitro blue tetrazolium staining of red and white fibres from each transverse section collected from specimen B; location also show by the white curved horizontal lines on the dorsal profile of Figure 3.1A. Nitro blue tetrazolium stains for the mitochondrial enzyme, succinate dehydrogenase, which is abundant in oxidative fibres, and thus a dark blue stain is produced in red muscle fibres and a sparse speckled stain in white muscle fibres. (H) Control sample for nitro blue tetrazolium stain was also taken from Specimen B.

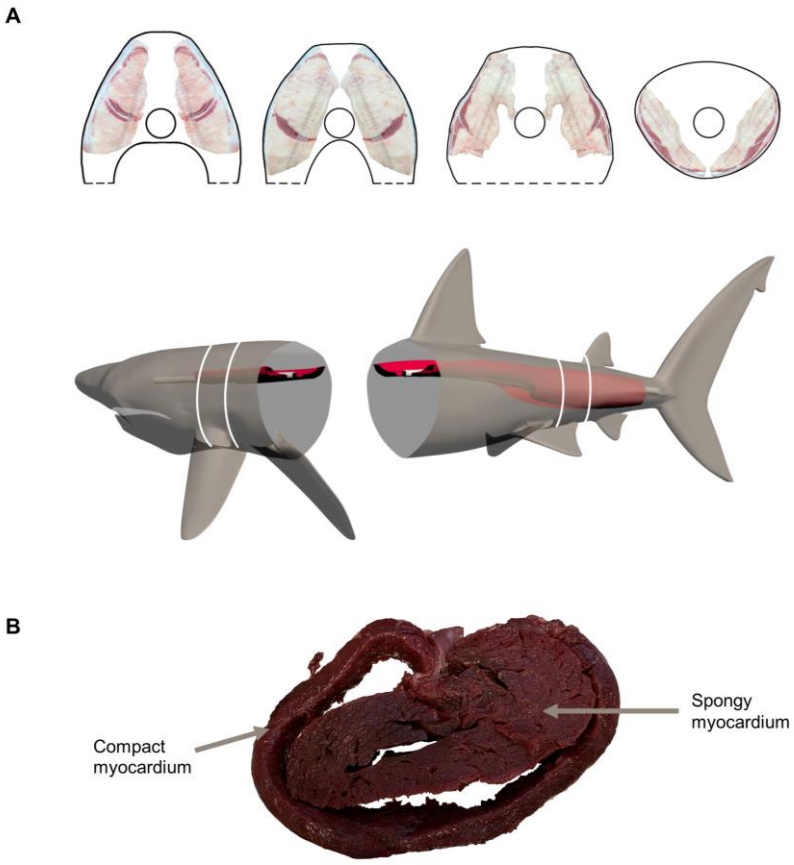

Figure 3.2: Anatomical measurements of red muscle distribution and compact myocardium in basking sharks. (A) Anterior to posterior red muscle distribution taken from transverse sections of Specimen A at positions indicated by the white curved vertical lines on the shark. Photographs of transverse sections are incomplete half sections that have been mirrored to aid visual representation (we have not extrapolated distribution anteriorly or posteriorly beyond the extents of our cross-section samples). (B) Ventricular cross-section showing the outer compact separated by inner spongy myocardium, taken from the atrioventricular junction of Specimen C.

3.4.2. Body and ambient water temperature

Biologging data showed that subcutaneous white muscle temperatures of free-swimming basking sharks (n = 4) were consistently 1.0 to 1.5°C higher than ambient water temperature for all four individuals across the 6 to 12 hours biologging deployments, with gradual declines in body temperature appearing to follow similar general declines in water temperature for three sharks (Figure 3.3A, Figure 3.3B).

3.4.3. Heat transfer coefficient model

Modelled subcutaneous white muscle temperature of a hypothetical fully ectothermic basking shark (Figure 3.4) steadily declines toward ambient water temperature over the duration of

deployment, whereas measured subcutaneous white muscle temperature remains consistently elevated above that of ambient for the entire duration of deployment (Figure 3.3B).

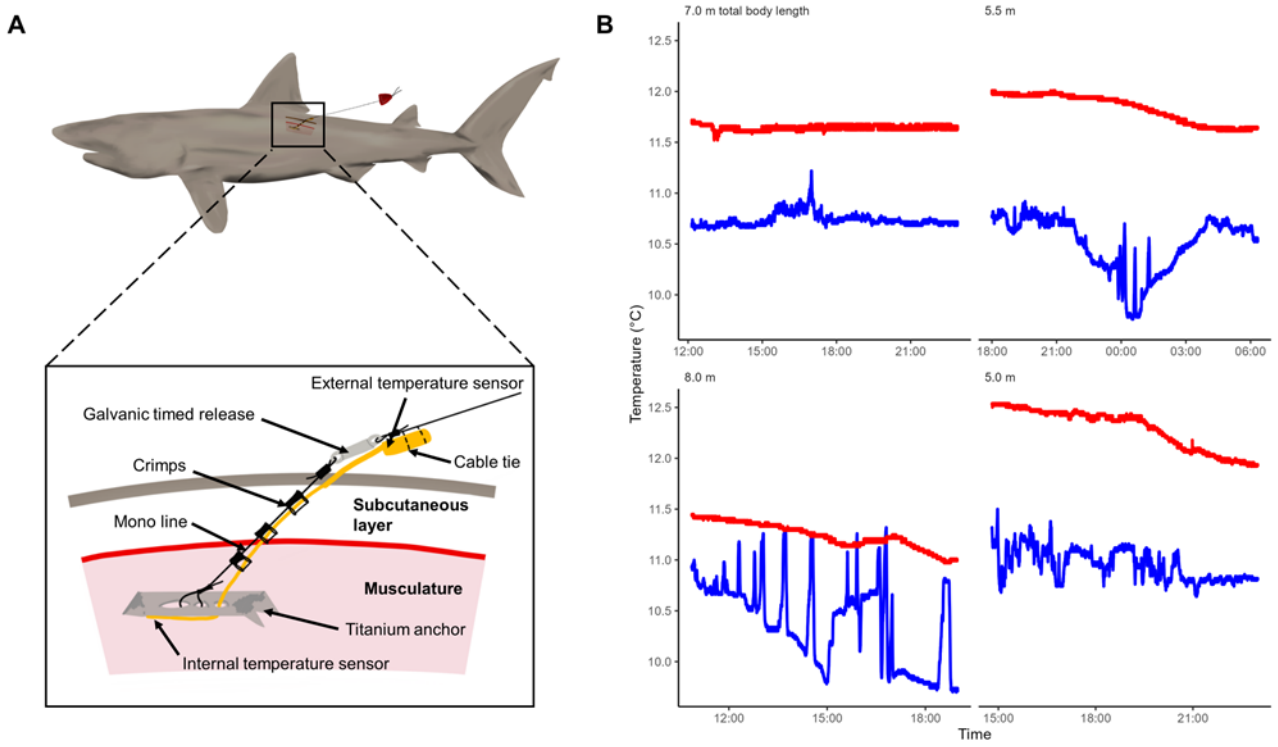

Figure 3.3: Biologging tag package and subcutaneous body temperature in free-swimming basking sharks. (A) Titanium anchor deployed into white muscle (between 5 to 7 cm under the subcutaneous layer) below the dorsal fin with a biologging device recording temperature (LAT1810S), and a towed float recovery package (shown in red behind the shark's dorsal fin) consisting of a VHF transmitter (model MM120, Advanced Telemetry Systems) and a satellite position only tag (model 258, Wildlife Computers). (B) Subcutaneous white muscle temperature (red lines) compared with ambient water temperature (blue lines) in four free-swimming basking sharks across entire deployment periods.

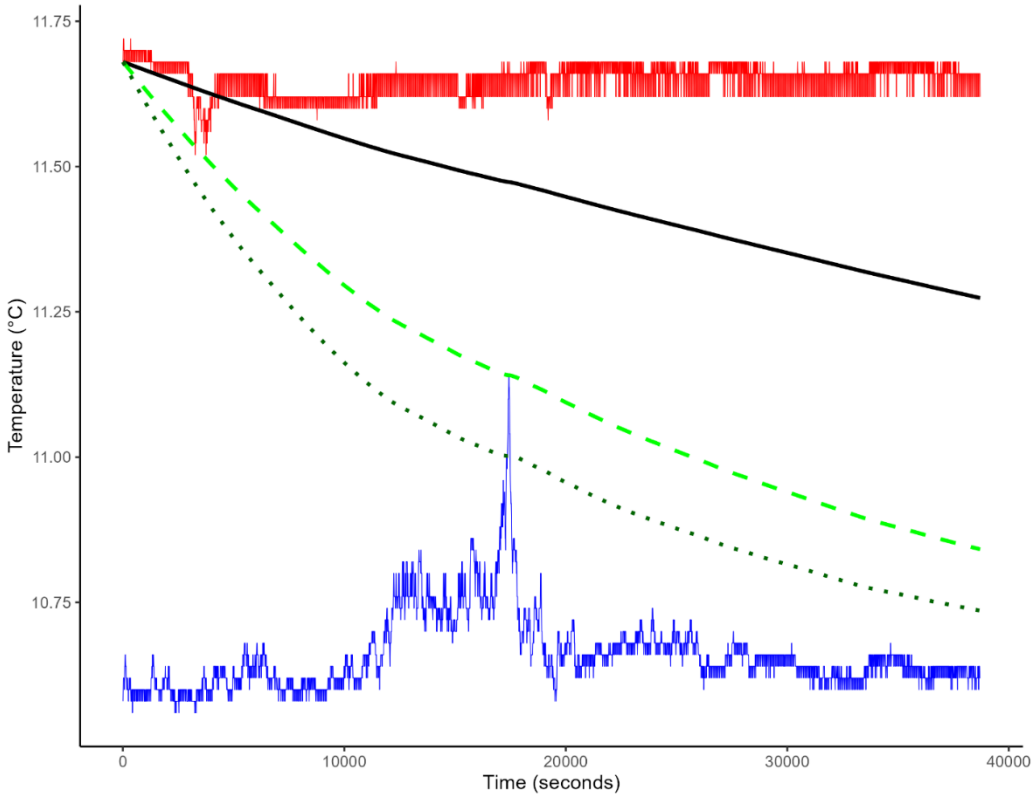

Figure 3.4: Measured basking shark subcutaneous white muscle temperature and modelled hypothetical ectothermic sharks of a similar body size. Red and blue lines represent measured subcutaneous white muscle temperature and ambient temperatures collected by 'basking shark 1', respectively. The black line, dashed light green line and dotted dark green line represent a modelled hypothetical fully ectothermic basking shark as well as two whale sharks (7.0, 7.0 and 7.2 m total length), respectively.

3.5. Discussion

While the proportion of red muscle could not be investigated in this study due to logistical constraints at dissections, its location in basking sharks is nonetheless more medial than in typical ectothermic species, such as the blue shark *Prionace glauca* and leopard shark *Triakis semifasciata* (Bernal et al. 2003a), which have most red muscle immediately beneath the subcutaneous layer. Basking shark red muscle does not form a cylindrical band adjacent to the vertebral column as seen in regionally endothermic salmon shark *Lamna ditropis* and shortfin mako shark *Isurus oxyrinchus* (Bernal et al. 2003a), however, there appears to be a paired small artery and large vein within the connective tissue of the basking shark, near the lateral extents of the red muscle; traits shared with regionally endothermic shortfin mako and white sharks *Carcharodon carcharias*, whose vessels then branch inwards towards the vertebrae to form the heat-exchanging rete (Carey et al. 1982).

Basking shark ventricles had an average 47% outer compact myocardium. Presence of well-developed compact myocardium is thought to facilitate higher blood pressures and blood flows, augmenting the uptake of oxygen across the gills and its offloading at the tissue, particularly the aerobic red muscle. It is often, but not exclusively, found in active, high-performance swimmers that ram ventilate (Brill & Bushnell 1991). Accordingly, highly active regional endotherms tend to have large proportions of compact myocardium, similar to basking sharks. For example, shortfin mako and white sharks have 36 and 42% compact myocardium respectively (Farrell & Smith 2017), and Pacific mackerel *Scomber japonicus* and Atlantic bluefin tuna *Thunnus thynnus* have approximately 40% (Brill & Bushnell 1991, Farrell & Smith 2017). In contrast, the vast majority of fish species have almost no compact myocardium at all (ca. 80%; Santer & Greer Walker 1980) and those that do generally have less of it. For example, the massive planktivorous and ectothermic whale shark has only 3% compact myocardium (Hirasaki et al. 2018). Nonetheless, some fully ectothermic and apparently less-active species also have high proportions of compact myocardium (e.g., common carp *Cyprinus carpio* (Brill & Bushnell 1991)), so it cannot be used as a clear distinguishing feature, but the regionally endothermic sharks examined to date all have a high percentage of compact myocardium (Emery et al. 1985, Bernal et al. 2003b, Farrell & Smith 2017, Hirasaki et al. 2018).

Biologging data showed that subcutaneous white muscle temperatures of free-swimming basking sharks were consistently 1.0 to 1.5°C higher than ambient water temperature. A temperature elevation of this magnitude in this location is similar to that reported for regionally endothermic shortfin mako shark (approximately 1.0°C elevation (Carey & Teal 1969)), and much greater than that of similarly sized – but fully ectothermic – whale sharks that showed no measurable elevation (Nakamura et al. 2020). Therefore, it is plausible that the deeper white and red muscle of basking sharks will be even warmer closer to the vertebrae, as reported in regionally endothermic sharks; for example, salmon shark *Lamna ditropis* subcutaneous white muscle is 1 to 2°C warmer than ambient, whereas its centrally-located red muscle can be more than 15°C warmer (Bernal et al. 2005). It is possible that the elevated subcutaneous body temperature of basking sharks arise in part from their large body size and associated thermal inertia; however the lack of consistent subcutaneous muscle temperature elevation above ambient water of the whale shark (Nakamura et al. 2020), that can reach lengths of 18 to 20 m, suggest this is unlikely the sole explanation for our results. Furthermore, heat-transfer models show ectothermic sharks exhibit subcutaneous body temperatures that converge toward ambient water temperature, just at slower rates for larger species (Nakamura et al. 2020, and results presented in this paper). In contrast, endothermic fishes at constant water temperature have a consistently elevated body temperature (as our basking shark data show) due to the greater contribution and retention of metabolic heat not seen in fully ectothermic species (Malte et al. 2007). Whether caused by large body size,

structures such as *rete mirabile*, or other phenomena, our data show basking sharks have consistent subcutaneous body temperature elevations that are similar to those seen in regional endothermic sharks and quite different to those seen in other large – but ectothermic – shark species.

When viewed collectively, our anatomical and physiological results show planktivorous basking sharks should at least not be considered fully ectothermic, and arguably should be classified with the 'regional endotherms' based on three key traits – red muscle found medially at the trunk, thick-walled ventricle, and elevated subcutaneous body temperatures. This challenges the current understanding that this collection of traits is confined to active, apex predatory fishes at high trophic levels; planktivorous basking sharks are therefore an exception in that respect. Notwithstanding, these findings may help reconcile their close phylogenetic placement to other regionally endothermic shark species (Bernal et al. 2001a), previous observations that basking sharks cruise at speeds (approximately 1.1 m s^{-1} (Sims 1999, 2000)) that are more similar to regionally endothermic fishes than their ectothermic counterparts (approximately 0.8 to 1.1 versus approximately 0.5 to 0.7 m s^{-1}, respectively (Harding et al. 2021)) and can undertake rapid, trans-oceanic movements (Gore et al. 2008) apparently at average speeds similar to those of regionally endothermic sharks (Watanabe et al. 2015). The basking shark is additionally unique among sharks in being an obligate ram filter-feeder that can occupy temperate waters (Gore et al. 2008, Johnston et al. 2022). The traits we report here could facilitate, in cooler water, the sustained mechanical power needed to overcome the regular and significant drag arising during ram filter-feeding at speeds averaging approximately 0.9 m s^{-1} (Sims 1999, 2000), while potentially preserving feeding efficiency (Paig-Tran et al. 2011).

Successful forecasting of population dynamics and distribution shifts is often improved by incorporating accurate physiological information (Kearney & Porter 2009). Globally 'Endangered' basking sharks (Rigby et al. 2021) can undertake long distance oceanic migrations in relatively short periods of time (82 days (Gore et al. 2008)) and can 'overwinter' in high and low latitudes (Sims et al. 2003, Witt et al. 2012, Doherty et al. 2017b, Dolton et al. 2020, Johnston et al. 2022). Taken collectively, the new anatomical and physiological insights provided here point toward basking sharks at least not being fully ectothermic and could help explain observed distribution patterns and refine estimates of how they may change in the future.

4. Chapter 4 Body temperature dynamics of regionally endothermic basking sharks

Authors: Haley R. Dolton, Andrew L. Jackson, David E Cade, Taylor K Chapple, Mason N Dean, David Edwards, Jeremy A. Goldbogen, Alexandra G McInturf, Edward P Snelling, Nicholas L. Payne.

Author contribution: Overall conception by NLP, ALJ, EPS and HRD. Fieldwork undertaken by HRD, NLP DEC, TKC, DE and AGM. Data analysis undertaken by HRD, NLP and ALJ. Writing led by HRD, EPS and NLP with contribution from all authors.

Status: This manuscript is *In Prep* for submission to the *Journal of Animal Ecology*.

4.1. Abstract

Regional endothermy has convergently evolved in several fish lineages. All currently described regionally endothermic sharks belong to the order Lamniformes with the largest bodied regionally endothermic species being the basking shark *Cetorhinus maximus*, which can measure up to 12 m in total length. As the first reported filter-feeding regional endotherm, basking sharks represent a unique biological system to explore dynamics of heat exchange in combination with such a feeding strategy, and in the largest regional endotherm reported to date. Through biologging and heat transfer coefficient (HTC) estimation, we show that basking sharks (n = 7; 5 to 8 m total length) consistently exhibit body temperatures elevated above ambient and rates of cooling faster than predicted for their given body mass, possibly due to their filter-feeding lifestyle. We also show subcutaneous white muscle temperature rapidly rises after acute increases in mechanical effort (e.g., burst swimming events) and subsequently cools approximately 100 times faster than normal HTC rates across most of the biologging timeseries. For the first time in the literature, our results provide an HTC estimate for a regionally endothermic extant filter-feeding shark species.

4.2. Introduction

Approximately 99.9% of all fish species are ectothermic (Carey et al. 1971, Block et al. 1993, Bernal et al. 2001a, Dickson & Graham 2004), with body temperature closely tracking ambient water. Most generated body heat of fish is assumed to be lost at the gills during respiration (Stevens & Sutterlin 1976, Carey & Gibson 1987). Several taxa (members of the tuna, shark and billfish families) have convergently evolved regional endothermy, the ability to both generate and retain body heat in certain tissues (Carey & Lawson 1973, Graham 1975, Graham & Dickson 2000, Bernal et al. 2001a, 2003a) via specialised anatomical traits such as aerobic red muscle found closer to the vertebrae and *rete mirabile*, a vascular counter current heat exchanger which transfers heat

generated by red muscle to cooler blood returning from the gills (Brill et al. 1994, Dickson & Graham 2004). Although metabolically expensive to generate and maintain muscle temperature above ambient (Bennett & Ruben 1979), regional endothermy is thought to confer advantages to fast, apex predatory fishes such as increased visual acuity, elevated cruising speeds and increasing the number of prey encounters (Block & Carey 1985, Watanabe et al. 2015, Harding et al. 2021).

The rate at which fish exchange body temperature can be modelled using a Heat Transfer Coefficient (HTC), which is derived from a coefficient of thermal conductance, *k* (typically measured as °C min^{-1} °C^{-1}), at which a fish's body (°C) exchanges heat with ambient temperature (°C) over time (t). Larger bodied fish typically have a lower *k* value, exchanging heat to the environment at a slower rate than smaller fish (Nakamura et al. 2020) due to established surface area to volume principles (Schmidt-Nielsen 1984). However, most studies of HTC have focused on comparatively small fishes, or large ectothermic fish such as the whale shark *Rhincodon typus* (Stevens & Fry 1970, Spigarelli et al. 1977, Fechhelm & Neill 1982, Malte et al. 2007, Nakamura et al. 2020). The rate of heat exchange of fishes can be influenced by both physiological and behavioural regulation, potentially allowing for exploitation of resources found in productive colder waters (Dewar & Graham 1994, Bernal et al. 2001b). For example, ectothermic fishes such as the whale and scalloped hammerhead shark *Sphyrna lewini* are able to exploit similar resources through large body sizes and 'breath holding' to reduce convective and conductive heat loss, respectively (Nakamura et al. 2020, Royer et al. 2023), albeit for shorter periods of time than regionally endothermic sharks. For example, the regionally endothermic salmon shark *Lamna ditropis* can spend months at <6°C due to their specialised physiology, whereas the whale shark has been recorded at temperatures of 4°C for no longer than one hour (Carlisle et al. 2011, Nakamura et al. 2020).

Basking sharks *Cetorhinus maximus* are the largest regionally endothermic shark species currently described in the literature, with a ram filter-feeding life history and tagged individuals experiencing ambient temperature ranges of 6.8 to 27.4°C (Johnston et al. 2022, Dolton et al. 2023). This species can physiologically retain generated body heat, likely due to the presence of anatomical structures such as medial to lateral red muscle distribution at the trunk of the shark. The aerobic medial red muscle used for sustained behaviours is likely the main source of metabolic heat production in Lamnidae (Bernal et al. 2001a), with steady swimming in the regionally endothermic shortfin mako shark *Isurus oxyrinchus* for example, increasing red muscle temperature within a laboratory setting by 0.3 to 3.0°C above ambient (Bernal et al. 2001b). Ram filter-feeding is a sustained behaviour displayed by basking sharks whereby the large drag associated with feeding at speeds of approximately 0.9 m s^{-1}, is likely overcome by increasing mechanical effort (Sims 1999, 2000, Cade et al. 2020). An increase in mechanical effort will be associated with increases in body temperature of all living things due to increased metabolic rate. However, the rate at which this

heat is exchanged with the environment for a large, ram filter-feeding regional endotherm is unknown.

The use of biologgers such as accelerometers that record tri-axial acceleration body movement, has allowed researchers to collect body movement data from large, free-swimming sharks that cannot be held in a laboratory setting. When body movement data is combined with internal temperature sensors, it is possible to assess whether increases in mechanical effort are associated with musculature temperature change. For example, burst events of free-swimming shortfin mako sharks led to increases in white muscle temperature within 12.5 minutes of an increase in mechanical effort (Waller et al. 2023). In this study we aimed to collect subcutaneous white muscle temperature and body movement data from free-swimming basking sharks to explore patterns in heat exchange. Specifically, we aimed to calculate the HTC for the largest regionally endothermic fish recorded to date and assess whether basking sharks follow established cooling rates for fishes, as they are uniquely, the only currently described regionally endothermic ram filter-feeding shark.

4.3. Materials & Methods

4.3.1. Biologging deployments

A biologging package (package configuration A; Figure C.1) recording subcutaneous white muscle temperature (T_m (fish muscle temperature in °C)) and T_a (ambient water temperature in °C) was deployed as in Dolton et al. 2023 on free-swimming basking sharks. Briefly, Lotek temperature sensors (recording at 0.1 Hz) with flexible stalks (LAT1810S, accuracy of 0.02°C, Lotek Wireless Inc., Newmarket, ON, Canada) were deployed using a modified pole spear in 2021 on five basking sharks (sharks 1 to 5; for basking shark tagging metadata linking Chapters 3 and 4 see Table C.1) in Irish waters.

Biologging packages were developed in 2022 to record T_m and T_a (recording at 1 Hz) using Lotek temperature sensors (LAT1810ST, resolution of 0.02°C, Lotek Wireless Inc., Newmarket, ON, Canada), video (Techcam, resolution 720p, TechnoSmart Europe) and accelerometer data (PD3GT, Little Leonardo Corp., resolution 0.01 g, where g is acceleration due to gravity) recording at 20 Hz and depth data at 1 Hz (resolution 0.4 m). A steel baseplate (measuring approximately 11 x 6 cm) with a foam covering on the ventral side of the plate was used as a platform to attach the body of the temperature sensor, accelerometer and video biologgers. A steel frame attached to the end of a modified pole was used to secure the baseplate during deployment and allow force-transmission to a modified spear (package configuration B and C; Figure C.1B and C). The internal temperature sensor (200 mm flexible stalk with 70 mm bend relief) was either threaded alongside a monofilament line using heat-shrink electrical tape, which attached to a titanium M-style dart

(Wildlife Computers (package configuration B; Figure C.1B; shark 6)) or was threaded alongside a spearfishing tip, also using heat-shrink electrical tape (package configuration C; Figure C.1C; shark 7) at the anterior end of the baseplate. Electrical tape was not fully taught to allow the flexible stalk to be removed from the shark when the biologging package detached from the baseplate. Biologgers were held in place on the baseplate using electrical tape and cable ties. Package configurations B and C were deployed into the subcutaneous white musculature no more than 14 and 15 cm, respectively, with recorded subcutaneous musculature temperature estimated at musculature depth of approximately 6 and 13 cm, respectively. Musculature depth was estimated by measuring the length of the Lotek flexible stalk once in the package and assuming the steel plate was approximately flush to the body. Package configuration B was deployed at a slight angle at the base of the first dorsal fin, likely approaching a thick subcutaneous white layer seen in that location (Dolton et al. 2023), resulting in lower subcutaneous musculature temperature estimation depth.

A galvanic timed-release link held the package attached to the plate. After approximately 12 to 25 hours the link corroded and allowed the biologgers to detach from the steel plate as the package was positively buoyant. A second monofilament line attached to the biologgers and a syntactic foam float which contained an ARGOS satellite tag and VHF telemetry device. A 3 m painters' pole was used to deploy the tags from the bow of a fishing vessel after manoeuvring slowly adjacent to a shark swimming at the surface, in a process lasting less than approximately five seconds. Sharks were not handled or approached subsequently to deployment.

Tagging of basking sharks was conducted under license from the Health Products Regulatory Authority of Ireland (#AE19136/P127) on sharks measured between 5 and 8 m total length (TL).

4.3.2. Data analysis

Accelerometery and temperature data were analysed using Igor Pro 6.3 (WaveMetrics Inc., Portland, OR, USA) with the Ethographer package (Sakamoto et al. 2009), Matlab v2022a (The MathWorks Inc., Natick, Massachusetts, USA) and R Studio (R Development Core Team 2019).

Lotek LAT1810S and 1810ST tags were calibrated by the manufacturer pre-deployment. Post-deployment data when biologging tags were floating at the sea surface, allowed for calibration between the external and internal temperature sensors. The mean value of $\Delta T = T_m - T_a$ during the calibration period was subtracted from the T_m recording (-0.08, -0.01, -0.19, -0.02, -0.01, 0.01 and -0.05°C, for sharks 1 to 7, respectively).

Accelerometer data were initially processed in Matlab using custom scripts to correct for tag attachment angles on sharks using methods described in (Cade et al. 2021). Firstly, the manufacturer acceleration axes were changed to match axes used in scripts (right-hand orientation; x, y, z). Secondly, biologger orientation on the shark was corrected to shark orientation by using

periods of steady surface swimming whereby, assuming depth remains relatively consistent during surface swimming, the axes x, y, z, should equal 0, 0, 1 g, respectively. Thirdly, occasional tag slips on shark 7 were corrected during the import process as in Cade et al. 2021. Briefly, when tag slips occur on the animal, axes orientation rapidly flips, meaning the strongest tailbeat accelerations (g) occur on the z axis, for example, rather than the y axis (following the right-hand orientation). Data were sub-sampled to 10 Hz and general noise from tag vibration was filtered out using a lowpass filter of 2 Hz. Pitch and roll were calculated using the methods described in Cade et al 2021 (code available at https://github.com/wgough/CATS-Methods-Materials).

Data collected from temperature and acceleration biologgers were aligned in Igor Pro by subsampling acceleration data to 1 Hz and matching pressure data collected from Lotek and Little Leonardo biologgers. Video data from sharks 6 and 7 will form part of a future study and were subsequently excluded from analysis.

4.3.1. Heat Transfer Coefficient Modelling

We used empirically recorded body and ambient water temperatures to estimate the parameters of a heat transfer coefficient model (Malte et al. 2007, Nakamura et al. 2020, Watanabe et al. 2021):

$$\frac{dT_m(t)}{dt} = k\big(T_a(t) - T_m(t)\big) + \dot{T}0$$

where $T_a(t)$ and $T_m(t)$ are the empirically observed ambient and body temperatures (respectively) in °C over time (t), k is the whole-body heat transfer coefficient (°C sec^{-1} $°C^{-1}$) to be estimated from the model and data and $\dot{T}0$ is a temperature elevation term arising from heat production and retention (°C sec^{-1}) also to be estimated from the model and data.

The differential equation was integrated numerically using the lsoda method to estimate body temperature ($\widehat{T_m}$) at times corresponding to the empirical observations. Nelder-Mead optimisation was used to minimise the sum of the squared residuals of the model prediction to the empirical data ($\sum\big(T_m - \widehat{T_m}\big)$) by optimising the unknown parameters k and $\dot{T}0$ to a given dataset. Within the integration step, T_a values were estimated at temperature values between observed time points using linear interpolation. For individual shark 6, Nelder-Mead optimisation could not produce an accurate $\widehat{T_m}$ likely due to large temperature variations at the start of the model. Instead, a Broyden-Fletcher-Goldfarb-Shanno (BFGS) optimisation was used, which is less sensitive to initial datapoints used in estimations as gradients per calculation are produced to minimise the sum of the squared residuals. The ODE model estimation was conducted using the package 'deSolve' (Soetaert et al. 2010).

Total length of basking sharks was estimated in the field to the nearest 0.5 m by experienced field biologists and used in established length-mass relationships to estimate body mass (kg), which was plotted with *k* estimates, overlaid with comparative analysis of body mass and thermoregulatory strategy (ectothermic or regionally endothermic). The reproduced figure in this study has corrected for the scale bar errors present from the original Nakamura et al. 2020 publication.

4.4. Results

Seven free-swimming basking sharks were tagged between 2021 and 2022 with devices which recorded depth, T_m and T_a (sharks 1 to 5: Table 4.1), or with devices that recorded depth, T_m, T_a and acceleration data (sharks 6 to 7; Table 4.1). Package configuration differed from 2021 (sharks 1 to 5; Figure C.1A) and in 2022 to accommodate a stable platform to record body acceleration data (sharks 6 to 7; Figure C.1B and C.1C, respectively). Sharks experienced a T_a range of 9.5 to 16.5°C and T_m ranged from 10.9 to 16.6°C (Table 4.1; note the late summer deployment of shark 6 and associated higher T_a than in spring). The T_m of each individual shark remained consistently elevated above T_a (Figure 4.1; Figure 4.2; Figure C.2), with average T_m of sharks being 0.5 (shark 6) to 1.5°C (shark 5) warmer than T_a (Table 4.1). A fixed HTC model produced estimated *k* and $\dot{T}0$ values for each individual shark (Table 4.1; Figure 4.2) with *k* estimates generally higher than predicated for their mass (Figure 4.3). Estimates of model T_m were similar to the measured free-swimming basking shark T_m recorded during deployments (Figure 4.2; Figure C.2) with a notable exception of shark 7 whose T_m increased rapidly and frequently throughout the time series (Figure 4.1C).

The two sharks fitted with accelerometer sensors revealed several interesting patterns of rolling events over 40° (rolling left to right; Figure 4.1) occurring during descents and with associated periods of high mechanical effort (increase in dynamic tailbeat (g)). These events were approximately 1 to 2 minutes in duration (Figure 4.4; Figure C.3) with the greatest roll angle reached from shark 7 of approximately 140° (Figure 4.4D). In addition, a notable rolling event occurred between a narrow depth range of 0 to 7 m, with an increase in mechanical effort and rapid changes of pitch (from 30 to -45°) lasting for approximately four minutes (Figure 4.4A, B; shark 7). Temperature increased rapidly in subcutaneous white muscle of shark 7 after these periods of increased mechanical effort. Given the observed spikes in T_m seen for this animal, we also fitted our HTC model to a reduced dataset (approximately eight minutes after a large mechanical event, a triple breach; Figure 4.5) to estimate *k* of a cool down period after this discrete event. The reduced dataset of a powered descent after breaching, had approximately 100 times increase in *k* when compared to the whole timeseries (Table 4.1; Figure 4.5; $k = 4.3 \times 10^{-3}$; $k = 4.0 \times 10^{-5}$, respectively).

Table 4.1: Metadata and estimated temperature parameters from heat transfer coefficient (HTC) modelling. *Potential shallow internal temperature sensor placement.

Shark ID	Total length (m)	Tag set up configuration	Empirically recorded ambient temperature range (°C)	Empirically recorded subcutaneous white muscle temperature range (°C)	Temperature sampling frequency (Hz)	*k* (°C sec^{-1} °C^{-1})	$\dot{T}0$ (°C sec^{-1})	Root-mean-square deviation of model (HTC)
1	7.0	A	10.6 to 11.1	11.5 to 11.7	0.1	7.0×10^{-05}	6.8×10^{-05}	0.02
2	5.5	A	9.7 to 10.9	11.6 to 12.0	0.1	2.4×10^{-05}	2.6×10^{-05}	0.05
3	8.0	A	9.5 to 11.5	11.0 to 11.5	0.1	4.4×10^{-05}	3.1×10^{-05}	0.03
4	5.0	A	10.6 to 11.5	11.9 to 12.5	0.1	2.7×10^{-04}	3.5×10^{-04}	0.05
5	8.0	A	11.8 to 18.0	13.8 to 16.6	0.1	3.7×10^{-05}	2.9×10^{-05}	0.09
6*	7.5	B	10.5 to 10.8	10.9 to 11.3	1.0	8.2×10^{-05}	2.7×10^{-05}	0.05
7	7.0	C	9.9 to 12.5	11.9 to 12.7	1.0	4.0×10^{-05}	3.4×10^{-05}	0.06

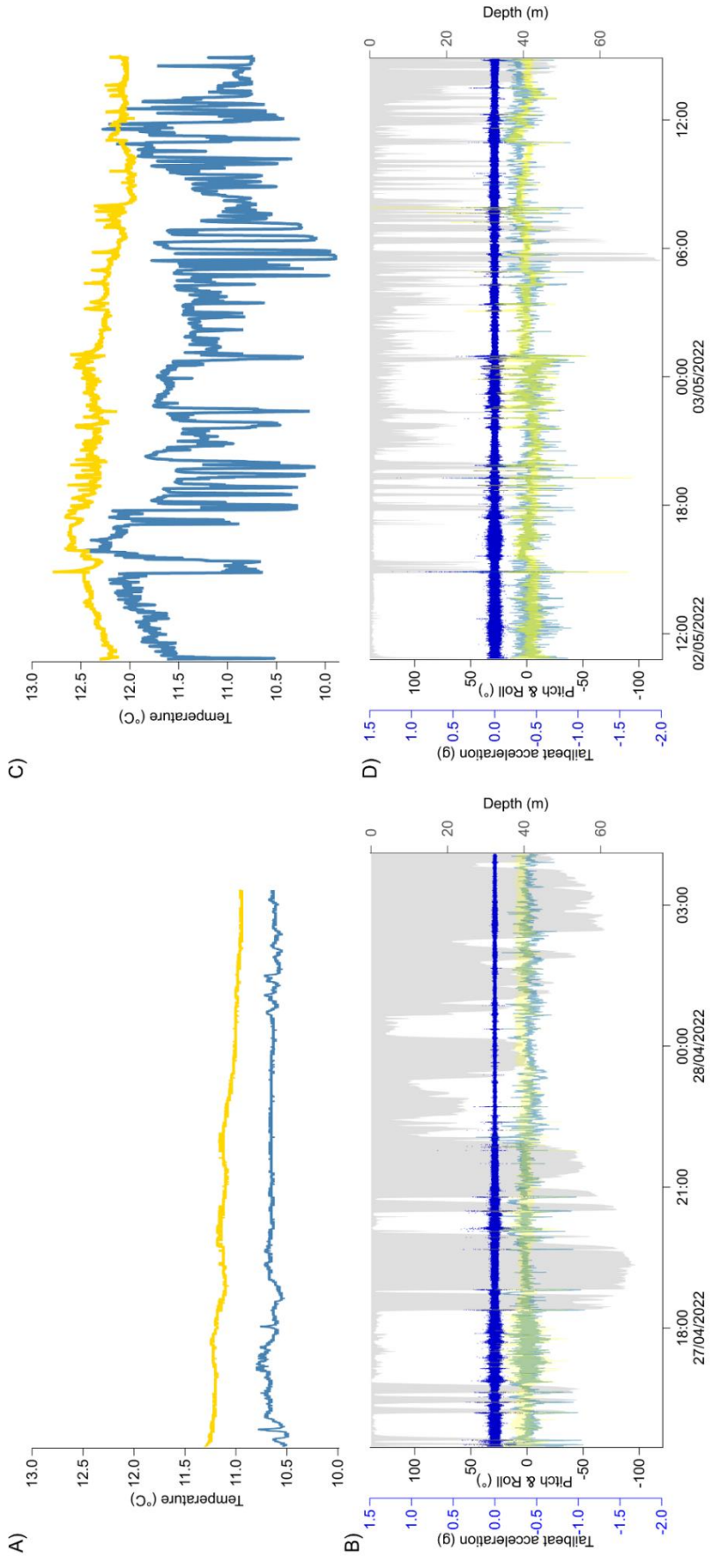

Figure 4.1: Temperature, depth and acceleration data from sharks 6 (A and B) and 7 (C and D). (A and C) Subcutaneous white muscle temperature (°C; gold line) and ambient water temperature (°C; steel blue line), respectively during the entire deployment period. (B and D) tailbeat acceleration (g; blue dots), pitch (°; teal line), roll (°; yellow line) and depth (m; shaded grey).

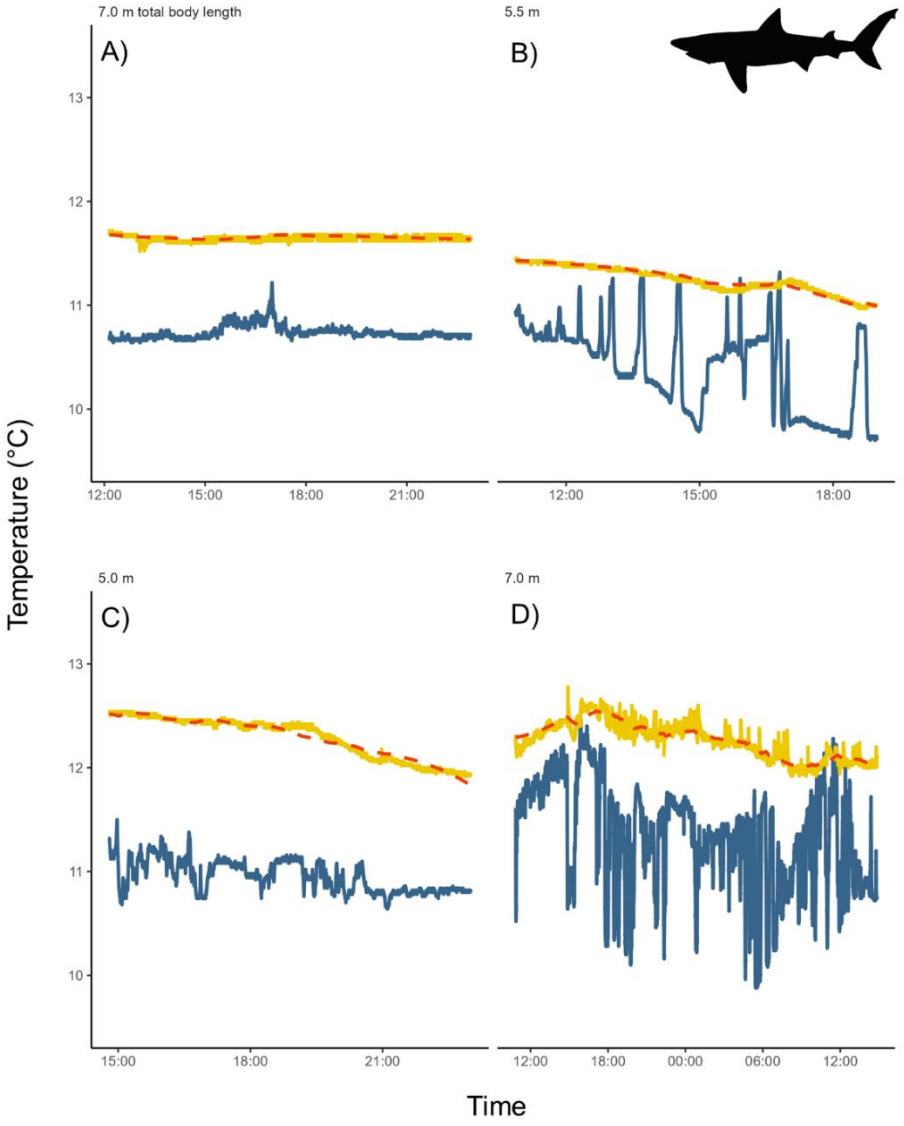

Figure 4.2: Entire time-series of water temperature, subcutaneous white muscle temperature and heat transfer coefficient estimates of four basking sharks. (A, B, C and D) subcutaneous white muscle temperature (gold lines) compared with fixed heat transfer coefficient model $\widehat{T_m}$ (orange dashed lines) and ambient water temperature (steel blue lines) in four free-swimming basking sharks (panels A, B, C and D are sharks 1, 3, 4 and 7, respectively).

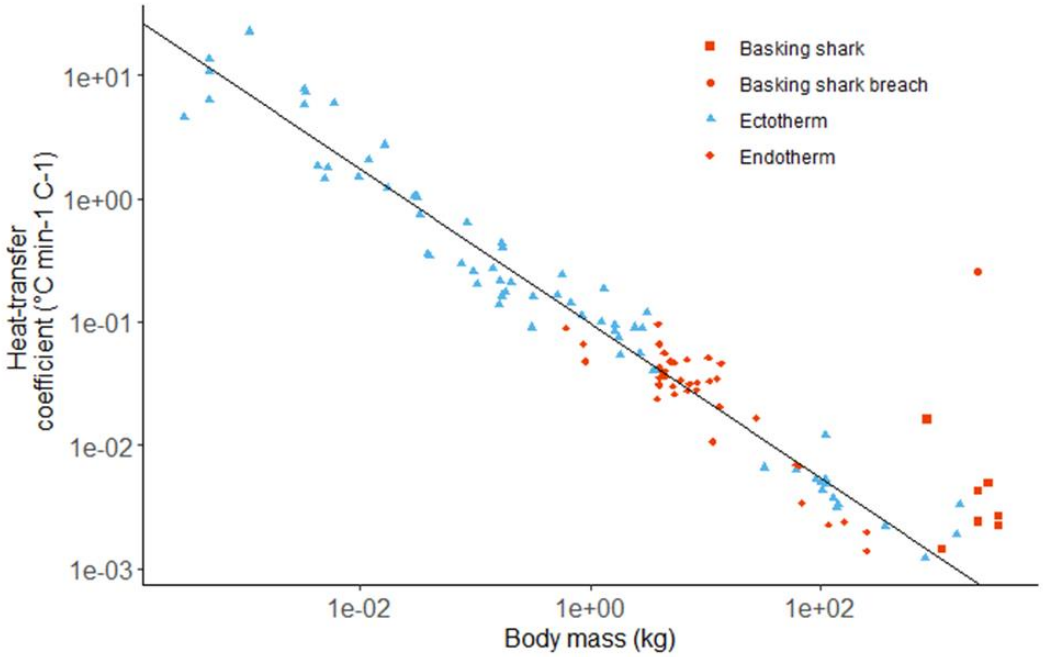

Figure 4.3: Relationship between body mass and heat transfer coefficient at cooling. Reproduced and modified from Nakamura et al. 2020. Relationship between body mass (kg) and heat transfer coefficients (°C min^{-1} $°C^{-1}$) at cooling from ectothermic fish (blue triangles), regionally endothermic fish (red diamonds). Fixed *k* estimates of regionally endothermic basking sharks are shown as red squares and a fixed *k* estimate after breaching is indicated by a red circle. The line through the data points was reproduced using the log intercept and slope given in Nakamura et al. 2020.

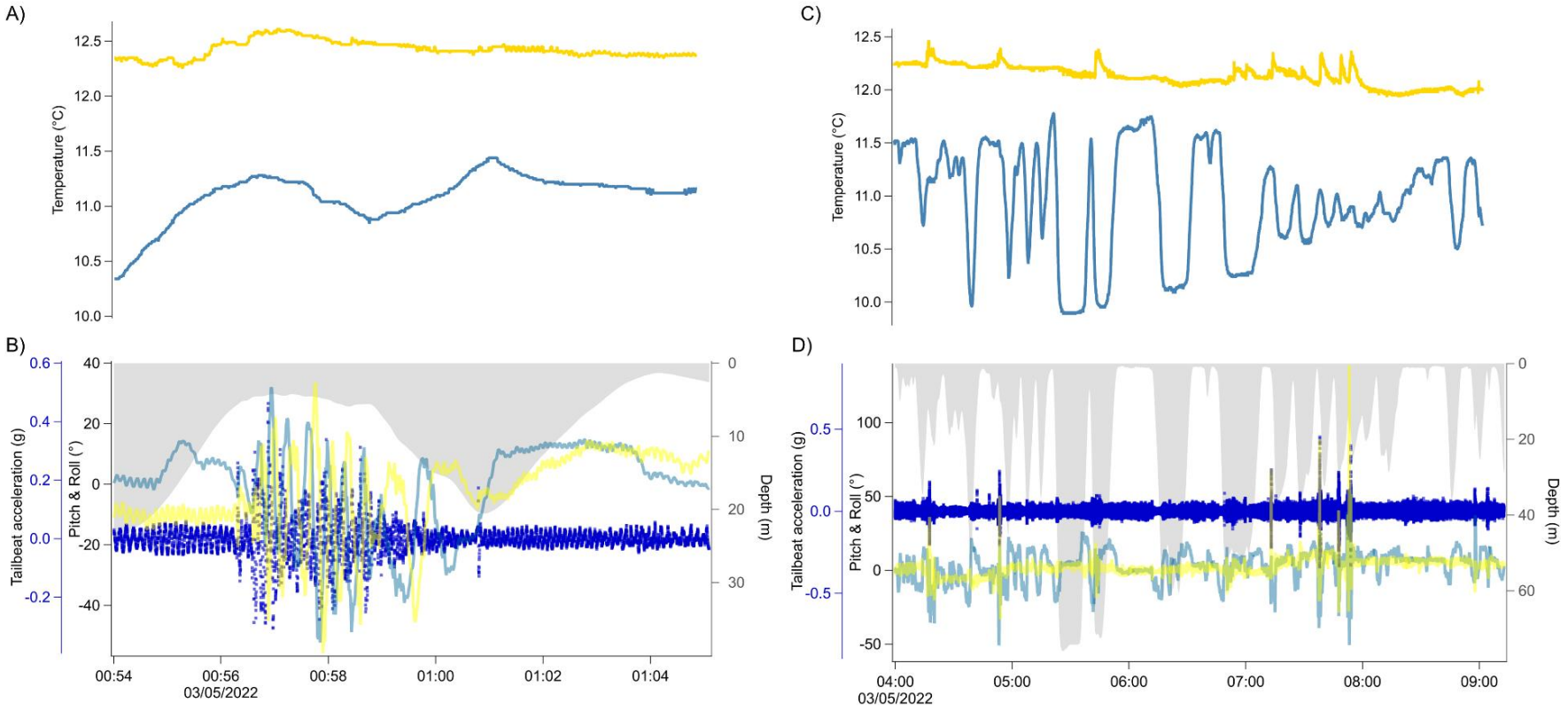

Figure 4.4: Time-series examples of increases in mechanical effort and associated subcutaneous musculature temperature increase from shark 7. (A and C) Subcutaneous white muscle temperature (°C; gold line) and ambient water temperature (°C; steel blue line). (B and D) Tailbeat acceleration (g; blue dots), pitch (°; teal line), roll (°; yellow line) and depth (m; shaded grey).

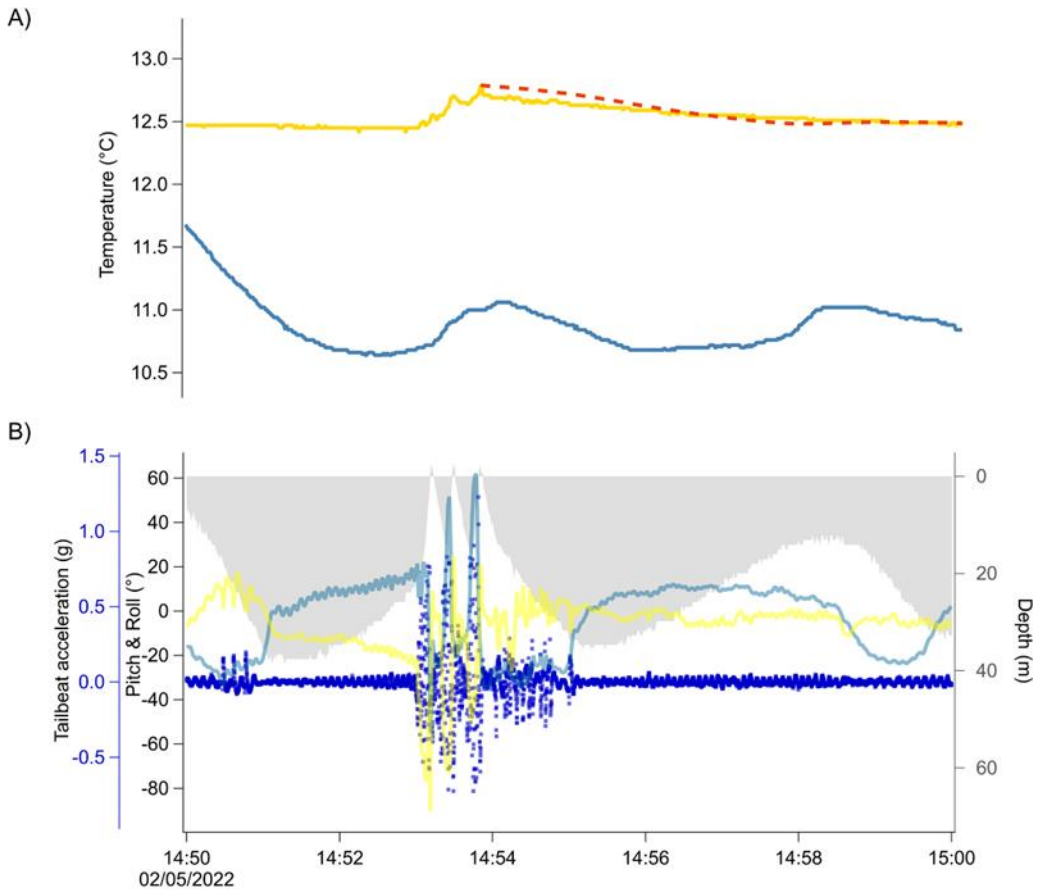

Figure 4.5: Subcutaneous white muscle temperature and heat transfer coefficient modelling of a cool down period after a triple breach event of shark 7. (A) Subcutaneous white muscle temperature (°C; gold line), ambient water temperature (°C; steel blue line) and fixed heat transfer coefficient model $\widehat{T_m}$ (orange dashed line). (B) Tailbeat acceleration (g; blue dots), pitch (°; yellow line), roll (°; teal line) and depth (m; shaded grey).

4.5. Discussion

Basing shark T_m was a minimum of 0.5°C and a maximum of 1.5°C above T_a. Inclusion of the heat generation term $\dot{T}0$ in the model was necessary to accurately predict the observed dynamics of body temperature change, which is unlike ectothermic shark species where $\dot{T}0$ drops out of HTC models due to a lack of anatomical traits for heat retention (Nakamura et al. 2020). The minimum T_m elevation of basking sharks is comparable to those of shortfin mako sharks whose minimum T_m taken from a musculature depth of approximately 5 to 6 cm, was 0.2°C above T_a (Waller et al. 2023). However, the maximum T_m of shortfin mako sharks was 4.0°C above T_a (Waller et al. 2023). Despite two of our T_m datasets being taken from a musculature depth of approximately 13 cm (implying a higher T_m due to thermal gradients of musculature (Q10) as seen in other regionally endothermic species (Bernal et al. 2005)), the larger difference between maximum T_m of shortfin mako sharks and basking sharks likely represents the differing dive behaviour displayed by each species during respective biologging deployments. For example, the shortfin mako sharks tagged in Waller et al. 2023 make rapid ascents and descents when compared to basking sharks in this study.

Consequently, shortfin mako sharks spent less time in water temperatures cooler than their T_m, with less time for exchange of heat.

Notwithstanding a consistently elevated body temperature above ambient, HTC estimates show basking sharks have fixed *k* values which are approximately an order of magnitude higher than predicted for their mass based on a comparative analysis of k_{cool} across 19 fish species (Nakamura et al. 2020). In ectothermic fishes the rate of heat loss at the gills is assumed to be equal to heat production (Brill et al. 1994). However, despite regionally endothermic fishes such as tuna and lamnids having a larger gill surface area than ectotherms (thought to facilitate a greater metabolic rate (Dewar & Graham 1994)), these fishes can still elevate T_m over T_a due to the presence of specialised structures such as rete (Dickson & Graham 2004). The fixed *k* estimates in this study include periods where basking sharks are heating and cooling, yet the *k* estimates are higher than predicted for their mass based on k_{cool} comparative analysis. This may represent an artefact of most sharks tagged in this study moving to cooler waters, which could cause T_m to decrease through convective and conductive heat loss (although T_m remains elevated above T_a). Or, because a ram filter-feeding life history might increase the bulk flow rate of water which is cooler than T_m over the gills.

Heat exchange at the gills also facilitates the recovery of oxygen after anaerobic, white muscle associated exercise (Dewar & Graham 1994, Royer et al. 2023, Waller et al. 2023), such as breaching behaviour observed in our data. The *k* estimate produced for a period after breaching was approximately 100 times higher than for the entire timeseries, with this period of rapid heat exchange potentially facilitated by the opening of the mouth and gill arches, exposing the lamellae to cooler water than T_m. Additionally, because breaching behaviour is powered by white muscle, which is distributed more laterally than red muscle, the generation of body heat from anaerobic exercise could possibly facilitate conductive heat loss across the body. The higher *k* value estimated after breaching also occurred during a powered descent made by the basking shark, which would have produced additional metabolic heat likely from the white muscle. To facilitate cooling during this powered descent, shunting of blood to the gills could occur as postulated for regionally endothermic lamnids and tunas (Carey et al. 1971), whilst not affecting oxygen binding affinity and gas exchange as seen in other regionally endothermic sharks (Morrison et al. 2023).

Despite basking sharks having a higher *k* estimate than predicted for their mass, rapid T_m elevations occur throughout the time series of shark 7. These acute increases in T_m were associated with an increase in mechanical effort. Similar rapid T_m elevations have also been recorded in free-swimming regionally endothermic shortfin mako sharks (Waller et al. 2023) and in ectothermic shark species (Harding et al. 2022). For example, the T_m of blue sharks *Prionace glauca* increased by 0.6°C to 2.7°C immediately following exhaustive exercise during capture, however body

temperature subsequently converges towards T_a within 30 minutes (Harding et al. 2022). This is comparable to basking shark T_m, which although remains consistently elevated above ambient, returns to pre-burst T_m within approximately eight minutes of a triple breaching event which lasted approximately one minute in duration. This rate of heat exchange after bursting behaviour of basking sharks is comparable to body temperature increase and decrease of shortfin mako sharks displaying similar increases in mechanical effort. For example, a bursting event lasted approximately 10 minutes and rapidly increased T_m, with T_m subsequently returning to pre-burst T_m within approximately 15 minutes (Waller et al. 2023).

Periods of acute temperature increase after bursting behaviours represent a high metabolic cost, which ultimately has to be repaid through acquisition of large, infrequent prey, or in the case of the basking shark, more abundant zooplankton. Indeed, although regional endothermy and its associated metabolic costs have been cited as one of the main contributors to the extinction of another massive and suspected regionally endothermic sharks such as the megatooth shark *Otodus megalodon* (Pimiento et al. 2017, 2019, Ferrón 2017), basking shark feeding ecology may provide the species with a metabolic advantage over extant, large, regionally endothermic, apex predatory sharks as their prey can currently be frequently encountered in the north-east Atlantic (Pimiento et al. 2019, Strand et al. 2020). Research on prey density for the massive ectothermic whale shark provides evidence of a filter-feeding life history having a low mass specific metabolic cost as the density of prey required to recover metabolic costs of foraging are low (Yowell & Vinyard 1993, Cade et al. 2020). However, a metabolic estimate for large, regionally endothermic, filter-feeding sharks has not been investigated. Future research should investigate the metabolic costs associated with regional endothermy and a filter-feeding life history where an increase in drag to feed at speed (Sims 1999, 2000) has to be overcome.

Our study shows basking sharks cool faster than expected for their body mass, possibly due to a filter-feeding life history. With the metabolic cost of free-swimming, regionally endothermic sharks largely understudied due to their size and rarity, it is difficult to assess how such species may respond to a changing environment (Waller et al. 2023). However, despite basking sharks maintaining their T_m above ambient, we show they cool faster than expected for their body mass. It is possible basking sharks have a high metabolic rate as predicted for regionally endothermic fish or possess other anatomical traits such as rete that enable T_m to remain above T_a. Additionally, if future research can accurately estimate the metabolic cost of this filter-feeding shark given the now known thermophysiology of the species, it could aid in the designation and protection of important feeding areas for basking sharks.

5. Chapter 5 Centralised red muscle in the smalltooth sand tiger shark *Odontaspis ferox* and the prevalence of regional endothermy in sharks

Authors: Haley R. Dolton, Edward P. Snelling, Robert Deaville, Andrew L. Jackson, Matthew W. Perkins, Jenny R. Bortoluzzi, Kevin Purves, David J. Curnick, Catalina Pimiento, Nicholas L. Payne.

Author contribution: HRD, JRB, KP and NLP collected samples in Ireland. HRD and NLP led the study conception and design. DC, RD and MWP arranged and collected samples in the UK. Material preparations were made by HRD. The first draft of the manuscript was written by HRD and NLP. All authors commented on previous versions of the manuscript. All authors read and approved the final manuscript.

Status: This manuscript is published in November 2023 in *Biology Letters* as a short correspondence (as results need to be discussed in the context of regional endothermy evolution, the results and discussion have been combined). In this chapter, additional methods and text that do not appear in the main published manuscript have been included.

5.1. Abstract

The order Lamniformes contains charismatic species such as the white shark *Carcharodon carcharias* and extinct megatooth shark, *Otodus megalodon*, and is of particular interest given their impact on marine ecosystems, and that some members have evolved regional endothermy. However, there remains significant debate surrounding the prevalence and evolutionary origins of regional endothermy in the order, and therefore the development of phenomena such as gigantism and filter-feeding in sharks generally. Here we show an extant, more basal Lamniform shark (smalltooth sand tiger shark *Odontaspis ferox*) to have centralised skeletal red muscle and a high percentage of compact myocardium of the heart; anatomical features consistent with regional endothermy. These results, together with the recent discovery of regional endothermy in filter-feeding basking sharks *Cetorhinus maximus*, suggests that regional endothermy is more prevalent in Lamniformes than previously thought, which in turn has important implications for understanding evolution of regional endothermy, gigantism, and differential extinction risk of warm-bodied shark species both past and present.

5.2. Introduction

While at least 99.9% of fish species are ectotherms (Wegner et al. 2015), regional endothermy is a remarkable example of convergent evolution seen in several lineages of large-bodied fish taxa (Bernal et al. 2001a). Tunas and several families of sharks have evolved a suite of traits such as centralised red muscle, a high percentage of compact myocardium of the heart and

counter-current heat exchangers that facilitate elevated temperature of key tissues above that of ambient water (Bernal et al. 2003a). Regional endothermy is thought to facilitate competitive advantages in apex 'high performance' fishes, such as faster cruising speeds, longer migration distances over short periods of time, enhanced visual perception, and niche expansion (Block & Carey 1985, Dickson & Graham 2004, Watanabe et al. 2015, Harding et al. 2021). The maintenance of elevated temperature within key tissues is an evolutionary triumph in fishes over the convective and conductive avenues of heat transfer that would otherwise transfer heat from the body to cooler ambient water (Brill et al. 1994). This is especially impressive considering all blood is circulated through the gills of ram ventilators and comes in close contact with water.

In sharks, all known regionally endothermic species are found within the order Lamniformes (Bernal et al. 2003a). Of 15 extant Lamniformes, two species are confirmed to be ectothermic by examination of musculature, six species are confirmed regional endotherms by virtue of significantly elevated body temperature above that of ambient water, and seven species are unknown or commonly assumed to be ectotherms (Pimiento et al. 2019). Recently, the thermophysiology and evolutionary history of Lamniformes has received significant attention given ongoing uncertainty about the origins of regional endothermy and associated consequences for the development of gigantism, filter-feeding, and extinction drivers of enigmatic species. For example, the extinct megatooth shark, *Otodus megalodon*, was a 15 to 20 m (total length (TL) Perez et al. 2021, Sternes et al. 2023) macropredator, which undoubtedly held a high trophic position (McCormack et al. 2022) during the prehistoric Micocene to early Pliocene (Cooper et al. 2022). The true Lamniformes phylogeny remains debated, and whether or not the megatooth shark had regional endothermy is focus of a flurry of recent papers (Cooper et al. 2022, Sternes et al. 2023, Shimada et al. 2023), likely due to its gigantic size and likely impact on the evolution and ecology of marine ecosystems (Cooper et al. 2022). Several lines of evidence from the fossil record have been used to infer that megatooth shark probably exhibited regional endothermy (e.g., isotopic analysis, inferred swim speeds and energy budget estimation) but also that the high whole-body metabolic demands of being such a gigantic, regional endothermic macropredator partly contributed to its extinction (Pimiento et al. 2017, 2019, Ferrón 2017, Shimada et al. 2020). However, an extant massive filter-feeding lamniform, basking shark *Cetorhinus maximus*, was recently shown to be the largest regional endotherm recorded to date, with centralised red muscle and elevated white subcutaneous muscle temperature (Dolton et al. 2023). This finding conflicts with the general consensus that all regionally endothermic sharks are high trophic level macropredators, and that evolutionary pathways to gigantism in elasmobranchs (such as for the megatooth shark) were facilitated by *either* regional endothermy *or* filter-feeding (Pimento et al. 2019); in basking sharks it appears *both* regional endothermy *and* filter-feeding may have played a role. Filter-feeding basking sharks were widely assumed to be ectothermic, as are several other species in Lamniformes (Ferrón

2017, Sternes et al. 2023). Nevertheless, many extant members of the order are difficult to study given their distribution and low abundance, which raises the possibility that regional endothermy is, and was, more prevalent in the evolutionary history of Lamniformes than previously thought. Indeed, it has been proposed based on fossil evidence that red muscle regional endothermy is an ancestral trait that evolved early in Lamniformes (approximately 113 Ma; Pimiento et al. 2019), but the point remains debated. In this study, we first present new data showing that the smalltooth sand tiger shark *Odontaspis ferox* – an extant Lamniformes species with a fossil record that goes as far back as late Oligocene (Mitchell & Tedford 1973) – exhibits anatomic features characteristic of regionally endothermic sharks. We then consider this result with the recent discovery of regional endothermy in basking sharks to propose a revision of the prevalence of regional endothermy in Lamniformes, and highlight several key implications of such a perspective.

5.3. Materials & Methods

One fresh carcass of a female smalltooth sand tiger shark, measuring 4.3 m TL, was stranded on the east coast of Ireland in 2023 (specimen 1). Due to logistics of beach dissections, four transverse cross sections of the body were just anterior of the first dorsal fin, anterior of the second dorsal fin, and anterior of the caudal peduncle to investigate red muscle distribution (Figure D.1A and D.1B). The heart was removed on site, rinsed with seawater and massaged of blood (Emery et al. 1985), and then stored in a –20°C freezer for two days before defrosting overnight to allow for dissection in the laboratory. Because the heart was large, the compact and spongey myocardium of the ventricle were dissected apart by eye using a scalpel and forceps, and then weighed on a digital scale. A second smalltooth sand tiger shark, this time a male measuring 2.9 m TL (specimen 2) was found floating at the surface by fishers, who retrieved the body and kept it in a refrigerated van between 3 to 4°C until collection and dissection four days later. This individual was gutted and sectioned into 11 full transverse cross sections of the body between the 4th gill slit and the precaudal pit (Bernal et al. 2003a (Figure D.1A and D1.C)).

A modified phylogram from Compagno 1990 which matches recent molecular analysis at the genus level was reconstructed in Procreate Software (version 5.2; Savage Interactive Pty Ltd.) to include all extant Lamniformes and the extinct megatooth shark. Although there is no clear phylogenetic arrangement of extant Lamniformes and the extinct megatooth shark due to conflicting results from morphological and molecular analysis (Bernal et al. 2001a, Naylor et al. 2012, Stone & Shimada 2019, Pimiento et al. 2019, Cade et al. 2020), multiple studies place the goblin shark *Mitsukurina owstoni* as the basal species, basking shark as sister to Lamnidae and, *Odontaspis spp*. being more basal to the more derived basking shark and Lamnidae (see Stone and Shimada 2019 for a review). The megatooth shark was included in this phylogram due to the interest in the origins of regional endothermy in this order and assumed historical life history in

this study. The placement of megatooth shark to extant Lamniformes, was based on analysis by Pimiento et al. 2019, whereby position of the megatooth shark did not interrupt extant Lamniformes placement (as in Compagno 1990) as the interrelationships between this extinct species and the extant order is unresolved (Pimiento et al. 2019, Cooper et al. 2020). Anatomical and physiological features described in Table D.1 were used to inform the modified phylogram.

5.4. Results and discussion

Dissection of two stranded smalltooth sand tiger shark carcasses showed the species exhibits centralised red muscle (it is a medial to lateral band along the trunk; Figure 5.1A, B), an anatomical trait shared by all confirmed regionally endothermic sharks examined to date (Bernal et al. 2003a, Bernal & Sepulveda 2005, Dolton et al. 2023). Analysis of smalltooth sand tiger shark hearts showed the species also has a high percentage of compact myocardium of the ventricle (48%); another trait shared with all regionally endothermic sharks examined to date. A high proportion of compact myocardium is typically, but not always, associated with elevated blood pressure and flow (Brill & Bushnell 1991), potentially servicing the metabolic demands of regional endothermy. While we could not confirm regional endothermy by taking *in-vivo* temperature measurements of our carcasses, all studied shark species with centralised red muscle along the trunk are regionally endothermic, with red muscle placement considered a "strong predictor" of regional endothermy (Sepulveda et al. 2005). If the smalltooth sand tiger shark is to be classified as having regional endothermy, then of the 15 extant species of Lamniformes, seven would have regional endothermy, two are ectothermic (Bernal et al. 2005), and the thermophysiology of the remaining six species are unknown (Figure 5.1C). Accordingly, finding regional endothermy (elevated white muscle temperature, 47% compact myocardium and centralised red muscle) in basking shark, and perhaps in the smalltooth sand tiger shark, suggests that regional endothermy is more prevalent in Lamniformes than previously thought, particularly given earlier classifications of ectothermic sharks are based partly on assumed links with feeding ecology that we now know to be tenuous (e.g., basking sharks are filter-feeders, and smalltooth sand tiger sharks are deep-water benthivores). Consequently, it is possible that the remaining six extant Lamniformes also exhibit features of regional endothermy. Dissecting further specimens in this order for red muscle placement and incorporating biologging of body temperature would be informative pursuits.

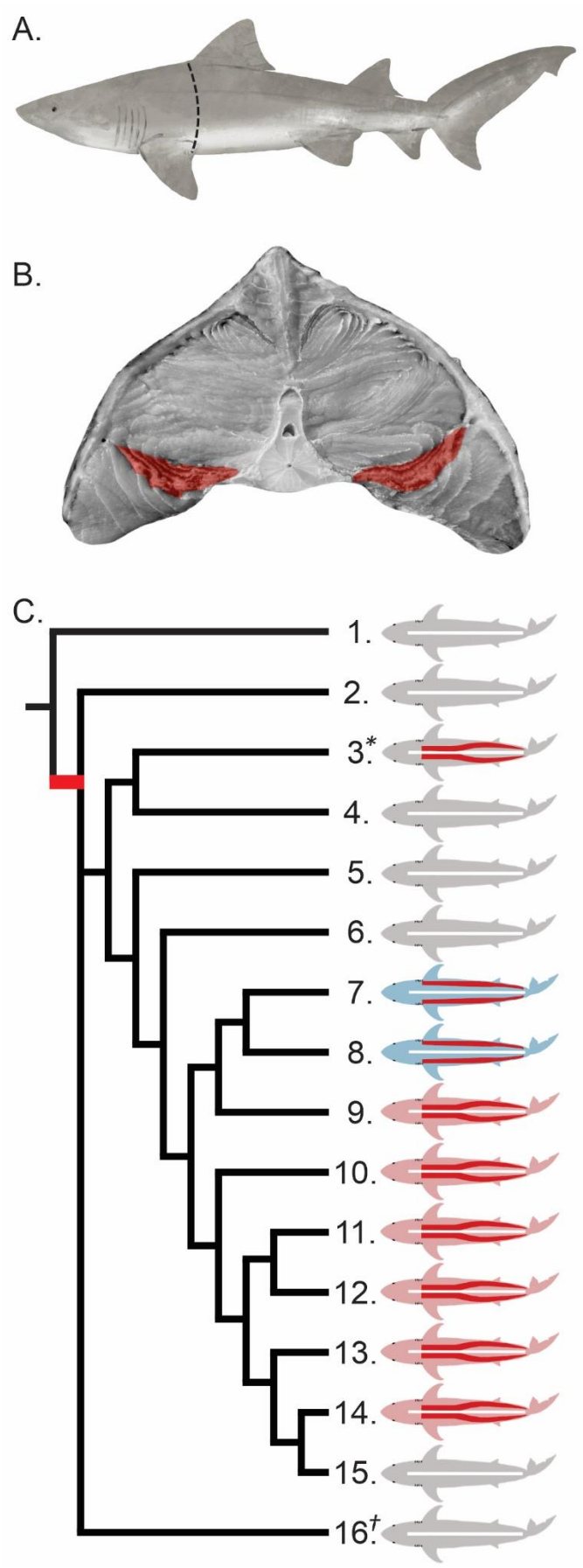

Figure 5.1: Red muscle distribution and prevalence of regional endothermy in Lamniformes. (A) Diagram of the smalltooth sand tiger shark showing location of transverse section indicated by black dashed line taken from specimen 1. (B). Posterior facing transverse section showing centralised (medial to lateral band) red muscle (red highlighted area) typical of regionally endothermic sharks. (C) Phylogram of Lamniformes adapted from Compagno 1990 and Piemento et al. 2019. Only extant species whose red muscle have been investigated are depicted by red lines on shark silhouettes on the reconstructed phylogram (Table D.1), and megatooth shark is also shown for context. Confirmed regional endothermy and centralised red muscle along the trunk (pink shark silhouette), confirmed laterally placed red muscle and probable ectothermy (light blue shark silhouette) and unconfirmed thermoregulatory strategy (grey silhouettes) with extinct species having a cross. Proposed single origin of regional endothermy indicated by red line. Species depicted are numbered as followed: (1.) *Mitsukurina owstoni* (2.) *Carcharias taurus* (3.) **Odontaspis ferox* (4.) *Odontaspis noronhai* (5.) *Pseudocarcharias kamoharai* (6.) *Megachasma pelagios* (7.) *Alopias superciliosus* (8.) *Alopias pelagicus* (9.) *Alopias vulpinus* (10.) *Cetorhinus maximus* (11.) *Lamna ditropis* (12.) *Lamna nasus* (13.) *Carcharodon carcharias* (14.) *Isurus oxyrinchus* (15.) *Isurus paucus* (16.) †*Otodus megalodon.*

These new findings help reconcile some conflicting versions of evolutionary pathways to regional endothermy in Lamniformes, such as why basking sharks cluster closely with regionally endothermic sharks based on morphology in phylogenetic analyses (Sternes et al. 2023), and whether regional endothermy evolved once and ancestrally, or multiple times convergently within the Lamniformes (Sepulveda et al. 2005, Pimiento et al. 2019, Sternes et al. 2023). With the higher general prevalence and indication that the smalltooth sand tiger shark has regional endothermy, our data support the single origin of regional endothermy in Lamniformes and that the megatooth shark was likely regionally endothermic. However, the findings also raise further questions regarding the role of regional endothermy in development of gigantism and filter-feeding in sharks, because it has been suggested that regional endothermy and filter-feeding are two mutually exclusive feeding strategies that evolved to facilitate extreme body size, but basking sharks seemingly developed filter-feeding while retaining regional endothermy (Pimiento et al. 2019, Dolton et al. 2023).

Vulnerabilities that gigantism and regional endothermy likely impose on species given the increased energy requirements of both features are currently debated, particularly extinction risks under changing ocean conditions (Griffiths et al. 2023). Previous work suggests regional endothermy tends to be associated with higher extinction risk (Pimiento et al. 2017), and the much-debated cause of the megatooth shark demise in the early Pliocene often focuses on high energetic demands due to regional endothermy coupled with changes in prey landscapes (Pimiento et al. 2016, 2017, Cooper et al. 2022, Griffiths et al. 2023). In this context, it is noteworthy that we now have evidence of possible regional endothermy in several extant Lamniformes with prey specialisation at rather different trophic levels than previously recognised, particularly since basking sharks are gigantic (up to 12 m TL). It is therefore possible that filter-feeding is a critical adaptation that ensures the persistence of gigantism, even throughout times of large environmental and biotic change. Indeed, it has been proposed that filter-feeding confers giant species with more resilience than being regionally endothermic because plankton is more abundant than large prey (Pimiento et al. 2019). So, while these new data improve understanding of the prevalence of regional endothermy in sharks and might help inform evolutionary pathways, they also enhance the currently active field of understanding the role of regional endothermy in contributing to extinction risk of elasmobranchs in light of warming oceans; most of which are severely vulnerable.

6. Discussion

Irish waters are rich with marine life and currently provide one of the best places in the world to study enigmatic, large, regionally endothermic fishes such as Atlantic bluefin tuna (ABFT) *Thunnus thynnus* and basking sharks *Cetorhinus maximus*. The technological development of biologging devices such as those used in **Chapters 2, 3 and 4** has provided the opportunity to collect previously unattainable data, and when combined with anatomical dissections (**Chapters 3 and 5**), has furthered our understanding of the biology and ecology of a 'hard to study' species (**Chapters 2 and 5**). In this thesis I have documented the response of a large regional endotherm to a stressful catch-and-release (C&R) event, challenged long-standing assumptions in the literature regarding the anatomy and physiology of shark species, questioned our view of the life history traits regional endothermy facilitates and investigated the thermal biology of the largest regionally endothermic fish in the world. Overall, this thesis has enhanced our knowledge of enigmatic, regionally endothermic fishes.

6.1. Short-term behavioural responses of Atlantic bluefin tuna to catch-and-release fishing

Recreational C&R of powerful fish, such as ABFT, is a popular practice which fosters the assumption that caught fishes continue to contribute to future populations. When managed appropriately, C&R of fishes can be a sustainable practice, whilst allowing financial gain for local communities (Cooke & Schramm 2007, Cosgrove et al. 2008, Donaldson et al. 2008). However, many studies have documented post-release mortality and sub-lethal impacts of fishes after a C&R event (Cooke & Suski 2005, Brownscombe et al. 2017). Although post-release mortality rates of ABFT have been studied, the fine-scale behavioural responses of this large, regionally endothermic fish were unknown. I show that ABFT display a behavioural response to C&R fishing by exhibiting an immediate powered descent response and an elevated dominant tailbeat frequency 5 to 10 hours post-release. This increase in mechanical effort of a species with a generally higher metabolic rate than its ectothermic counterparts (Dewar & Graham 1994) will likely impact the behaviour of ABFT until oxygen and energetic debt can be recovered. The initial powered descent observed in my data is in contrast to other research on C&R of ABFT who show a gliding behaviour immediately post-release for likely energy conservation (Gleiss et al. 2019). Our recorded powered descent may facilitate an important recovery period for the fish as displaying a post-release behaviour (increased mechanical effort) of exhaustive exercise indicates a powered descent behaviour might have a net positive outcome for the fish (e.g., reoxygenation). Although I was unable to classify this behaviour as an 'escape' or 'recovery' response it does highlight that water depth at the point of release is

likely an important species-specific consideration in the management of C&R fisheries of ABFT. The increase in dominant tailbeat frequency for 5 to 10 hours post-release is also documented in other fish species (Iosilevskii et al. 2022) and may represent a period of physiological recovery after exhaustive exercise. It would be beneficial to further explore this relationship with longer deployments of fine-scale biologgers to establish when ABFT 'recover' and to quantitatively assess the effects of ABFT being exposed to air during capture versus being kept submerged. It may also be important to explore these relationships and how we record responses to C&R in terms of thermophysiology. For example, as ectothermic fish have been recorded to exhibit an increase in body temperature by as much as 2.7°C after capture in recreational fisheries (Harding et al. 2022), it is reasonable to assume this increase in body temperature of a regionally endothermic fish undergoing capture would be greater and even higher towards the core of the fish due to a deep centralised red muscle position and associated heat retaining rete (Bernal et al. 2005). It would be beneficial to explore the body temperature of regional endotherms after a C&R event to aid in the understanding of their behaviour and physiology post-release. Such studies could be greatly informed by monitoring body temperatures of caught fishes on deck to ensure they remain below known lethal temperature thresholds or by preventing potential thermal stress of regionally endothermic fishes in cold waters post-release. Given my finding that ABFT make powered descents when caught in environments such as those in Irish waters (and by using the methods described in this study), it could be productive to also explore site-specific guidelines in addition to species-specific guidelines of C&R fisheries if they are to be managed appropriately (Bartholomew & Bohnsack 2005).

6.2. Regionally endothermic traits in planktivorous basking sharks *Cetorhinus maximus*

One of the biggest harvests of basking sharks in the north-east Atlantic occurred in Irish waters during 1946 to 1976, with the fishery collapsing due to overfishing (McNally 1976). A lack of knowledge of the biology and ecology of this species, along with unregulated fishing, ultimately led to the species being becoming globally 'Endangered' (Rigby et al. 2021). It is assumed regionally endothermic sharks produce fewer young less frequently than ectothermic sharks because of the energetic demands of regional endothermy (Shimada et al. 2020). The basking shark has exclusively been referred to as being ectothermic and having the associated anatomy, with just one implicit mention in recent literature of being a 'plausible candidate' (Dove & Pierce 2021). This led to many questions regarding basking shark biology and ecology; for example, how they were capable of elevated cruising speeds of approximately 1.1 m s^{-1}, which is similar to regionally endothermic fishes (Sims 1999, 2000, Harding et al. 2021) and why they would cluster with regionally endothermic species in comparative morphological analyses (Sternes et al. 2023). In my thesis, I

was able to provide evidence that the assumption of basking sharks being ectothermic is incorrect. I showed this through anatomical investigations of stranded carcasses and by developing a completely new method of deploying internal temperature probes into free-swimming basking sharks. The findings from this chapter directly challenges our understanding of regional endothermy being confined to apex, predatory sharks (Bernal et al. 2003a, 2005). It also casts doubt onto the assumed ectothermic life history of seven species within Lamniformes as evidence to support these claims in the literature are lacking (as highlighted by **Chapter 4**). It could be that regional endothermy is more prevalent than we assumed in shark species, and it facilitates more life histories than we had considered before (e.g., it is not confined to apex, predatory sharks). It is important to understand the physiology of a species if we are to be able to better predict how pressures might affect them. For example, regionally endothermic fish were considered to be less susceptible to sea temperature rises due to the thermal niche expansion hypothesis; however, it is now known that regional endothermy supports swimming performance rather than a tolerance of wider temperatures (Harding et al. 2021). By finding basking sharks are regionally endothermic, it is possible to better inform population forecasting and distribution shifts as accurate physiological data can improve modelling (Kearney & Porter 2009).

There is still much to learn regarding basking shark anatomy and physiology. The only access to specimens of this globally 'Endangered' species comes from stranded carcasses whereby tissue quality is poor. Consequently, investigations into regionally endothermic anatomical traits, such as proportional red muscle distribution, rete structures or myoglobin concentration within red muscles, which facilities oxygen transfer from the blood to muscle tissue, could not be investigated (Bernal et al. 2003a). Their large size also means it is not possible to accurately measure metabolic rates or muscle fibre twitch rates in a controlled environment (Bernal et al. 2001b, Seamone & Syme 2015). Our existing knowledge of this species is currently restricted to what can be hard won in the field. However, this chapter serves as a major update into the understanding of this species.

6.3. Body temperature dynamics of regionally endothermic basking sharks

Despite the difficulty of studying anatomy and physiology of basking sharks, it is possible to investigate the rate at which basking shark body heat is exchanged with ambient temperature through the estimation of heat transfer coefficients (HTC) (Malte et al. 2007, Nakamura et al. 2020, Watanabe et al. 2021). In doing so it is possible to further understand fish physiology and behaviour. A key result from this chapter, which will be of use in future comparative analyses regarding thermophysiology and HTC estimations, is that we now have an HTC estimate of the world's largest regionally endothermic fish, the basking shark. These estimates show basking sharks as an outlier to established comparative analysis between body mass and HTC as basking sharks are shown to

lose heat faster than predicted for their mass (Nakamura et al. 2020), and also cool approximately 100 times faster than their 'routine' HTC over the entire biologging deployment. This is possibly due to their ram filter-feeding life history as water is constantly following over the gills. It would be instructive to explore this further by examining the bulk flow of water over the gills and re-examining the gill surface area of this species.

A novelty of this study is that it is the first study to combine accelerometers and internal temperature probes on a large free-swimming basking shark that was not handled pre- or post-deployment, reducing the stress that fishing and handling normally has on shark species. Additionally, I found white muscle temperature spikes were associated with increases in mechanical effort, which is also seen in the regionally endothermic shortfin mako shark *Isurus oxyrinchus*. It would be of interest to compare the HTC of both species before and after these increases in mechanical effort to assess firstly, whether a potential 'ramp up' or 'cool down' of musculature temperature occurs, and secondly if they do occur, whether these periods differ between these two regional endotherms with vastly differing feeding ecologies. The response of regional endotherms to sea surface temperature increases is currently understudied and unknown (Waller et al. 2023), and as such, investigating the physiology of these species could facilitate improved predictions of population fluctuations for example under a changing climate.

6.4. Prevalence and origin of regional endothermy in sharks

Identifying a previously unrecognised regionally endothermic ram filter-feeder suggests the ability to elevate and maintain body temperature above ambient is more prevalent in shark species than the literature currently suggests. In **Chapter 5**, I find anatomical traits associated with regionally endothermic sharks in a more basal Lamniformes species to basking sharks, the smalltooth sand tiger shark *Odontaspis ferox*. In doing so, I challenge current assumptions about the ectothermic life history of seven species of Lamniformes and support a single origin hypothesis of the evolution of regional endothermy in shark species (Pimiento et al. 2019). Furthermore, I challenge an existing hypothesis that regional endothermy and filter-feeding have facilitated two independent pathways to gigantism (Sternes et al. 2023) and that regional endothermy facilitates an apex predatory lifestyle in shark species (Bernal et al. 2003a, 2005). Although regional endothermy has not been confirmed in smalltooth sand tiger sharks, the results from this chapter highlight the accepted broadscale assumption within this order regarding anatomy. The phylogenetic placement of species within Lamniformes is debated with different morphometric and molecular analysis revealing differing results (Bernal et al. 2001a, Naylor et al. 2012, Stone & Shimada 2019, Pimiento et al. 2019). However, the findings from this chapter might help to reconcile phylogenetic relationships within Lamniformes species and to explain recent forays into northerly waters in the north-east Atlantic, which extends their known range (Curnick et al. 2023).

It is broadly unknown how regionally endothermic sharks will respond to the effects of sea temperature rise (as discussed in Waller et al. 2023). However, the recent range shift of the smalltooth sand tiger shark at a time of a sea temperature rise in the north-east Atlantic region possibly indicates the species will make additional migrations north to stay within preferred sea temperature ranges that are not harmful to their physiology.

6.5. Regional endothermy in a changing environment

Fine and broad-scale effects of sea temperature change on regionally endothermic fishes are largely unknown with studies reporting both positive and negative impacts of temperature fluctuations on the mechanical outputs of large, regionally endothermic shark species (Carey & Lawson 1973, Block 1991, Dickson & Graham 2004, Horodysky et al. 2016, Waller et al. 2023). Although changing sea temperatures may make it possible for fishes to explore environments which were previously outside their thermal niche (Curnick et al. 2023), recent research shows the benefit of regional endothermy is to increase in cruising swimming speeds rather than expand thermal niches (Watanabe et al. 2015, Harding et al. 2021). Regionally endothermic anatomical traits have now been found in two species which were previously assumed to have ectothermic anatomy (**Chapters 3 and 5**), which potentially changes our understanding of their metabolism, how these fishes move through their environment and how we forecast future population fluctuations. For example, the accuracy of species distribution modelling is improved by incorporating accurate physiological data by taking purely correlative modelling into a mechanistic understanding of species (Kearney & Porter 2009). This could potentially benefit conservation planning by designating seasonal, important feeding areas for those species with high routine metabolic rates or improving species distribution modelling of a species as they make forays into waters previously outside of their thermal niche. Additional monitoring of shifting distributions and exploration into the physiological capabilities of regionally endothermic sharks are needed to establish species-specific thermal tolerance estimations to further improve species distribution estimates under climatic changes.

6.6. Implications and future research

My thesis has directly addressed and answered long-standing gaps in knowledge regarding the ecology and biology of regionally endothermic fish in Irish waters. We now know the fine-scale behavioural response of ABFT to a stressful C&R event and the differing response post-release to handling techniques (i.e., on deck or in the water). Species-specific guidelines for the capture and handling of fish species are thought to be key in managing sustainable C&R fisheries. It is this area of research which excites me the most when thinking about improvements to ever increasing C&R practice of ABFT. An area of future research could explore the response of ABFT to C&R when left

submerged in the water during tagging versus those fish brought on deck. Deploying video cameras has also been used to great effect to assess feeding rates of marine species (Nakamura et al. 2015, Del Caño et al. 2021, Watanabe et al. 2021). When used in combination with accelerometers these types of data can help answer when a fish has returned to 'homeostasis' as they begin resumption of normal behaviours such as feeding. The addition of internal temperature probes into biologging packages could also aid in the understanding of the energetic costs of C&R to regionally endothermic fishes and help estimate the metabolic costs of free-swimming fishes (Waller et al. 2023).

My thesis has shown there remain large assumptions regarding the anatomy and life history of an enigmatic order of shark species. Basking sharks are regionally endothermic, which challenges what we thought we knew about species and the regionally endothermic trait in general. Basking sharks are considered a relatively well-studied shark species in terms of satellite tracking studies (Sims et al. 2003, Gore et al. 2008, Skomal et al. 2009, Witt et al. 2016, Doherty et al. 2017a, Dolton et al. 2020), but finding these relatively basic anatomical traits highlights the knowledge gaps within anatomical and physiological research of shark species, which can ultimately be used to effectively conserve species within this order. I would suggest further anatomical investigations of this order and beyond, rather than relying on assumptions made in literature. Only by uncovering the true prevalence of regional endothermic traits within shark species can we begin to understand when the trait evolved and for which functions it serves, as has been done to a greater extent in tuna species (Bernal et al. 2001a). I've also shown that regionally endothermic basking sharks do not fit with comparative analysis of body mass and expected rates of cooling. This could be due to relatively short deployments of biologgers meaning fewer heating and cooling periods to include in the analyses to assess a variable *k*, but it would be informative to explore relationships between anatomical structures, feeding ecology, regional endothermy and body mass to assess the extent to which basking sharks are a true outlier.

In summary, the trait of regional endothermy in fishes is overwhelmingly rare. Species which possess this trait are an evolutionary triumph, with their anatomy, behaviour, and physiological nuances still to be truly understood. From the development of new biologgers and continued practice of dissections, we can continue to add to the knowledge base of these ecologically important fishes. My thesis has shown there are large assumptions about which species possess regional endothermy and for which purpose. By broadening our definitions of the form and function of regional endothermy, my thesis demonstrates that the relationships between feeding ecology, size and thermophysiology need to be better understood to inform future conservation and management strategies of these evolutionary marvels.

7. Bibliography

Adobe Photoshop Creative Cloud (2019) *Adobe Incorporated*, San Jose, California.

Arends RJ, Mancera JM, Mun JL, Bonga SEW, Flik G (1999) The stress response of the gilthead sea bream (*Sparus aurata L.*) to air exposure and confinement. *Journal of Endocrinology* 163:149–157.

Arlinghaus R, Cooke SJ, Lyman J, Policansky D, Schwab A, Suski C, Sutton SG, Thorstad EB (2007) Understanding the complexity of catch-and-release in recreational fishing: An integrative synthesis of global knowledge from historical, ethical, social, and biological perspectives. *Reviews in Fisheries Science* 15:75–167.

Bartholomew A, Bohnsack JA (2005) A review of catch-and-release angling mortality with implications for no-take reserves. *Reviews in Fish Biology and Fisheries* 15:129–154.

Beitinger TL (1990) Behavioral Reactions for the Assessment of Stress in Fishes. *Journal of Great Lakes Research* 16:495–528.

Bennett AF, Ruben JA (1979) Endothermy and Activity in Vertebrates. *Science* 206:649–654.

Bernal D, Carlson JK, Goldman KJ, Lowe CG (2012) Energetics, Metabolism, and Endothermy in Sharks and Rays. In: *Biology of Sharks and Their Relatives*. Carrier J, Simpfendorfer CA, Heithaus MR, Yopak K (eds) Taylor and Francis Group, Oxfordshire, UK, p 211–237

Bernal D, Dickson KA, Shadwick RE, Graham JB (2001a) Review: Analysis of the evolutionary convergence for high performance swimming in lamnid sharks and tunas. *Comparative Biochemistry and Physiology - A Molecular and Integrative Physiology* 129:695–726.

Bernal D, Donley JM, Shadwick RE, Syme DA (2005) Mammal-like muscles power swimming in a cold-water shark. *Nature* 437:1349–1352.

Bernal D, Sepulveda C, Graham JB (2001b) Water-tunnel studies of heat balance in swimming mako sharks. *Journal of Experimental Biology* 204:4043–4054.

Bernal D, Sepulveda C, Mathieu-Costello O, Graham JB (2003a) Comparative studies of high performance swimming in sharks: I. Red muscle morphometrics, vascularization and ultrastructure. *Journal of Experimental Biology* 206:2831–2843.

Bernal D, Sepulveda CA (2005) Evidence for temperature elevation in the aerobic swimming musculature of the common Thresher Shark, *Alopias vulpinus*. *Copeia*:146–151.

Bernal D, Smith D, Lopez G, Weitz D, Grimminger T, Dickson K, Graham JB (2003b) Comparative studies of high performance swimming in sharks: II. Metabolic biochemistry of locomotor and myocardial muscle in endothermic and ectothermic sharks. *Journal of Experimental Biology* 206:2845–2857.

Bernvi DC (2016) Ontogenetic Influences on Endothermy in the Great White Shark (*Carcharodon carcharias*). PhD thesis, Stockholm University, Sweden

Bivand R, Keitt T, Rowlingson B, Pebesma E, Sumner M, Hijmans R, Baston D, Rouault E, Warmerdam F, Ooms J, Rundel C (2012) Rgdal: Bindings for the "Geospatial" Data Abstraction Library. R-CRAN.

Block BA (1991) Endothermy in fish: thermogenesis, ecology and evolution. In: *Biochemistry and Molecular Biology of Fishes.* Hochachka PW, Mommsen TP (eds) Elsevier, Netherlands

Block BA, Carey FG (1985) Warm brain and eye temperatures in sharks. *Journal of Comparative Physiology B* 156:229–236.

Block BA, Finnerty JR, Stewart AFR, Kidd J (1993) Evolution of endothermy in fish: Mapping physiological traits on a molecular phylogeny. *Science* 260:210–214.

Block BA, Teo SLH, Walli A, Boustany A, Stokesbury MJW, Farwell CJ, Weng KC, Dewar H, Williams TD (2005) Electronic tagging and population structure of Atlantic bluefin tuna. *Nature* 434:1121–1127.

Braekken O (1959) Red Muscle as a Possible Character for the Identification of Sharks. *Nature* 183:556–557.

Brewster LR, Dale JJ, Guttridge TL, Gruber SH, Hansell AC, Elliott M, Cowx IG, Whitney NM, Gleiss AC (2018) Development and application of a machine learning algorithm for classification of elasmobranch behaviour from accelerometry data. *Marine Biology* 165:doi.org/10.1007/s00227-018-3318-y.

Brill RW, Bushnell PG (1991) Metabolic and cardiac scope of high energy demand teleosts, the tunas. *Canadian Journal of Zoology* 69:2002–2009.

Brill RW, Dewar H, Graham JB (1994) Basic concepts relevant to heat transfer in fishes, and their use in measuring the physiological thermoregulatory abilities of tunas. *Environmental Biology of Fishes* 40:109–124.

Brownscombe JW, Danylchuk AJ, Chapman JM, Gutowsky LFG, Cooke SJ (2017) Best practices for catch-and-release recreational fisheries – angling tools and tactics. *Fisheries Research* 186:693–705.

Brownscombe JW, Nowell L, Samson E, Danylchuk AJ, Cooke SJ (2014) Fishing-Related Stressors Inhibit Refuge-Seeking Behavior in Released Subadult Great Barracuda. *Transactions of the American Fisheries Society* 143:613–617.

Brownscombe JW, Thiem JD, Hatry C, Cull F, Haak CR, Danylchuk AJ, Cooke SJ (2013) Recovery bags reduce post-release impairments in locomotory activity and behavior of bonefish (*Albula* spp.) following exposure to angling-related stressors. *Journal of Experimental Marine Biology and Ecology* 440:207–215.

Cade DE, Gough WT, Czapanskiy MF, Fahlbusch JA, Kahane-Rapport SR, Linsky JMJ, Nichols RC, Oestreich WK, Wisniewska DM, Friedlaender AS, Goldbogen JA (2021) Tools for integrating inertial sensor data with video bio-loggers, including estimation of animal orientation, motion, and position. *Animal Biotelemetry* 9:34.

Cade DE, Levenson JJ, Cooper R, de la Parra R, Webb DH, Dove ADM (2020) Whale sharks increase swimming effort while filter feeding, but appear to maintain high foraging efficiencies. *Journal of Experimental Biology* 223:jeb224402.

Carey FG, Casey JG, Pratt HL, Urquhart D, McCosker JE (1985) Temperature, heat production and heat exchange in lamnid sharks. *Memoirs of the California Academy of Sciences* 9:92–108.

Carey FG, Gibson QH (1987) Blood Flow in the Muscle of Free-Swimming Fish. *Physiological Zoology* 60:138–148.

Carey FG, Kanwisher JW, Brazier O, Gabrielson G, G J, Pratt HL, Casey JG (1982) Temperature and Activities of a White Shark, *Carcharodon carcharias*. *Copeia* 1982:254–260.

Carey FG, Teal JM (1969) Mako and porbeagle: Warm-bodied sharks. *Comparative Biochemistry and Physiology* 28:199–204.

Carey FG, Teal JM, Kanwisher JW, Lawson KD (1971) Warm-bodied fish. *American Zoologist* 11:137–145.

Carey G, Lawson D (1973) Temperature regulation in free-swimming bluefin tuna. *Comparative Biochemistry and Physiology Part A: Physiology* 44:375–392.

Carlisle AB, Perle CR, Block BA (2011) Seasonal changes in depth distribution of salmon sharks (*Lamna ditropis*) in Alaskan waters: implications for foraging ecology. *Canadian Journal of Fisheries and Aquatic Sciences* 68:1905–1921.

Ciezarek AG, Dunning LT, Jones CS, Noble LR, Humble E, Stefanni SS, Savolainen V (2016) Substitutions in the Glycogenin-1 Gene Are Associated with the Evolution of Endothermy in Sharks and Tunas. *Genome Biology and Evolution* 8:3011–3021.

Compagno LJV (1990) Relationships of the Megamouth Shark, *Megachasma pelagios* (Lamniformes: Megachasmidae), with Comments on Its Feeding Habits. In: *Elasmobranchs as living resources: Advances in the Biology, Ecology, Systematics and the Status of the Fisheries*. Pratt HL, Gruber SH, Taniuichi T (eds) NMFS, Washington, USA, p 357–379

Cooke SJ, Hinch SG, Wikelski M, Andrews RD, Kuchel LJ, Wolcott TG, Butler PJ (2004) Biotelemetry: A mechanistic approach to ecology. *Trends in Ecology and Evolution* 19:334–343.

Cooke SJ, Schramm HL (2007) Catch-and-release science and its application to conservation and management of recreational fisheries. *Fisheries Management and Ecology* 14:73–79.

Cooke SJ, Schreer JF, Dunmall KM, Philipp DP (2002) Strategies for quantifying sublethal effects of marine catch-and-release angling: Insights from novel freshwater applications. In:

American Fisheries Society Symposium. Lucy JA, Studholme AL (eds) Maryland, USA, p 121–134

Cooke SJ, Suski CD (2005) Do we need species-specific guidelines for catch-and-release recreational angling to effectively conserve diverse fishery resources? *Biodiversity and Conservation* 14:1195–1209.

Cooper JA, Hutchinson JR, Bernvi DC, Cliff G, Wilson RP, Dicken ML, Menzel J, Wroe S, Pirlo J, Pimiento C (2022) The extinct shark *Otodus megalodon* was a transoceanic superpredator: Inferences from 3D modeling. *Science Advances* 8:eabm9424.

Cooper JA, Pimiento C, Ferrón HG, Benton MJ (2020) Body dimensions of the extinct giant shark *Otodus megalodon*: a 2D reconstruction. *Scientific Reports* 10:14596.

Corriero A, Heinisch G, Rosenfeld H, Katavić I, Passantino L, Zupa R, Grubišić L, Lutcavage ME (2020) Review of Sexual Maturity in Atlantic Bluefin Tuna, *Thunnus thynnus* (Linnaeus, 1758). *Reviews in Fisheries Science & Aquaculture* 28:182–192.

Cosgrove R, Stokesbury MJW, Browne D, Boustany A, Block BA, Farrell M (2008) Bluefin tuna tagging in Irish waters. *Fisheries Resource Series* 6:1–16.

Curnick DJ, Deaville R, Bortoluzzi JR, Cameron L, Carlsson J, Carlsson J, Dolton HR, Gordan CA, Hosegood P, Nilsson A, Perkins MW, Purves KJ, Spiro S, Vecchiato M, Williams R, Payne NL (2023) Northerly range expansion and first confirmed records of the smalltooth sand tiger shark, *Odontaspis ferox*, in the United Kingdom and Ireland. *Journal of Fish Biology* Accepted Author Manuscript.

Danylchuk AJ, Adams A, Cooke SJ, Suski CD (2008) An evaluation of the injury and short-term survival of bonefish (*Albula* spp.) as influenced by a mechanical lip-gripping device used by recreational anglers. *Fisheries Research* 93:248–252.

Davis MW (2007) Simulated fishing experiments for predicting delayed mortality rates using reflex impairment in restrained fish. *ICES Journal of Marine Science* 64:1535–1542.

Del Caño M, Quintana F, Yoda K, Dell'Omo G, Omo D, Blanco GS, Laich AG (2021) Fine-scale body and head movements allow to determine prey capture events in the Magellanic Penguin (*Spheniscus magellanicus*). *Marine Biology* 168:1–15.

Dewar H, Graham JB (1994) Studies of Tropical Tuna Swimming Performance in a Large Water Tunnel:I. Energetics. *Journal of Experimental Biology* 192:13–31.

Dickson KA, Graham JB (2004) Evolution and consequences of endothermy in fishes. *Physiological and Biochemical Zoology* 77:998–1018.

Doherty PD, Baxter JM, Gell FR, Godley BJ, Graham RT, Hall G, Hall J, Hawkes LA, Henderson SM, Johnson L, Speedie C, Witt MJ (2017a) Long-term satellite tracking reveals variable seasonal migration strategies of basking sharks in the north-east Atlantic. *Scientific Reports* 7:1–10.

Doherty PD, Baxter JM, Godley BJ, Graham RT, Hall G, Hall J, Hawkes LA, Henderson SM, Johnson L, Speedie C, Witt MJ (2017b) Testing the boundaries: Seasonal residency and inter-annual site fidelity of basking sharks in a proposed Marine Protected Area. *Biological Conservation* 209:68–75.

Dolton H, Jackson A, Deaville R, Hall J, Hall G, McManus, G., Perkins MW, Rolfe RA, Snelling EP, Houghton JDR, Sims DW, Payne N (2023) Regionally endothermic traits in planktivorous basking sharks *Cetorhinus maximus*. *Endangered Species Research* 51:227–232.

Dolton HR, Gell FR, Hall J, Hall G, Hawkes LA, Witt MJ (2020) Assessing the importance of Isle of Man waters for the basking shark *Cetorhinus maximus*. *Endangered Species Research* 41:209–223.

Donaldson MR, Arlinghaus R, Hanson KC, Cooke SJ (2008) Enhancing catch-and-release science with biotelemetry. *Fish and Fisheries* 9:79–105.

Dove ADM, Pierce SJ (2021) Whale sharks: biology, ecology, and conservation. CRC Press, Florida, USA.

Emery SH, Mangano C, Randazzo V (1985) Ventricle morphology in pelagic elasmobranch fishes. *Comparative Biochemistry and Physiology - Part A: Physiology* 82:635–643.

Farrell AP, Smith F (2017) Cardiac Form, Function and Physiology. *Fish Physiology* 36:155–264.

Fechhelm RG, Neill WH (1982) Predicting Body-Core Temperature in Fish Subjected to Fluctuating Ambient Temperature. *Physiological Zoology* 55:229–239.

Ferrón HG (2017) Regional endothermy as a trigger for gigantism in some extinct macropredatory sharks. PLOS ONE 12:e0185185.

French RP, Lyle J, Tracey S, Currie S, Semmens JM (2015) High survivorship after catch-and-release fishing suggests physiological resilience in the endothermic shortfin mako shark (*Isurus oxyrinchus*). *Conservation Physiology* 3:1–15.

Gallagher AJ, Serafy JE, Cooke SJ, Hammerschlag N (2014) Physiological stress response, reflex impairment, and survival of five sympatric shark species following experimental capture and release. *Marine Ecology Progress Series* 496:207–218.

Gleiss AC, Schallert RJ, Dale JJ, Wilson SG, Block BA (2019) Direct measurement of swimming and diving kinematics of giant Atlantic bluefin tuna (*Thunnus thynnus*). *Royal Society Open Science* 6:doi.org/10.1098/rsos.190203.

Gore MA, Rowat D, Hall J, Gell FR, Ormond RF (2008) Transatlantic migration and deep mid-ocean diving by basking shark. *Biology Letters* 4:395–398.

Graham JB (1975) Heat exchange in the yellowfin tuna, *Thunnus albacares* and skipjack tuna, *Katsuwonus pelamis* and the adaptive significance of elevated body temperatures in scombroid fishes. *Fishery Bulletin* 73:2199–229.

Graham JB, Dickson KA (2000) The evolution of thunniform locomotion and heat conservation in scombrid fishes: New insights based on the morphology of *Allothunnus fallai*. *Zoological Journal of the Linnean Society* 129:419–466.

Graham JB, Koehrn FJ, Dickson KA (1983) Distribution and relative proportions of red muscle in scombrid fishes: consequences of body size and relationships to locomotion and endothermy. *Canadian Journal of Zoology* 61:2087–2096.

Griffiths ML, Eagle RA, Kim SL, Flores RJ, Becker MA, Maisch HM, Trayler RB, Chan RL, McCormack J, Akhtar AA, Tripati AK, Shimada K (2023) Endothermic physiology of extinct megatooth sharks. *Proceedings of the National Academy of Sciences* 120:e2218153120.

Hanke A, Macdonnell A, Dalton A, Busawon D, Rooker JR, Secor DH (2018) Stock mixing rates of bluefin tuna from Canadian landings: 1975-2015. *ICCAT Collective Volume of Scientific Papers* 74:2622–2634.

Harding L, Gallagher A, Jackson A, Bortoluzzi J, Dolton HR, Shea B, Harman L, Edwards D, Payne N (2022) Capture heats up sharks. *Conservation Physiology* 10:doi.org/10.1093/conphys/coac065.

Harding L, Jackson A, Barnett A, Donohue I, Halsey L, Huveneers C, Meyer C, Papastamatiou Y, Semmens JM, Spencer E, Watanabe Y, Payne N (2021) Endothermy makes fishes faster but does not expand their thermal niche. *Functional Ecology* 35:1951–1959.

Hirasaki Y, Tomita T, Yanagisawa M, Ueda K, Sato K, Okabe M (2018) Heart Anatomy of *Rhincodon typus*: Three-Dimensional X-Ray Computed Tomography of Plastinated Specimens. *Anatomical Record* 301:1801–1808.

Holder PE, Griffin LP, Adams AJ, Danylchuk AJ, Cooke SJ, Brownscombe JW (2020) Stress, predators, and survival: Exploring permit (*Trachinotus falcatus*) catch-and-release fishing mortality in the Florida Keys. *Journal of Experimental Marine Biology and Ecology* 524:doi.org/10.1016/j.jembe.2019.151289.

Holland KN, Brill RW, Chang RKC (1990) Horizontal and vertical movements of yellowfin and bigeye tuna associated with fish aggregating devices. *Fishery Bulletin* 88:493–507.

Holts D, Bedford D (1993) Horizontal and vertical movements of the shortfin mako shark, *Isurus oxyrinchus*, in the Southern California Bight. *Marine and Freshwater Research* 44:901–909.

Horodysky AZ, Cooke SJ, Graves JE, Brill RW (2016) Fisheries conservation on the high seas: linking conservation physiology and fisheries ecology for the management of large pelagic fishes. *Conservation Physiology* 4:doi:10.1093/conphys/cov059.

Horton TW, Block BA, Drumm A, Hawkes LA, Cuaig MO, Neill RO, Schallert RJ, Stokesbury MJW, Witt MJ (2020) Tracking Atlantic bluefin tuna from foraging grounds off the west coast of Ireland. *ICES Journal of Marine Science* 77:2066–2077.

Hounslow JL, Brewster LR, Lear KO, Guttridge TL, Daly R, Whitney NM, Gleiss AC (2019) Assessing the effects of sampling frequency on behavioural classification of accelerometer data. *Journal of Experimental Marine Biology and Ecology* 512:22–30.

Humason GL (1979) Animal Tissue Techniques. Johns Hopkins University Press, Baltimore, USA.
Huveneers C, Watanabe YY, Payne NL, Semmens JM (2018) Interacting with wildlife tourism increases activity of white sharks. *Conservation Physiology* 6:1–10.
ICCAT (2020) 2020 SCRS Advice to the Commission. Madrid, Spain.
ICCAT (2002) ICCAT workshop on bluefin tuna mixing. *ICCAT Collective Volume of Scientific Papers* 54:261–352.
Igor Pro 6.3 (WaveMetrics Incorporated, Portland, Oregon, USA)
Iosilevskii G, Kong JD, Meyer CG, Watanabe YY, Papastamatiou YP, Royer MA, Nakamura I, Sato K, Doyle TK, Harman L, Houghton JDR, Barnett A, Semmens JM, Maoiléidigh NÓ, Drumm A, O'Neill R, Coffey DM, Payne NL (2022) A general swimming response in exhausted obligate swimming fish. *Royal Society Open Science* 9:doi.org/10.1098/rsos.211869.
Jacoby DMP, Siriwat P, Freeman R, Carbone C (2015) Is the scaling of swim speed in sharks driven by metabolism? *Biology Letters* 11:1–4.
Johnston EM, Houghton JDR, Mayo PA, Hatten GKF, Klimley AP, Mensink PJ (2022) Cool runnings: behavioural plasticity and the realised thermal niche of basking sharks. *Environmental Biology of Fishes* 105:2001–2015.
Kearney M, Porter W (2009) Mechanistic niche modelling: combining physiological and spatial data to predict species' ranges. *Ecology Letters* 12:334–350.
Kielhorn CE, Dillaman RM, Kinsey ST, McLellan WA, Mark Gay D, Dearolf JL, Ann Pabst D (2013) Locomotor muscle profile of a deep (*Kogia breviceps*) versus shallow (*Tursiops truncatus*) diving cetacean. *Journal of Morphology* 274:663–675.
Kroeger JP, McLellan WA, Arthur LH, Velten BP, Singleton EM, Kinsey ST, Pabst DA (2020) Locomotor muscle morphology of three species of pelagic delphinids. *Journal of Morphology* 281:170–182.
LaRochelle L, Chhor AD, Brownscombe JW, Zolderdo AJ, Danylchuk AJ, Cooke SJ (2021) Ice-fishing handling practices and their effects on the short-term post-release behaviour of Largemouth bass. *Fisheries Research* 243:doi.org/10.1016/j.fishres.2021.106084.
Lennox RJ, Brownscombe JW, Cooke SJ, Danylchuk AJ (2018) Post-release behaviour and survival of recreationally-angled arapaima (*Arapaima* cf. *arapaima*) assessed with accelerometer biologgers. *Fisheries Research* 207:197–203.
Lennox RJ, Brownscombe JW, Cooke SJ, Danylchuk AJ, Moro PS, Sanches EA, Garrone-neto D (2015) Ocean & Coastal Management Evaluation of catch-and-release angling practices for the fat snook *Centropomus parallelus* in a Brazilian estuary. *Ocean and Coastal Management* 113:1–7.
Malte H, Larsen C, Musyl M, Brill R (2007) Differential heating and cooling rates in bigeye tuna (*Thunnus obesus* Lowe): a model of non-steady state heat exchange. *Journal of Experimental Biology* 210:2618–2626.
Marcek BJ, Graves JE (2014) An Estimate of Postrelease Mortality of School-Size Bluefin Tuna in the U.S. Recreational Troll Fishery. *North American Journal of Fisheries Management* 34:602–608.
Matlab v2022a (2022) The MathWorks Incorporated, Natick, Massachusetts, USA.
McArley TJ, Herbert NA (2014) Journal of Experimental Marine Biology and Ecology Mortality, physiological stress and reflex impairment in sub-legal *Pagrus auratus* exposed to simulated angling. *Journal of Experimental Marine Biology and Ecology* 461:61–72.
McCormack J, Griffiths ML, Kim SL, Shimada K, Karnes M, Maisch H, Pederzani S, Bourgon N, Jaouen K, Becker MA, Jöns N, Sisma-Ventura G, Straube N, Pollerspöck J, Hublin J-J, Eagle RA, Tütken T (2022) Trophic position of *Otodus megalodon* and great white sharks through time revealed by zinc isotopes. *Nature Communications* 13:2980.
McNally K (1976) The Sunfish Hunt. Blackstaff Press, Belfast, UK.
Medina A (2020) Reproduction of Atlantic bluefin tuna. *Fish and Fisheries* 21:1109–1119.
Mitchell ED, Tedford RH (1973) The Enaliarctinae. A new group of extinct aquatic Carnivora and a consideration of the origin of the Otariida. *Bulletin of the American Museum of Natural History* 151:201–284.

Mohan JA, Jones ER, Hendon JM, Falterman B, Boswell KM, Eric R, Wells RJD (2020) Capture stress and post-release mortality of blacktip sharks in recreational charter fisheries of the Gulf of Mexico. *Conservation Physiology* 8:doi.org/10.1093/conphys/coaa041.

Morrison PR, Bernal D, Sepulveda CA, Brauner CJ (2023) The effect of temperature on haemoglobin–oxygen binding affinity in regionally endothermic and ectothermic sharks. *Journal of Experimental Biology* 226:doi.org/10.1242/jeb.244979.

Muoneke MI, Childress WM, Muoneke MI, Childress WM (2008) A review for recreational fisheries Hooking Mortality: A Review for Recreational Fisheries. *Reviews in Fish Biology and Fisheries* 2:123–156.

Nachlas MM, Tsou KC, De Souza E, Cheng CS, Seligman AM (1957) Cytochemical demonstration of succinic dehydrogenase by the use of a new p-nitrophenyl substituted ditetrazole. *The journal of histochemistry and cytochemistry* 5:420–436.

Nakamura I, Goto Y, Sato K (2015) Ocean sunfish rewarm at the surface after deep excursions to forage for siphonophores. *Journal of Animal Ecology* 84:590–603.

Nakamura I, Matsumoto R, Sato K (2020) Body temperature stability in the whale shark, the world's largest fish. *Journal of Experimental Biology* 223:1–10.

Naylor G, Caira J, Jensen K, Rosana K, Straube N, Lakner C (2012) Elasmobranch Phylogeny: A Mitochondrial Estimate Based on 595 Species. In: *Biology of Sharks and Their Relatives, Second Edition*. Marine Biology, Carrier J, Musick J, Heithaus M (eds) CRC Press, Florida, USA, p 31–56

Paig-Tran EWM, Bizzarro JJ, Strother JA, Summers AP (2011) Bottles as models: predicting the effects of varying swimming speed and morphology on size selectivity and filtering efficiency in fishes. *Journal of Experimental Biology* 214:1643–1654.

Patterson JC, Sepulveda CA, Bernal D (2011) The vascular morphology and in vivo muscle temperatures of thresher sharks (Alopiidae). *Journal of Morphology* 272:1353–1364.

Payne NL, Snelling EP, Fitzpatrick R, Seymour J, Courtney R, Barnett A, Watanabe YY, Sims DW, Squire L, Semmens JM (2015) A new method for resolving uncertainty of energy requirements in large water breathers: The "mega-flume" seagoing swim-tunnel respirometer. *Methods in Ecology and Evolution* 6:668–677.

Payne NL, Taylor MD, Watanabe YY, Semmens JM (2014) From physiology to physics: Are we recognizing the flexibility of biologging tools? *Journal of Experimental Biology* 217:317–322.

Perez V, Leder R, Badaut T (2021) Body length estimation of Neogene macrophagous lamniform sharks (*Carcharodon* and *Otodus*) derived from associated fossil dentitions. *Palaeontologia Electronica*:doi.org/10.26879/1140.

Pimiento C, Cantalapiedra JL, Shimada K, Field DJ, Smaers JB (2019) Evolutionary pathways toward gigantism in sharks and rays. *Evolution* 73:588–599.

Pimiento C, Griffin JN, Clements CF, Silvestro D, Varela S, Uhen MD, Jaramillo C (2017) The Pliocene marine megafauna extinction and its impact on functional diversity. *Nature Ecology & Evolution* 1:1100–1106.

Pimiento C, MacFadden BJ, Clements CF, Varela S, Jaramillo C, Velez-Juarbe J, Silliman BR (2016) Geographical distribution patterns of *Carcharocles megalodon* over time reveal clues about extinction mechanisms. *Journal of Biogeography* 43:1645–1655.

Policansky D (2002) Catch-and-release recreational fishing: A historical perspective. In: *Recreational Fisheries: Ecological, Economic and Social Evaluation*. Pitcher T, Hollingworth C (eds) Blackwell Science, Oxford, UK

Procreate Software (version 5.2; Savage Interactive Pty Ltd.).

QGIS Development Team (2018) QGIS Geographic Information System. QGIS Association.

R Development Core Team (2020) RStudio:integrated development for R. RStudio. Boston, MA.

R Development Core Team (2019) RStudio:integrated development for R. RStudio. Boston, MA.

Raby GD, Cooke SJ, Cook KV, McConnachie SH, Donaldson MR, Hinch SG, Whitney CK, Drenner SM, Patterson DA, Clark TD, Farrell AP (2013) Resilience of Pink Salmon and Chum Salmon to Simulated Fisheries Capture Stress Incurred upon Arrival at Spawning Grounds. *Transactions of the American Fisheries Society* 142:524–539.

Rigby C, Barreto R, Carlson J, Fernando D, Fordham S, Francis M, Herman K, Jabado RW, Liu KM, Marshall A, Romanov E, Kyne PM (2021) *Cetorhinus maximus* (amended version of 2019 assessment) The IUCN Red List of Threatened Species. doi.org/10.2305/IUCN.UK.2021 (accessed January 1, 2022)

Rodríguez-Ezpeleta N, Díaz-Arce N, Walter JF, Richardson DE, Rooker JR, Nøttestad L, Hanke AR, Franks JS, Deguara S, Lauretta MV, Addis P, Varela JL, Fraile I, Goñi N, Abid N, Alemany F, Oray IK, Quattro JM, Sow FN, Itoh T, Karakulak FS, Pascual-Alayón PJ, Santos MN, Tsukahara Y, Lutcavage M, Fromentin JM, Arrizabalaga H (2019) Determining natal origin for improved management of Atlantic bluefin tuna. *Frontiers in Ecology and the Environment* 17:439–444.

Rooker JR, Arrizabalaga H, Fraile I, Secor DH, Dettman DL, Abid N, Addis P, Deguara S, Karakulak FS, Kimoto A, Sakai O, Macías D, Santos MN (2014) Crossing the line: Migratory and homing behaviors of Atlantic bluefin tuna. *Marine Ecology Progress Series* 504:265–276.

Rooker JR, Secor DH, De Metrio G, Schloesser R, Block BA, Neilson JD (2008) Atlantic Bluefin Tuna Populations. *Science* 322:742–744.

Royer M, Meyer C, Royer J, Maloney K, Cardona E, Blandino C, Fernandes Da Silva G, Whittingham K, Holland KN (2023) "Breath holding" as a thermoregulation strategy in the deep-diving scalloped hammerhead shark. *Science* 380:651–655.

Ryan LA, Meeuwig JJ, Hemmi JM, Collin SP, Hart NS (2015) It is not just size that matters: shark cruising speeds are species-specific. *Marine Biology* 162:1307–1318.

Sakamoto KQ, Sato K, Ishizuka M, Watanuki Y, Takahashi A (2009) Can Ethograms Be Automatically Generated Using Body Acceleration Data Can Ethograms Be Automatically Generated Using Body Acceleration Data from Free-Ranging Birds? *PLOS ONE* 4.

Santer RM, Greer Walker M (1980) Morphological studies on the ventricle of teleost and elasmobranch hearts. *Journal of Zoology* 190:259–272.

Schmidt-Nielsen K (1984) Scaling: Why Is Animal Size So Important? Cambridge University Press, Cambridge, UK.

Seamone SG, Syme DA (2015) Elasmobranch Muscle Structure and Mechanical Properties. Elsevier Incorporated, Netherlands.

Sepulveda CA, Heberer C, Aalbers SA, Spear N, Kinney M, Bernal D, Kohin S (2015) Post-release survivorship studies on common thresher sharks (*Alopias vulpinus*) captured in the southern California recreational fishery. *Fisheries Research* 161:102–108.

Sepulveda CA, Wegner NC, Bernal D, Graham JB (2005) The red muscle morphology of the thresher sharks (family Alopiidae). *Journal of Experimental Biology* 208:4255–4261.

Shimada K, Becker MA, Griffiths ML (2020) Body, jaw, and dentition lengths of macrophagous lamniform sharks, and body size evolution in Lamniformes with special reference to 'off-the-scale' gigantism of the megatooth shark, *Otodus megalodon*. *Historical Biology* 33:2543–2559.

Shimada K, Yamaoka Y, Kurihara Y, Takakuwa Y, Maisch HM, Becker MA, Eagle RA, Griffiths ML (2023) Tessellated calcified cartilage and placoid scales of the Neogene megatooth shark, *Otodus megalodon* (Lamniformes: Otodontidae), offer new insights into its biology and the evolution of regional endothermy and gigantism in the otodontid clade. *Historical Biology*:1–15.

Sims DW (2000) Filter-feeding and cruising swimming speeds of basking sharks compared with optimal models: They filter-feed slower than predicted for their size. *Journal of Experimental Marine Biology and Ecology* 249:65–76.

Sims DW (2008) Sieving a living: A review of the biology, ecology and conservation status of the plankton-feeding basking shark Cetorhinus maximus. *Advances in Marine Biology* 54:171–220.

Sims DW (1999) Threshold foraging behaviour of basking sharks on zooplankton: life on an energetic knife edge? *Proceedings of the Royal Society B* 266:1437–1443.

Sims DW, Southall EJ, Richardson AJ, Reid PC, Metcalfe JD (2003) Seasonal movements and behaviour of basking sharks from archival tagging: No evidence of winter hibernation. *Marine Ecology Progress Series* 248:187–196.

Skomal GB, Zeeman SI, Chisholm JH, Summers EL, Walsh HJ, McMahon KW, Thorrold SR (2009) Transequatorial Migrations by Basking Sharks in the Western Atlantic Ocean. *Current Biology* 19:1019–1022.

Soetaert K, Petzoldt T, Woodrow Setzer R (2010) "Solving Differential Equations in R: Package deSolve." *Journal of Statistical Software* 33:1–25.

Spigarelli SA, Thommes MM, Beitinger TL (1977) The influence of body weight on heating and cooling of selected Lake Michigan fishes. *Comparative Biochemistry and Physiology A* 56:51–57.

Sternes P, Wood J, Shimada K (2023) Body forms of extant lamniform sharks (Elasmobranchii: Lamniformes), and comments on the morphology of the extinct megatooth shark, *Otodus megalodon*, and the evolution of lamniform thermophysiology. *Historical Biology* 35:doi.org/10.1080/08912963.2021.2025228.

Stevens ED, Fry FEJ (1970) The rate of thermal exchange in a teleost, *Tilapia mossambica*. *Canadian Journal of Zoology* 48:221–226.

Stevens ED, Sutterlin AM (1976) Heat transfer between fish and ambient water. *Journal of Experimental Biology* 65:138–148.

Stokesbury M, Cosgrove R, Boustany A, Browne D, Teo S, O'Dor R, Block B (2007) Results of satellite tagging of Atlantic bluefin tuna, *Thunnus thynnus*, off the coast of Ireland. *Hydrobiologia* 582:91–97.

Stokesbury MJW, Neilson JD, Susko E, Cooke SJ (2011) Estimating mortality of Atlantic bluefin tuna (*Thunnus thynnus*) in an experimental recreational catch-and-release fishery. *Biological Conservation* 144:2684–2691.

Stone N, Shimada K (2019) Skeletal anatomy of the bigeye sand tiger shark, *Odontaspis noronhai* (Lamniformes: odontaspididae), and its implications to lamniform phylogeny, taxonomy, and conservation biology. *Copeia* 107:632–652.

Strand E, Bagøien E, Edwards M, Broms C, Klevjer T (2020) Spatial distributions and seasonality of four Calanus species in the Northeast Atlantic. *Progress in Oceanography* 185:102344.

Taylor NG, Mcallister MK, Lawson GL, Carruthers T, Block BA (2011) Atlantic Bluefin Tuna: A Novel Multistock Spatial Model for Assessing Population Biomass. *PLOS ONE* 6:doi.org/10.1371/journal.pone.0027693.

Tubbesing VA, Block BA (2000) Orbital rete and red muscle vein anatomy indicate a high degree of endothermy in the brain and eye of the salmon shark. *Acta Zoologica* 81:49–56.

Waller MJ, Queiroz N, Da Costa I, Cidade T, Loureiro B, Womersley FC, Fontes J, Afonso P, Macena BCL, Loveridge A, Humphries NE, Southall EJ, Sims DW (2023) Direct measurement of cruising and burst swimming speeds of the shortfin mako shark (*Isurus oxyrinchus*) with estimates of field metabolic rate. *Journal of Fish Biology* Online Version of Record before inclusion in an issue:doi.org/10.1111/jfb.15475.

Watanabe Y, Sato K (2008) Functional dorsoventral symmetry in relation to lift-based swimming in the ocean sunfish *Mola mola*. *PLOS ONE* 3:doi.org/10.1371/journal.pone.0003446.

Watanabe Y, Wei Q, Yang D, Chen X, Du H, Yang J, Sato K, Naito Y, Miyazaki N (2008) Swimming behavior in relation to buoyancy in an open swimbladder fish, the Chinese sturgeon. *Journal of Zoology* 275:381–390.

Watanabe YY, Goldman KJ, Caselle JE, Chapman DD, Papastamatiou YP (2015) Comparative analyses of animal-tracking data reveal ecological significance of endothermy in fishes. *Proceedings of the National Academy of Sciences* 112:6104–6109.

Watanabe YY, Nakamura I, Chiang WC (2021) Behavioural thermoregulation linked to foraging in blue sharks. *Marine Biology* 168:1–10.

Watanabe YY, Takahashi A (2013) Linking animal-borne video to accelerometers reveals prey capture variability. *Proceedings of the National Academy of Sciences of the United States of America* 110:2199–2204.

Wegner NC, Snodgrass OE, Dewar H, Hyde JR (2015) Whole-body endothermy in a mesopelagic fish, the opah, *Lampris guttatus*. *Science* 348:786–789.

Weihs D (1973) Mechanically efficient swimming techniques for fish with negative buoyancy. *Journal of Marine Research* 31:194–209.

Weng KC, Block BA (2004) Diel vertical migration of the bigeye thresher shark (*Alopias superciliosus*), a species possessing orbital retia mirabilia. *Fishery Bulletin* 102:221–229.

Weng KC, Castilho PC, Morrissette JM, Landeira-Fernandez AM, Holts DB, Schallert RJ, Goldman KJ, Block BA (2005) Satellite tagging and cardiac physiology reveal niche expansion in salmon sharks. *Science* 310:104–106.

Whitney NM, White CF, Anderson PA, Hueter RE, Skomal GB (2017) The physiological stress response, postrelease behavior, and mortality of blacktip sharks (*Carcharhinus limbatus*) caught on circle and J-hooks in the Florida recreational fishery. *Fishery Bulletin* 115:532–543.

Whitney NM, White CF, Gleiss AC, Schwieterman GD, Anderson P, Hueter RE, Skomal GB (2016) A novel method for determining post-release mortality, behavior, and recovery period using acceleration data loggers. *Fisheries Research* 183:210–221.

Wickham H, Averick M, Bryan J, Chang W, McGowan L, François R, Grolemund G, Hayes H, Henry L, Hester J, Kuhn M, Pedersen T, Miller E, Bache S, Müller K, Ooms J, Robinson D, Seidel D, Spinu V, Takahashi K, Vaughan D, Wilke C, Woo K, Yutani H (2019) Welcome to the tidyverse. *Journal of Open Source Software* 4:doi.org/10.21105/joss.016861.

Witt MJ, Graham BJ, Hawkes RT (2016) Basking shark satellite tagging project: insights into basking shark (*Cetorhinus maximus*) movement, distribution and behaviour using satellite telemetry. Final Report. *Scottish Natural Heritage Commissioned Report No 908*.

Witt MJ, Hardy T, Johnson L, McClellan CM, Pikesley SK, Ranger S, Richardson PB, Solandt JL, Speedie C, Williams R, Godley BJ (2012) Basking sharks in the northeast Atlantic: Spatio-temporal trends from sightings in UK waters. *Marine Ecology Progress Series* 459:121–134.

Wolf NG, Swift PR, Carey FG (1988) Swimming muscle helps warm the brain of lamnid sharks. *Journal of Comparative Physiology B: Biochemical, Systemic and Environmental Physiology* 157:709–715.

Yowell DW, Vinyard GL (1993) An energy-based analysis of particulate-feeding and filter-feeding by blue tilapia, *Tilapia aurea*. *Environmental Biology of Fishes* 36:65–72.

Appendix A Supplementary information to Chapter 2:

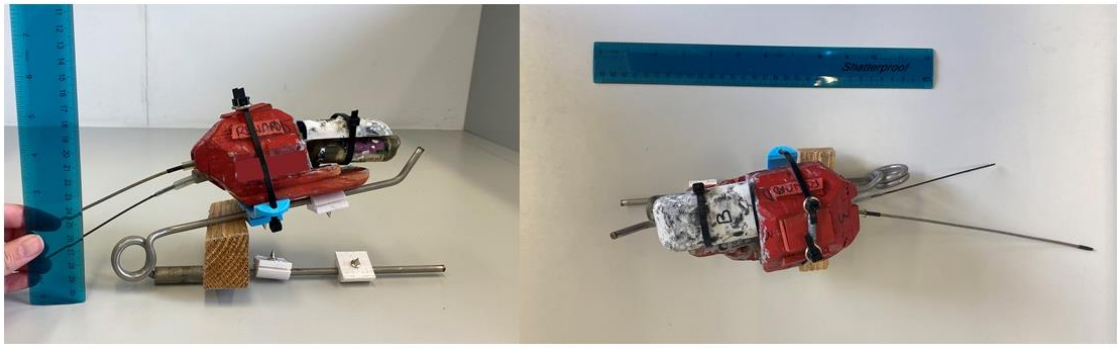

Figure A.1: Biologging package and clamp attachment. Biologging package containing a multi-channel data logger (recording tri-axial acceleration), a very high frequency transmitter and Satellite Position Only Tag. A clamp is held open with a block of wood in preparation for deployment. Recovery telephone number has been obscured on red float material.

Table A.1: Metrics (measured in cm) and weight (g) of biologging package contents used during this study. Length, width, and height measurements were made at the maximum point of the main body of devices or clamp package.

Device	**Length (cm)**	**Width (cm)**	**Height (cm)**	**Weight in air (g)**
Technosmart AGM-1	7.0	4.0	1.3	57.0
Little Leonardo Corp. ORI1300 3MPD3GT	7.5	1.5	2.5	37.0
Advanced Telemetry Systems transmitter MM170B (main body)	6.2	2.0	2.0	42.0
Satellite Position Only Tag (SPOT, Wildlife Computers Model 258 (main body)	11.0	2.0	1.8	52.0
Clamp and float package	26.5	7.5	12.5	252.0

A map of deployment location and pop-off location was produced in QGIS software (QGIS Development Team 2018). Shapefiles were written in R Studio (RStudio Team, 2020) using the package 'rgdal' (Bivand et al. 2012). The 50 m and 100 m contour lines have been displayed as to not overcomplicate the map.

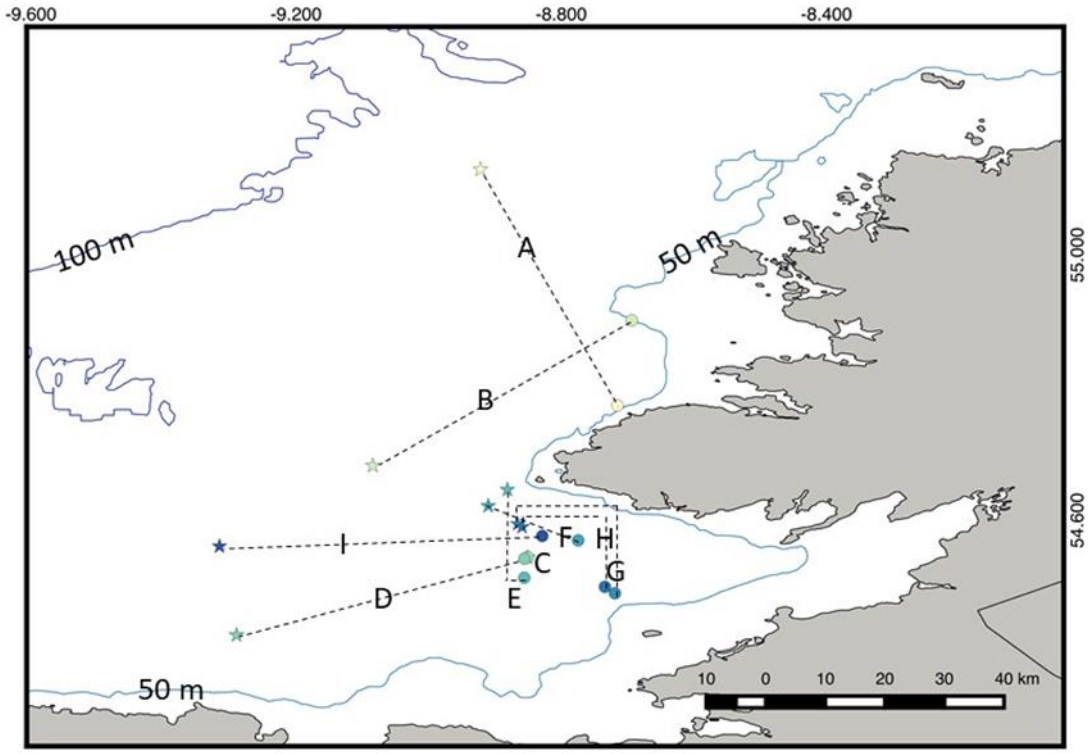

Figure A.2: Deployment locations (circle shapes) of Atlantic bluefin tuna (tuna ID indicated on the map) tagged off the coast of Donegal, Ireland. Black dashed line indicates a connecting line between deployment location and pop-off location (star shape) of the biologging package. It does not represent actual movement of Atlantic bluefin tuna. The biologging package came off of Tuna C within 1.0 km of the deployment location. Consequently, there is no connecting black dashed line. Tuna X is not shown due to a suspected mortality event within minutes of release.

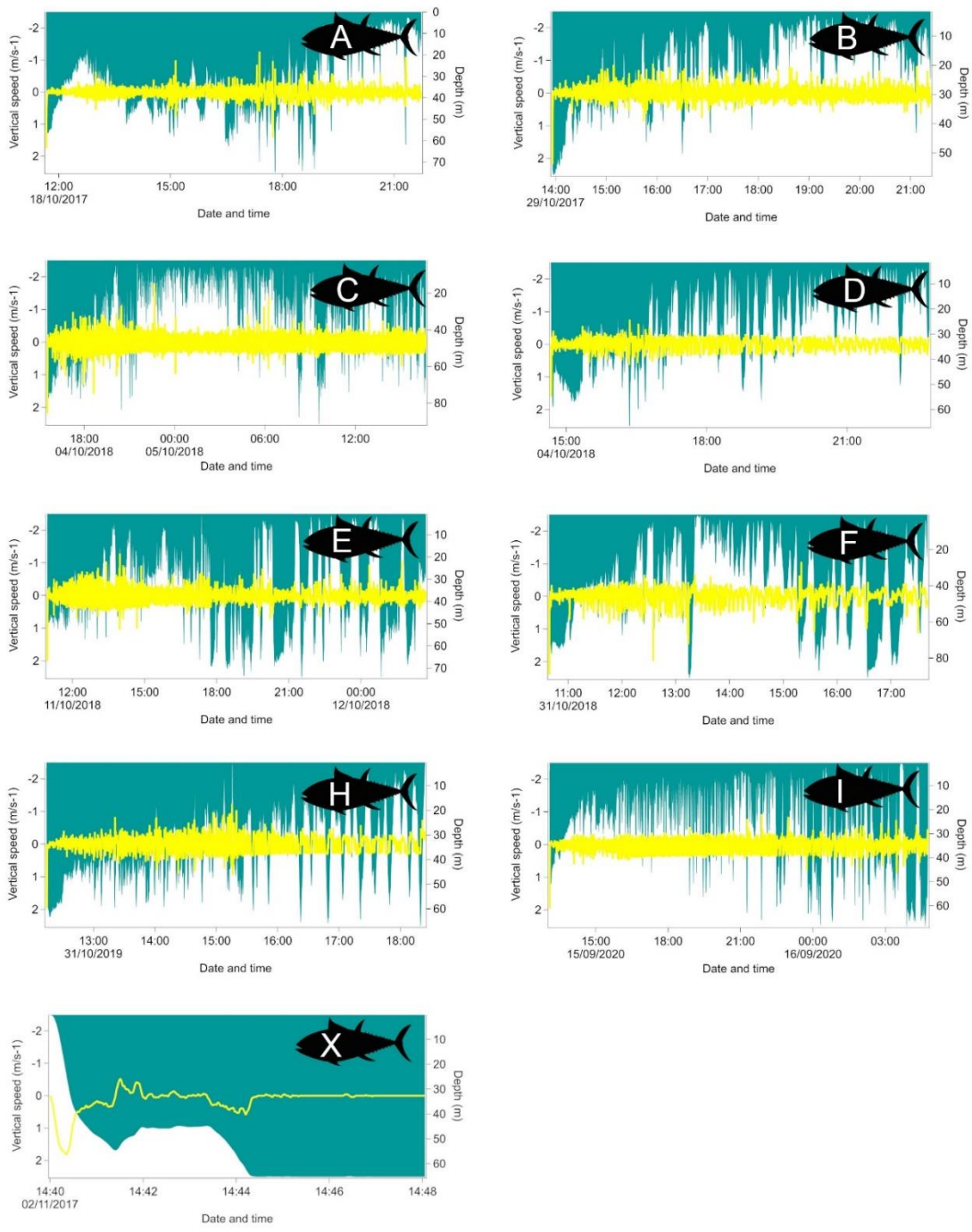

Figure A.3: Vertical speed and depth use of Atlantic bluefin tuna during the respective whole deployment. Vertical speed (m s^{-1}) (yellow) and depth (m) (green) use of Atlantic bluefin tuna tagged in this study. Atlantic bluefin tuna identification shown in plots.

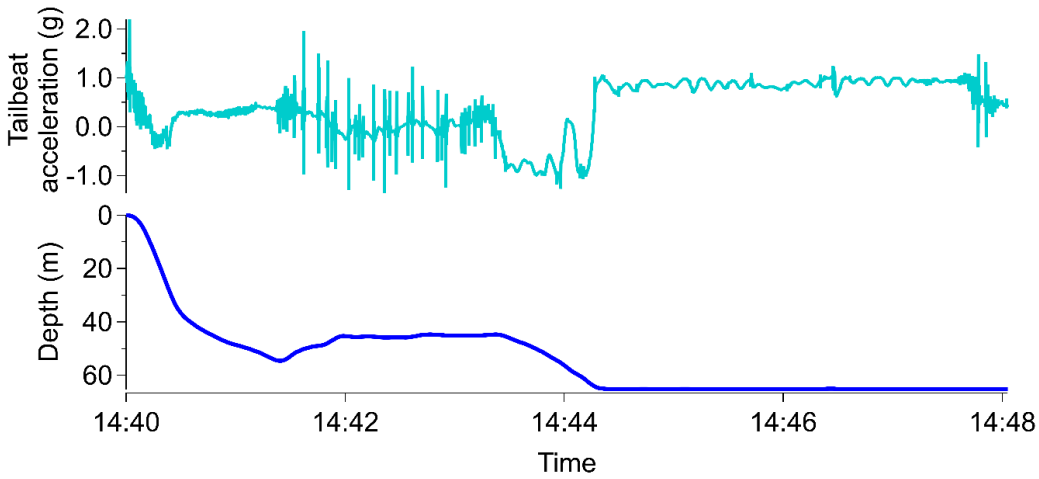

Figure A.4: Suspected mortality event of tuna X. Release event of tuna X showing unfiltered acceleration (teal line (g)) and smoothed depth data (blue line (m)).

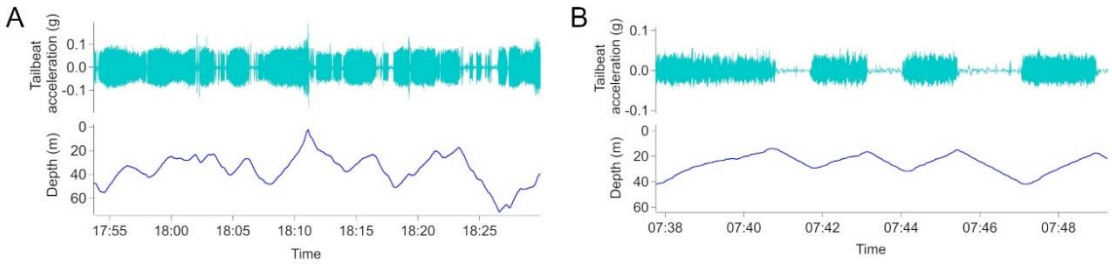

Figure A.5: Classic intermittent locomotion of Atlantic bluefin tuna. (A) Examples of classic intermittent locomotion of tuna A 6 hours post-release and (B) tuna C 16 hours post-release. Increased tailbeat activity (teal line (g)) is seen on ascents and gliding on descents (depth shown with a blue line (m)).

Appendix B Supplementary information to Chapter 3:

Specimen A was found stranded in Cornwall, southwest England, and Specimen B was live stranded at Scarborough, in the north-east of England. Thirteen approximate half cross-sections were made, without piercing the abdominal cavity, on Specimen A at intervals along the body length every 5% of the fork length of the shark, or every 18 cm (Bernvi 2016). Attempts to re-float Specimen B were unsuccessful and the shark was humanely euthanised with barbiturate drugs by a qualified veterinarian operating under The Wildlife and Countryside Act 1981 (as amended) and The Animal and Welfare Act 2006. A field examination of Specimen B was conducted two days later by the Cetacean Strandings Investigation Programme under license from Natural England (Class License CL01). Five approximate half cross-sections were taken from Specimen B, starting from just anterior of the pectoral fins, between the pectoral fins, under the first dorsal fin, posterior to the first dorsal fin and posterior to the second dorsal fin. Due to logistical and regulatory constraints of the beach dissections, thorough examination of relevant heat retention tissues such as a 'lamnid specific red muscle vein' or rete mirabile could not be conducted. Beach dissection of Specimen B was exploratory in nature. As a result, full transverse sections could not be taken, and photographs were unable to be taken from 90° to the musculature. Photographic angles were corrected from Specimen B in Adobe Photoshop CC (Adobe Photoshop Creative Cloud 2019) using distortion panel and backgrounds of all photographs were removed using the lasso tool.

The Lotek LAT1810S tags were calibrated by the manufacturer before deployment and concurrent data collected by the tag after release from individual sharks allowed for calibration between the external and internal temperature sensors to be calculated post-deployment. DeltaT (the difference in temperature from one timepoint to the next) was calculated as the difference between the internal and external temperature sensors post-deployment (while the tag was floating on the water surface) for each individual shark. The mean value of deltaT was calculated and added to each body temperature recording of the relevant individual (0.08, 0.01, 0.19 and 0.02°C for the shark measuring 7.0, 5.5, 8.0 and 5.0 m respectively) to correct the internal body temperature recording.

Figure 3.2A schematic was created in Procreate Software (version 5.3, Savage Interactive Pty Ltd.).

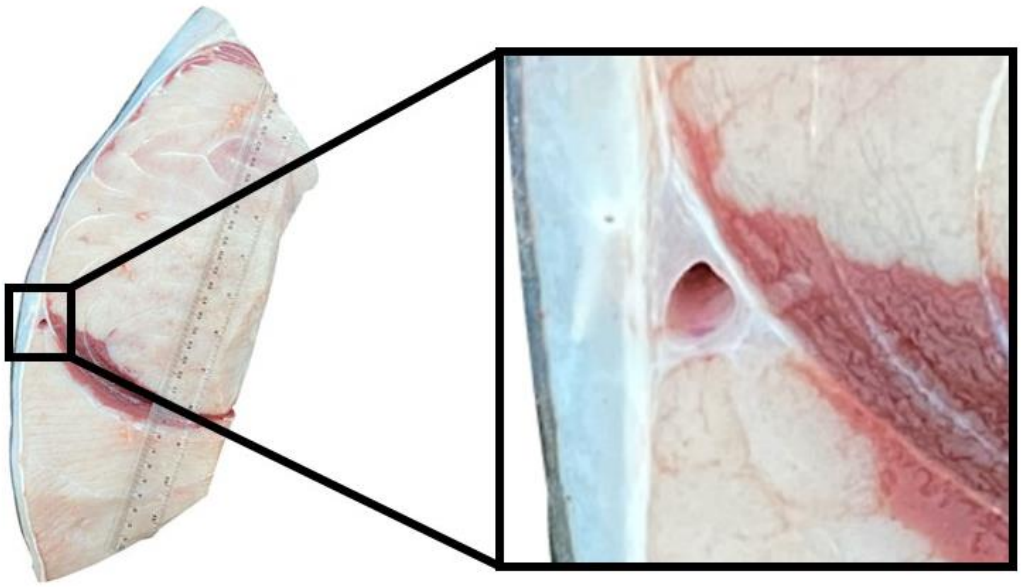

Figure B.1: Lateral subcutaneous vessels of basking sharks. Within the connective tissue there appears a small lateral subcutaneous artery and large lateral subcutaneous vein located near the lateral extents of the red muscle. Image taken from specimen A from near the pectoral fin region

Appendix C Supplementary information to Chapter 4:

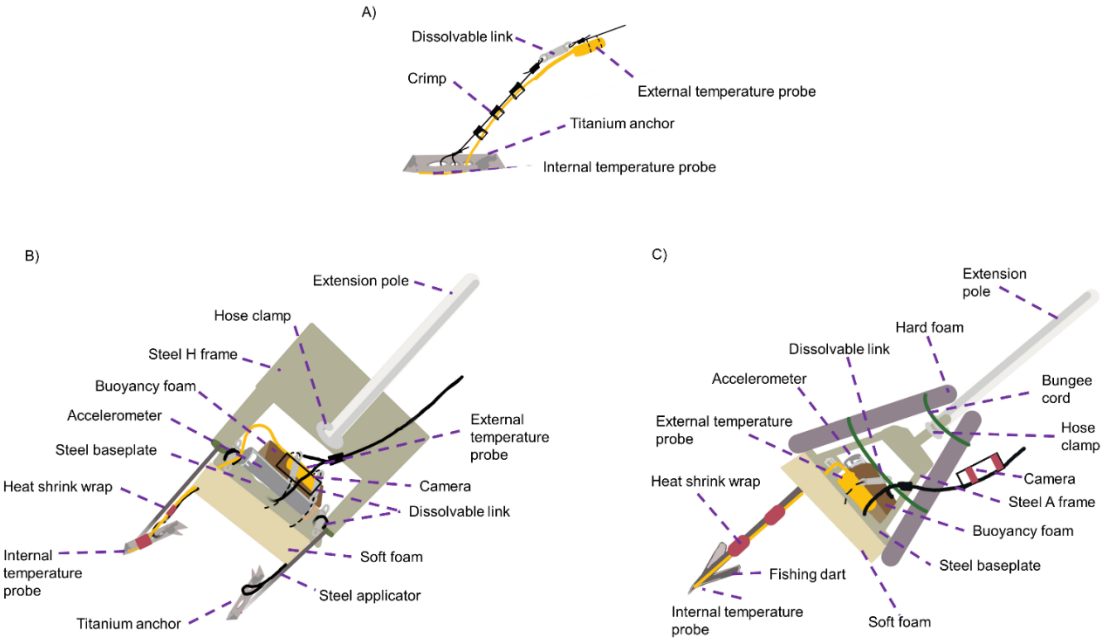

Figure C.1: Biologging configurations. Tag deployment set up (solid black line represent monofilament line and dashed black lines represent cable ties). (A) Titanium anchor deployed into white muscle using a modified tagging spear as described in Dolton et al 2023. (B) Two titanium anchors used to hold internal temperature in the musculature. Steel H frame used to transmit force down the extension pole to steel baseplate and steel applicators. Biologging devices (Lotek LAT100ST, Technosmart 720hp video camera, and PD3GT Little Leonardo accelerometer) secured onto baseplate. Steel frame and extension pole removed from shark upon deployment. (C) Fishing dart used to deploy internal temperature probe (Lotek LAT100ST) into the musculature. Steel A frame used to transmit force down the extension pole to steel baseplate (held in place with hard foam) and fishing dart. Biologging devices (Lotek LAT100ST and PD3GT Little Leonardo accelerometer) secured onto baseplate, with Technosmart 720hp video camera secured to the anchor line. Steel frame, hard foam and extension pole removed from shark upon deployment.

Table C.1: basking shark identification from Chapters 3 and 4 including deployment latitude, longitude and total length of each relevant shark.

Shark ID (basking shark number)	Shark used in Chapter 3	Shark used in Chapter 4	Date tagged	Deployment lat (N)	Deployment long (W)	Total length (m)
1	Yes	Yes	29/04/2021	51.567017	8.703350	7.0
2	Yes	Yes	30/04/2021	51.542188	8.940992	5.5
3	Yes	Yes	01/05/2021	51 32.5313	8 56.4595	8.0
4	Yes	Yes	01/05/2021	51.585400	8.698600	5.0
5	No	Yes	28/08/2021	52.721267	9.685217	8.0
6	No	Yes	27/04/2022	52.095320	10.61082	7.5
7	No	Yes	02/05/2022	51.583000	8.665500	7.0

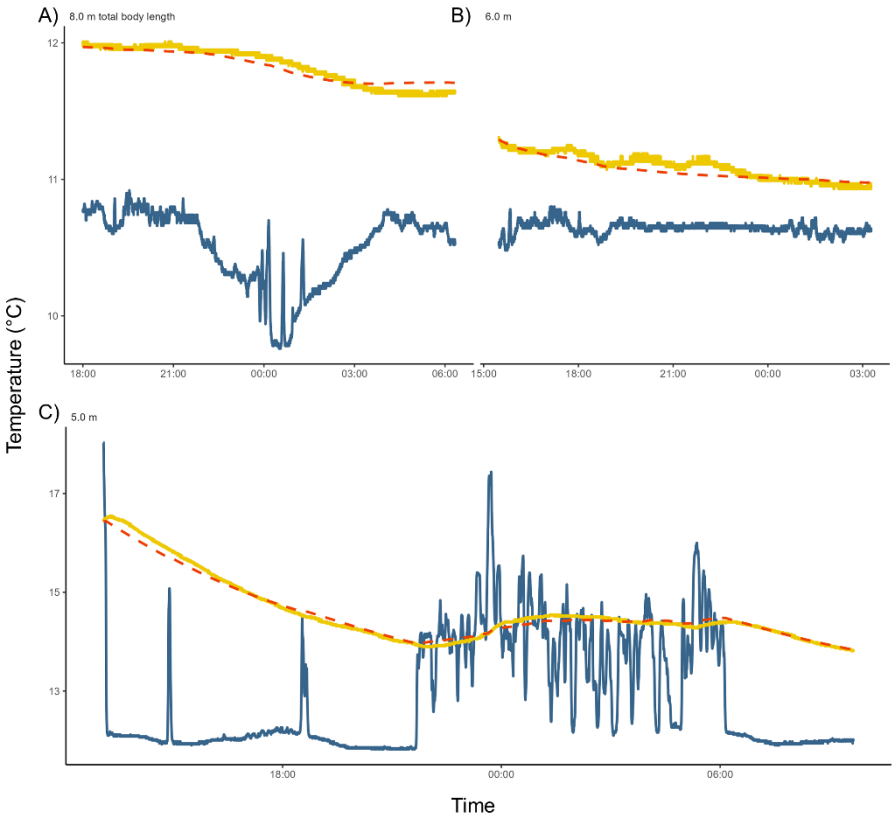

Figure C.2: Entire time-series of water temperature, subcutaneous white muscle temperature and heat transfer coefficient estimates of three basking sharks. (A, B, and C) subcutaneous white muscle temperature (gold lines) compared with fixed heat transfer coefficient model $\widehat{T_m}$ (orange dashed lines) and ambient water temperature (steel blue lines) in three free-swimming basking sharks (panels A, B and C are sharks 2, 6, and 5, respectively).

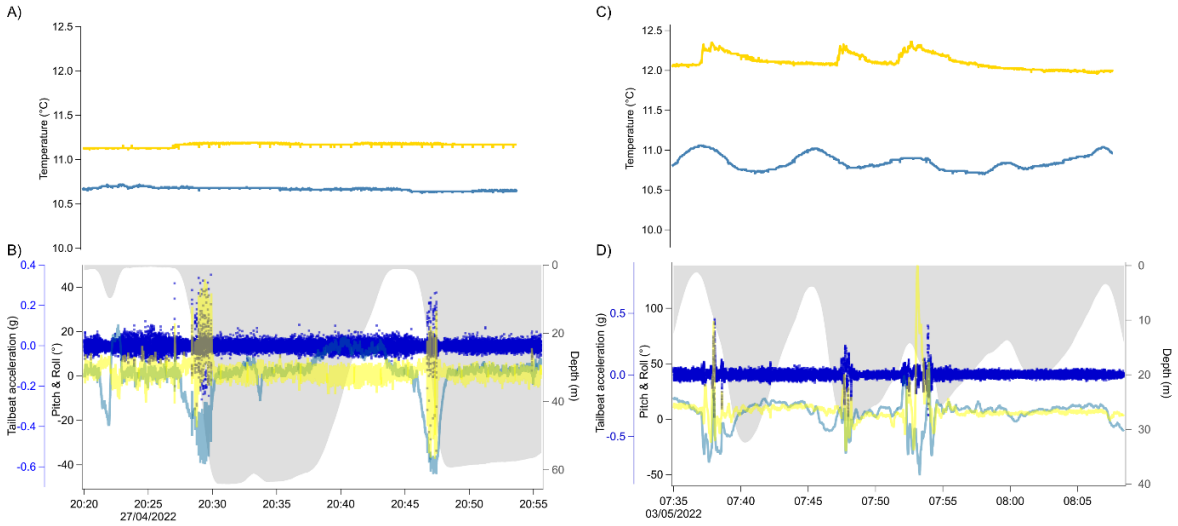

Figure C.3: Time-series examples of rolling events from shark 6 and 7. (A and C) Subcutaneous white muscle temperature (°C; gold line) and ambient water temperature (°C; steel blue line) of two separate rolling events. (B and D) Tailbeat acceleration (g; blue dots), pitch (°; teal line), roll (°; yellow line) and depth (m; shaded grey) of rolling events of shark 6 and 7, respectively.

Appendix D Supplementary information to Chapter 5:

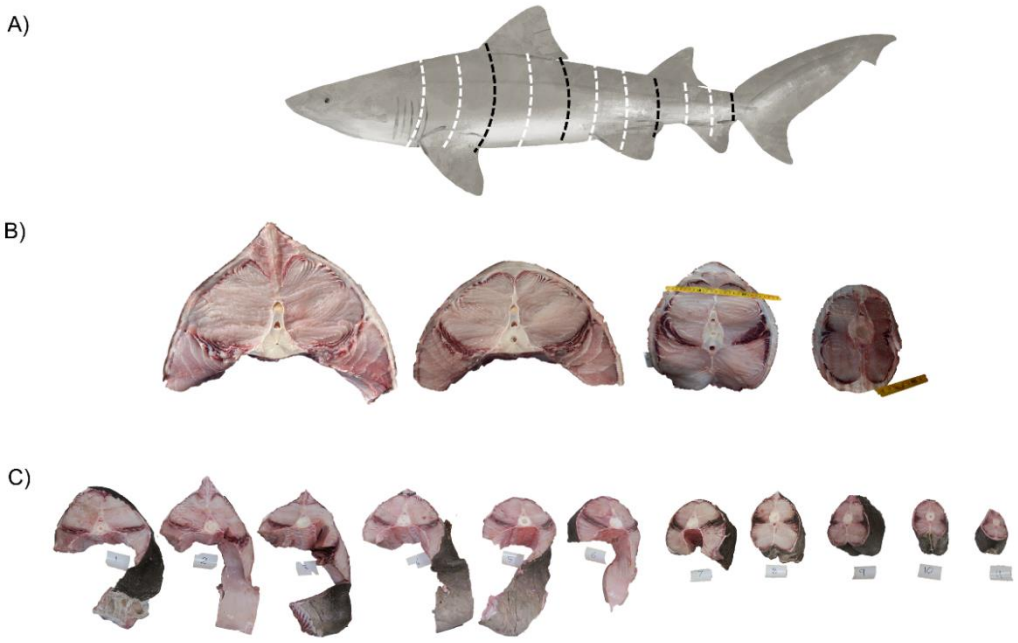

Figure D.1: Red muscle distribution of the smalltooth sand tiger shark *Odontaspis ferox*. (A) Diagram of the smalltooth sand tiger shark showing location of transverse sections. (B) Transverse cross sections of specimen 1 taken from locations indicted on panel A as black dashed lines. (C) Transverse cross sections of specimen 2 taken from locations indicted on panel A as white and black dashed lines. The first dashed line on the left matching first transverse cross section on the left in panels B and C.

Table D.1: Species in the order Lamniformes that have regionally endothermic anatomical traits (yes; Y, no; N or Unknown) and thermoregulatory life history investigated (Regional endotherm, Ectotherm or Unknown).

Species	Myocardium assessed	Medial to lateral red muscle at the trunk	Paired lateral vasculature	Rete (either in red muscle, viscera, brain, eyes)	Red muscle vein	Thermoregulatory strategy	Reference
Cetorhinus maximus	Y	Y	Y	Unknown	Unknown	Regional endotherm (skeletal muscle)	(Dolton et al. 2023)
Lamna nasus	N	Y	Y	Y	Y	Regional endotherm (skeletal muscle)	(Braekken 1959, Carey & Teal 1969, Block & Carey 1985, Wolf et al. 1988)
Lamna ditropis	Y	Y	Y	Y	Y	Regional endotherm (skeletal muscle)	(Block & Carey 1985, Wolf et al. 1988, Tubbesing & Block 2000, Bernal et al. 2003a b, 2005, 2012)
Carcharodon carcharias	Y	Y	Y	Y	Y	Regional endotherm (skeletal muscle)	(Carey et al. 1982, Block & Carey 1985, Wolf et al. 1988, Bernvi 2016, Farrell & Smith 2017)
Isurus paucus	Unknown	Unknown	Unknown	Y	Unknown	Unknown	(Carey et al. 1985, Block & Carey 1985, Bernal et al. 2001a)
Isurus oxyrinchus	Y	Y	Y	Y	Y	Regional endotherm (skeletal muscle)	(Carey & Teal 1969, Block & Carey 1985, Wolf et al. 1988, Holts & Bedford 1993, Bernal et al. 2001a, 2003a, Farrell & Smith 2017)
Alopias superciliosus	Unknown	N	N	Y	N	Ectotherm (possible cranial endothermy)	(Weng & Block 2004, Bernal & Sepulveda 2005, Patterson et al. 2011)
Alopias vulpinus	Y	Y	Y	Y	N	Regional endotherm (skeletal muscle)	(Emery et al. 1985, Weng & Block 2004, Bernal & Sepulveda 2005, Sepulveda et al. 2005)
Alopias pelagicus	Unknown	N	N	Y	N	Ectotherm	(Weng & Block 2004, Bernal & Sepulveda 2005, Patterson et al. 2011)
Odontaspis ferox	Y	Y	Y	Unknown	Unknown	Unknown	This study